PERSPECTIVES OF NUCLEAR STRUCTURE AND NUCLEAR REACTIONS

Joint Institute for Nuclear Research

PERSPECTIVES OF NUCLEAR STRUCTURE AND NUCLEAR REACTIONS

Collection of papers, dedicated to the 60th anniversary of the birthday of Rostislav Jolos

Dubna 2002

УДК 539.14
539.17.01
ББК 22.383
22.383.5
Р47

The contributions are reproduced directly from the originals presented by the Organizing Committee.

Perspectives of Nuclear Structure and Nuclear Reactions: Collection
Р47 of papers, dedicated to the 60th anniversary of the birthday of Rostislav Jolos. — Dubna: JINR, 2002. — 112 p.; 12 p. photos.

ISBN 5-85165-704-9

This book is a collection of papers dedicated to the 60th anniversary of the birthday of Professor Rostislav Jolos. Recent achievements in the theoretical study of nuclear structure and nuclear reactions at low energies are presented.

Перспективы в изучении структуры ядра и ядерных реакций: Сборник статей, посвященный 60-летию со дня рождения Р. В. Джолоса. — Дубна: ОИЯИ, 2002. — 112 с.; 12 с. фото.

ISBN 5-85165-704-9

Сборник статей посвящен 60-летию профессора Р. В. Джолоса. Представлены последние достижения в теоретическом изучении структуры ядер и ядерных реакций при низких энергиях.

УДК 539.14
539.17.01
ББК 22.383
22.383.5

ISBN 5-85165-704-9

Rostislav Jolos

Biographical Sketch

On January 11, 2002, we celebrated the 60th anniversary of Prof. Rostislav Jolos's birth. His scientific carrier began with the study of collective nuclear excitations at low energies using the microscopical methods. Starting with the nuclear Hamiltonian as that of a system of interacting nucleons, and using the finite boson expansion method, R.V. Jolos jointly with his colleagues has managed to construct a Hamiltonian containing only collective quadrupole degrees of freedom. Then the collective nuclear parameters can be calculated on the grounds of the known data on the average nuclear potential and effective nucleon interaction. The analysis of the collective Hamiltonian symmetry has shown that the Hamiltonian can also be used for describing quadrupole movement in stiff spherical nuclei and in the nuclei of the so-called transitional region, where quadrupole oscillations are very far from being harmonic. It is also applicable to the strongly deformed nuclei, where the rotational and oscillatory degrees of freedom can be singled out. These works were the first to point out that the collective Hamiltonian of quadrupole movement has in the general case the SU(6) symmetry, which, in the case of the strongly deformed nuclei, is reduced to a simpler symmetry, SU(3). On the basis of the microscopically grounded collective Hamiltonian, analysed and explained have been many properties of the excited levels of the nuclei in the transitional areas.

These works had great resonance. In 1977, they won the First Prize of the Central Institute of Nuclear Research in Rossendorf, and in 1980 – the JINR Prize. The approach developed by R.V. Jolos has been appreciated by the community of nuclear theorists. It has initiated the development of the so-called algebraic models in nuclear theory, of which the interacting boson model is the most known. The authors of this model, which was immensely popular in the 1980s, F. Iachello and A. Arima, used the ideas and approaches of Dubna's physicists and themselves repeatedly admitted it.

The story of the finite boson expansion and Hamiltonian of collective quadrupole movement can create the impression that R.V. Jolos's style is purely mathematical and he makes his discoveries following the formal logic of mathematical calculations. However, it is not so. He rather chooses a mathematical apparatus on the grounds of his almost intuitive understanding of the physics phenomenon being studied. The style of his works and his way of reasoning are always clear. He begins to consider a problem starting from the physics of

the phenomenon and using the simplest qualitative assessments. But apparent simplicity hides his subtle intuition in physics, which sometimes leaves behind logical constructions and long calculations. So lectures by R.V. Jolos have always drawn a diverse audience, including students, postgraduates, and eminent scientists.

Up to now, R.V. Jolos's studies have been focused on the theory of low-energy nuclear excitations, or, in other terms, theoretical nuclear spectroscopy. But since the early 1980s, a new subject has been present and gaining strength in his works: theory of collisions of heavy nuclei at the energies of several tens of MeV. In his numerous works, R.V. Jolos tries to resolve quite a complicated issue in this field: does the structure of the heavy nuclei affect the result of their collision? This question has an answer now: yes, it does, and very strongly, which is confirmed in the experiments on the deep inelastic collisions and fusion of heavy nuclei. The model developed at R.V. Jolos's group has great predictive power and is successful in the description of the experiment. For example, it has allowed the description of mass and charge distribution of reaction products and explanation of non-statistical effects in the excitation energy distribution between fragments. It has been shown that the dominating mechanism of collision kinetic energy dissipation consists in the colliding nuclei exchanging nucleons, neutron exchange being more important. Some of these works won the 1992 JINR Encouraging Prize. One of the makings of this success should be specially noted: in the 1990s, a fruitful team of young researchers formed around R.V. Jolos. His group is supported by the Russian Foundation for Basic Research as well as by various International Foundations (Alexander von Humboldt Stiftung, Volkswagen-Stiftung, DFG, and DAAD).

R.V. Jolos continues his research in the theory of nuclear structure. He won the 1996 JINR Prize for his studies of the octupole correlations in nuclei. In this area, he is most interested in the display of supersymmetry in the properties of the low-energy nuclear excitations. In popular scientific publications and communications from physics institutes and laboratories worldwide, the word "supersymmetry" appears so often that there is hardly any need to explain how urgent and interesting is this topic. In their recent works, R.V. Jolos and his colleagues suggested that the octupole vibrations in nuclei be regarded as the oscillations in the mass asymmetry coordinate. The new approach allows us to explain in the same manner many experimental data on parity splitting in actinides and to propose experiments on the search of the octupole states.

This book is dedicated to Prof. Rostislav Jolos, to whom we wish further successes.

Bibliography of Rostislav Jolos

1. J. Bang, R.V. Jolos, A.S. Markov, I.N. Mikhailov, On accuracy of the calculations of the frequency of the collective nuclear vibrations in the framework of the $u - v$ transformation method, *Phys. Atomic Nuclei (Rus)*, **3** 227 (1966).

2. R.V. Jolos, I.N. Mikhailov, A method for solving the nucleon–phonon interaction problem, *Acta Physica Polonica*, **30** 237 (1966).

3. R.V. Jolos, The interaction of the nucleon on the isolated level with the quadrupole phonon, *Dubna, Preprint JINR*, **P4–2985** (1966).

4. E.B. Balbutzev, R.V. Jolos, I.N. Mikhailov, Calculation of nucleon–phonon interaction effects in a simple nuclear model, *Acta Physica Polonica*, **31** 371 (1967).

5. R.V. Jolos, V.G. Soloviev, K.M. Zheleznova, Anharmonic effects in even–even deformed nuclei, *Phys. Lett. B*, **25** 393 (1967).

6. R.V. Jolos, The anharmonic effects and the appearance of the nuclear deformation in even–even deformed nuclei, *Proc. 7th Cracow school on Theor. Phys.*, 125 (1967).

7. E.B. Balbutzev, R.V. Jolos, Magnetic moments of the collective states of the spherical even–even nuclei, *Dubna, Preprint JINR*, **P4–3611** (1967).

8. E.B. Balbutzev, R.V. Jolos, Quadrupole moments of the spherical even–even nuclei, *Phys. Atomic Nuclei (Rus)*, **7** 788 (1968).

9. R.V. Jolos, V.G. Soloviev, K.M. Zheleznova, U.M. Finer, Anharmonic effects in nuclei of the transition region, *Phys. Lett. B*, **27** 614 (1968).

10. R.V. Jolos, Collective modes associated with nuclear pair correlations, *Phys. Lett. B*, **30** 390 (1969).

11. R.V. Jolos, Mass coefficient in the collective nuclear Hamiltonian and the sum rules for E2–transition probabilities and quadrupole moments, *Dubna, JINR preprint*, **P4–5346** (1970).

12. R.V. Jolos, V.G. Soloviev, Selfconsistent field method in nuclear theory, *Particles and Nuclei*, **1** 365 (1970).

13. R.V. Jolos, Pair correlations and collective 0^+–states in nuclei. 1, *Theor. Math. Phys. (Rus)*, **6** 403 (1971).

14. D.A. Arseniev, R.V. Jolos, Isomer transition $8^- \to 6^+$ in ^{130}Ba, *Izv. AN SSSR, (ser. fyz.) (Rus)*, **35** 2281 (1971).

15. R.V. Jolos, V. Rybarska, Correlations between quasiparticle and collective excitations in nuclei, *Dubna, Preprint JINR*, **E4–5578** (1971).

16. R.V. Jolos, Phenomenological approach to description of the nuclear rotational excitations, *Dubna, Preprint JINR*, **P4–5982** (1971).

17. F. Dönau, D. Janssen, S. Frauendorf, R.V. Jolos, Boson description of collective states 1. Derivation of the boson transformation for even fermion system, *Nucl. Phys. A*, **172** 145 (1971).

18. R.V. Jolos, V.P. Permjakov, Energies of the low lying collective states in odd spherical nuclei, *Conference on nuclear spectroscopy and nuclear structure, Dubna*, 41 (1971).

19. R.V. Jolos, V. Rybarska, Pair rotations and the problem of the host states, *Dubna, Preprint JINR*, **P4–6258** (1972).

20. R.V. Jolos, V. Rybarska, Method of the boson representations of the fermion operators in nuclear theory, *Particles and Nuclei (Rus)*, **3** 739 (1972).

21. R.V. Jolos, V.G. Kartavenko, To foundation of the Crancking model, *Dubna, Preprint JINR*, **P4–6543** (1972).

22. R.V. Jolos, V.G. Kartavenko, Method of N.N. Bogoliubov in the problem of pair vibrations, *Dubna, Preprint JINR*, **P4–6590** (1972).

23. R.V. Jolos, V.G. Kartavenko, On analog of Bohr's hamiltonian for pair vibrations, *Dubna, Preprint JINR*, **P4–6782** (1972).

24. R.V. Jolos, V.G. Kartavenko, Pair correlations and collective 0^+–states in nuclei with $A \sim 56$, *Dubna, Preprint JINR*, **P4–6781** (1972).

25. R.V. Jolos, V.G. Kartavenko, F. Dönau, D. Janssen, Pair correlations and collective 0^+–states in nuclei. 2, *Theor. Math. Fyz. (Rus)*, **14** 70 (1973).

26. R.V. Jolos, F. Dönau, V.G. Kartavenko, D. Janssen, Structure of transitional nuclei in the region of Sm and Gd, *Dubna, Preprint JINR*, **P4–7223** (1973).

27. Ch. Fuya, A.B. Chalikulov, V.A. Morozov, T.M. Muminov, R.V. Jolos, l-forbidden M1–transitions in neutron deficient La, Ce and Pr isotopes, *Proc. Int. Conf. on Nucl. Phys., Munich*, **1** 291 (1973).

28. R.V. Jolos, V.P. Permjakov, The role of the nonadiabatic effects in the process of the Coulomb interaction of the complex nuclei, *Dubna, Preprint JINR*, **P4–8416** (1974).

29. R.V. Jolos, F. Dönau, D. Janssen, Construction of the collective hamiltonian in microscopic nuclear model, *Theor. Math. Phys. (Rus)*, **20** 112 (1974).

30. R.V. Jolos, V.G. Kartavenko, Pair correlations and collective 0^+–states in nuclei with $A \sim 56$, *Phys. Atomic Nuclei (Rus)*, **19** 964 (1974).

31. R.V. Jolos, F. Dönau, V.G. Kartavenko, D. Janssen, Properties of collective states of even Mo isotopes, *Phys. Atomic Nuclei (Rus)*, **20** 310 (1974).

32. R.V. Jolos, V.G. Kartavenko, V. Rybarska, Method of N.N. Bogoliubov in the problem of pair vibrations and the problem of exclusion of the host states, *Theor. Math. Phys.*, **20** 353 (1974).

33. G.N. Afanasyev, R.V. Jolos, V.G. Kartavenko, Influence of the isospin invariant pair correlations on the mean square nuclear radii, *Izv. AN SSSR, (ser. fyz.) (Rus)*, **38** 730 (1974).

34. R.V. Jolos, F. Dönau, V.G. Kartavenko, D. Janssen, Properties of collective states of transitional Sm and Gd isotopes, *Izv. AN SSSR, (ser. fyz.) (Rus)*, **38** 2059 (1974).

35. D. Janssen, R.V. Jolos, F. Dönau, An algebraic treatment of nuclear quadrupole degree of freedom, *Nucl. Phys. A*, **224** 93 (1974).

36. R.V. Jolos, The method of calculations of the energies and the wave functions of low lying states in odd nuclei, *Dubna, Preprint JINR*, **P4–7967** (1974).

37. R.V. Jolos, F. Dönau, V.G. Kartavenko, D. Janssen, Microscopic theory of collective motion in transitional nuclei, *Proc. Int. Symp. on correlations in nuclei, Budapest*, 71 (1974).

38. R.V. Jolos, F. Dönau, D. Janssen, Microscopic approach to the construction of collective nuclear hamiltonian. 2, *Theor. Math. Phys.*, **23** 374 (1975).

39. R.V. Jolos, F. Dönau, V.G. Kartavenko, D. Janssen, E2–transitions in ^{108}Pd without changing of phonon number, *Izv. AN SSSR, (ser. fyz.) (Rus)*, **39** 532 (1975).

40. R.V. Jolos, V.G. Kartavenko, S.M. Semenov, Pair correlations and two–nucleon transfer reaction cross–sectionson nuclei with A = 46 – 64, *Phys. Atomic Nuclei (Rus)*, **22** 1121 (1975).

41. R.V. Jolos, F. Dönau, D. Janssen, Symmetry properties of the collective states of deformed nuclei, *Phys. Atomic Nuclei (Rus)*, **22** 965 (1975).

42. R.V. Jolos, D. Janssen, Generator coordinate method and the construction of the collective hamiltonian, *Dubna, Preprint JINR*, **E4–8692** (1975).

43. R.V. Jolos, Collective models and microscopic approach to description of the properties of spherical and transitional nuclei, *Dubna, Preprint JINR*, **P4–8743** (1975).

44. T. Fenes, I. Mahunka, Z. Mate, R.V. Jolos, V. Paar, Excitation of light Hg nuclei in the decay of Tl, *Nucl. Phys. A*, **247** 103 (1975).

45. R.V. Jolos, Calculations of the energies of low lying states of short living isotopes ^{193,195,197}Hg, *Dubna, Preprint JINR*, **P4–9357** (1975).

46. R.V. Jolos, D. Janssen, Anomalous 0_2^+ excited states in spherical even–even nuclei, *Dubna, Preprint JINR*, **P4–9358** (1975).

47. R.V. Jolos, D. Janssen, Method of calculations of the matrix elements of microscopic nuclear hamiltonian in the space of collective fermion states, *Izv. AN SSSR, (ser. fyz.) (Rus)*, **40** 1273 (1976).

48. G. Holzwart, D. Janssen, R.V. Jolos, On the validity of the boson method for transitional nuclei, *Nucl. Phys. A*, **261** 1 (1976).

49. R.V. Jolos, F. Dönau, D. Janssen, Properties of transitional nuclei (theory and experiment), *Proc. of Intern. School on Nucl. Phys., Bucharest*, 381 (1976).

50. R.V. Jolos, V.P. Permjakov, G. Röpke, H. Schulz, Friction forces in the reactions with complex nuclei. 1, *Dubna, Preprint JINR*, **E4–9670** (1976).

51. R.V. Jolos, V.P. Permjakov, G. Röpke, H. Schulz, Friction forces in the reactions with complex nuclei. 2, *Dubna, Preprint JINR*, **E4–9671** (1976).

52. R.V. Jolos, V.P. Permjakov, H. Schulz, Nonadiabatic effects in the interaction of complex nuclei, *Proc. Int. Conf. on Heavy Ion Collision, Caen, France*, 155 (1976).

53. R.V. Jolos, D. Janssen, Spherical states in transitional nuclei, *Phys. Atomic Nuclei (Rus)*, **25** 499 (1977).

54. R.V. Jolos, D. Janssen, Microscopic approach to the description of the properties of quadrupole nuclear excitations, *Particles and Nuclei*, **8** 330 (1977).

55. R.V. Jolos, S.I. Fedotov, Coupling of the volume and surface vibrations in nuclei, *Proc. Int. Conf. on Nucl. Interactions, Australia*, 123 (1978).

56. G.N. Afanasyev, R.V. Jolos, V.P. Permjakov, V.M. Shilov, Coulomb energy dissipation in heavy ion reactions, *Izv. AN SSSR, (ser. fyz.) (Rus)*, **42** 1961 (1978).

57. G.N. Afanasyev, R.V. Jolos, V.P. Permjakov, V.M. Shilov, Influence of the nonadiabaticity on the elastic scattering, *Dubna, Preprint JINR*, **P4–11319** (1978).

58. R.V. Jolos, Ch.L. Molina, V.G. Soloviev, Influence of the Pauli principle on the properties of two–phonon states, *Theor. Math. Phys. (Rus)*, **40** 245 (1979).

59. R.V. Jolos, Ch.L. Molina, V.G. Soloviev, Effect of the Pauli principle on the excited states of double–even nuclei, *Z. Phys. A*, **295** (1980).

60. R.V. Jolos, V.G. Kartavenko, S.I. Fedotov, Kinetic energy dissipation in heavy ion collisions and nuclear matter density vibrations, *Dubna, Preprint JINR*, **E4–80–730** (1980).

61. R.V. Jolos, V.G. Kartavenko, Preequilibrium light particles emission in heavy ion reactions, *Dubna, Preprint JINR*, **P4–80–37** (1980).

62. R.V. Jolos, V. Navrozka, Self–consistent QRPA in the theory of nuclear structure, *Z. Phys. A*, **296** 73 (1980).

63. R.V. Jolos, R.V. Jolos, Interaction of heavy ions at energies 10 MeV/A and the nonequilibrium processes in nuclei, *Proceeding of the International school on nuclear structure, Alushta, Dubna*, **D4–80–385** 277 (1980).

64. R.V. Jolos, V.G. Kartavenko, S.I. Fedotov, Dissipation of kinetic energy in heavy ion reactions, *Phys. Atomic Nuclei (Rus)*, **33** 1511 (1981).

65. R.V. Jolos, R. Schmidt, Interaction of heavy ions at energies about 10 MeV/nucleon, *Particles and Nuclei (Rus)*, **12** №2 324 (1981).

66. R.V. Jolos, V.G. Kartavenko, V.P. Permyakov, Nuclear hydrodynamics and nuclear surface vibrations, *Phys. Atomic Nuclei (Rus)*, **34** 1444 (1981).

67. R.V. Jolos, S.P. Ivanova, V.G. Kartavenko, Light particle emission in heavy ion reactions, *Izv. AN SSSR, (ser. fyz.) (Rus)*, **45** 1927 (1981).

68. R.V. Jolos, R. Schmidt, I. Teichert, Particle–hole description of HIC, *Proc. 12 Int. Symp. on Nucl. Phys., Gaussig*, 72 (1982).

69. R.V. Jolos, M.M. Mihailova, Excited states of ^{131}Ba in the framework of the particle–core coupling model, *Bulg. Journ. Phys.*, **6** 569 (1982).

70. R.V. Jolos, Z. Vylov, Z. Zhelev, M. Mihailova, Investigation of the excited states of ^{135}Ba, *Izv. AN SSSR, (ser. fyz.) (Rus)*, **47** 2108 (1983).

71. R.V. Jolos, A.K. Nasirov, Multinucleon transfer in deep inelastic collisions of heavy ions, *Phys. Atomic Nuclei (Rus)*, **40** 721 (1984).

72. R.V. Jolos, S.P. Ivanova, Microscopic model of preequilibrium nucleon emission, *Proc. of the Workshop on Coinc. Part. Emission from Continuum states in Nucl., Bad Honnef, ed. H.Machner and Jahn*, 410 (1984).

73. R.V. Jolos, R. Schmidt, I. Teichert, One–body collisions and classical collective dynamics in heavy ion reactions, *Nucl. Phys. A*, **429** 139 (1984).

74. R.V. Jolos, S.P. Ivanova, V.V. Ivanov, Initial stage of heavy ion interaction and mechanism of the kinetic energy dissipation, *Phys. Atomic Nuclei (Rus)*, **40** 117 (1984).

75. R.V. Jolos, S.P. Ivanova, V.V. Ivanov, Description of the relative motion of nuclei in deep inelastic collisions of heavy ions, *Izv. AN SSSR, (ser. fyz.) (Rus)*, **40** 2180 (1985).

76. R.V. Jolos, V.M. Mihailov, I.Ch. Lemberg, Interacting boson model. Physical grounds and applications, *Particles and Nuclei*, **16** 280 (1985).

77. R.V. Jolos, H. Reinhardt, R. Schmidt, R. Schvengler, Microscopic model of the kinetic energy damping in deep inelastic heavy ion collisions, *Phys. Atomic Nuclei (Rus)*, **41** 906 (1985).

78. R.V. Jolos, S.P. Ivanova, Heavy ion collisions: kinetic energy damping and nucleon emission, *Proc. Int. Conf. on Nucl. Structure, Dubna*, 304 (1985).

79. R.V. Jolos, S.P. Ivanova, Effect of the nonorthogonality of the wave functions in the description of the collision of nuclei, *Phys. Atomic Nuclei (Rus)*, **41** 677 (1985).

80. R.V. Jolos, A.K. Nasirov, Influence of the residual forces on the width of charge distributions of the products of multinucleon transfer reactions, *Phys. Atomic Nuclei (Rus)*, **42** 175 (1985).

81. R.V. Jolos, S.P. Ivanova, R. Pedrosa, Investigation of the structure of 0_2^+ states of even–even isotopes of Ge and Se, *Dubna, Preprint JINR*, **P4–85–452** (1985).

82. R.V. Jolos, S.P. Ivanova, A model for the description of fast particle emission and multinucleon transfer in deep inelastic collisions of heavy ions, *Proc. of the 2nd Int. Conf. on nucleus–nucleus collisions, Visbu*, 71 (1985).

83. R.V. Jolos, S.P. Ivanova, Model for description of neutrons emission in heavy ion collisions, *Phys. Atomic Nuclei (Rus)*, **43** 1463 (1986).

84. R.V. Jolos, A.K. Nasirov, A.I. Muminov, Influence of the nuclear structure on the cross sections of the multinucleon transfer reactions, *Phys. Atomic Nuclei (Rus)*, **44** 357 (1986).

85. S.P. Ivanova, R.V. Jolos, SU(6)–symmetry in the IBM: a convenient tool or physical requirement?, *Proc. Int. Conf. on symmetries and nuclear structure, Dubrovnik, Yugoslavia*, **3** 3 (1986).

86. R.V. Jolos, A.K. Nasirov, Charge distributions of the multinucleon transfer reaction products at large kinetic energy losses, *Dubna, Preprint JINR*, **P4–86–546** (1986).

87. S.P. Ivanova, R.V. Jolos, SU(6)–symmetry in the Interacting boson model, *Dubna, Preprint JINR*, **P4–86–507** (1986).

88. M.M. Mihailova, Zh. Zhelev, R.V. Jolos, Low–energy excitations in odd–mass barium nuclei, *Journ. Phys. G*, **12** L191 (1986).

89. R.V. Jolos, S.P. Ivanova, P.P. Korovin, Isovector polarization of nuclei in heavy ion collisions, *Phys. Atomic Nuclei (Rus)*, **46** 779 (1987).

90. R.V. Jolos, S.P. Ivanova, R. Pedrosa, V.G. Soloviev, Investigation of the shifts of the two–phonon poles in deformed nuclei by the boson expansion technique, *Theor. Math. Phys.*, **70** 154 (1987).

91. R.V. Jolos, A.K. Nasirov, Influence of the nucleon exchange on the nucleus–nucleus interaction potential, *Phys. Atomic Nuclei (Rus)*, **45** 1298 (1987).

92. R.V. Jolos, V.P. Permyakov, Influence of the nuclear shape vibrations on the sub-barrier fusion cross section, *JINR Rapid Communications*, № **1(21)** 46 (1987).

93. G. Kyrchev, V. Paar, R.V. Jolos, Collective nuclear model based on dynamical SU(6)–symmetry, *Particles and Nuclei*, **18** 1173 (1987).

94. R.V. Jolos, A.K. Nasirov, V.P. Permjakov, Inhancement of the sub-barrier fusion of complex nuclei due to dynamical changings of the entrance channel interaction potential, *Izv. AN SSSR, (ser. fyz.) (Rus)*, **51** 2041 (1987).

95. S.P. Ivanova, R.V. Jolos, V.P. Permjakov, Isovector polarization of nuclei in heavy ion collisions and the dynamical nucleus–nucleus interaction potential, *Proc. of the 1st topical meeting, Legnaro*, 21 (1987).

96. R.V. Jolos, A.K. Nasirov, V.P. Permjakov, Total kinetic energies of deep inelastic collisions of heavy ions and quasifission, *Phys. Atomic Nuclei (Rus)*, **48** 1304 (1988).

97. R.V. Jolos, V.P. Permjakov, Enhancement of the sub-barrier fusion by the excitations of quadrupole shape vibrations during collisions, *Phys. Atomic Nuclei (Rus)*, **47** 58 (1988).

98. S.P. Ivanova, R.V. Jolos, V.P. Permjakov, Isovector polarization of nuclei in heavy ion collisions and the dynamical nucleus–nucleus interaction potential, *Nucl. Phys. A*, **482** 263 (1988).

99. S.P. Ivanova, R.V. Jolos, Current and density algebra approach to HIC, *Proc.18 Int. Symp. on Nucl. Phys., Gaussig*, 300 (1988).

100. R.V. Jolos, M.M. Mihailova, Low energy spectra of Odd–Mass transitional nuclei in the framework of the particle–core coupling model, *Proc. 9th Int. Conf. on Nucl. Phys., Neutron. Phys. and Nucl. Energy, Varna, Bulgaria, World Scientific*, 171 (1989).

101. R.V. Jolos, S.P. Ivanova, R. Pedrosa, Approximate treatment of the Holstein–Primakov type boson mapping, *Journ. Phys. G*, **15** 55 (1989).

102. N.V. Antonenko, R.V. Jolos, Influence of the shell effects on the productions of light nuclei in heavy ion collisions, *Phys. Atomic Nuclei (Rus)*, **50** 98 (1989).

103. R.V. Jolos, S.M. Lukyanov, A.K. Nasirov et al., Investigation of the influence of the nuclear shell structure on mass distributions of the multinucleon transfer reaction products, *Phys. Atomic Nuclei (Rus)*, **50** 382 (1989).

104. J. Dobes, S.P. Ivanova, R.V. Jolos, R. Pedrosa, Boson representation of the microscopic nuclear Hamiltonian, *Proc. Int. Conf. on Selected topics in Nucl. Structure, Dubna*, **2** 320 (1990).

105. J. Dobes, S.P. Ivanova, R.V. Jolos, R. Pedrosa, Projection operator in the boson expansion technique, *Phys. Rev. C*, **341** 1840 (1990).

106. N.V. Antonenko, R.V. Jolos, Coulomb effects in the microscopic theory of the multinucleon transfer reactions, *Phys. Atomic Nuclei (Rus)*, **51** 690 (1990).

107. N.V. Antonenko, R.V. Jolos, Influence of the shell effects on charge distributions of the heavy ion reaction products, *Phys. Scripta T*, **32** 27 (1990).

108. A. Zilges, P. von Brentano, A. Richter, R.V. Jolos et al., Phonon scattering experiments in the rare earth region–a new approach to low lying dipole modes, *Proc. of the 7th Int. Symp. on capture gamma– ray spectroscopy and related topics, Asilomar, Pacific Grove, California*, 47 (1990).

109. J. Dobes, S.P. Ivanova, R.V. Jolos, R. Pedrosa, Boson mapping and the microscopic collective nuclear hamiltonian, *Journ. Phys. G*, **17** 125 (1991).

110. S.P. Ivanova, R.V. Jolos, R. Pedrosa, Description of the 8^+ states in Kr isotopes, *Phys. Atomic Nuclei (Rus)*, **53** 86 (1991).

111. N.V.Antonenko, R.V. Jolos, Microscopic treatment of the proton and neutron multiple transfer in DIC, *Z. Phys. A*, **338** 423 (1991).

112. S.P. Ivanova, R.V. Jolos, Current and density algebra approach to low energy heavy ion collisions, *Nucl. Phys. A*, **530** 232 (1991).

113. N.V. Antonenko, R.V. Jolos, Mechanism of enhanced yield of light particles in compound nucleus formation, *Z. Phys. A*, **339** 453 (1991).

114. S.P. Ivanova, R.V. Jolos, R. Pedrosa, Interacting boson approximation for two-quasiparticle and collective states, *Czech. Jour. of Phys.*, **41** 1099 (1991).

115. N.V. Antonenko, R.V. Jolos, Mechanism of enhanced yield of light particles in compound nucleus formation: diffusion description, *Z. Phys. A*, **341** 459 (1992).

116. A. Zilges, P. von Brentano, R.V. Jolos et al., Evidence of dipole transition to a two phonon plus particle multiplet in ^{143}Nd, *Proc. of the 6th Int. Conf. on nuclei far from stability and 9th Int. Conf. on Atomic Mass. and Fundamental const., Germany, eds. R.Neugart and A.Wöhr*, 27 (1992).

117. R.V. Jolos, P. von Brentano, A. Gelberg, Description of staggering in energy spectra of odd triaxial nuclei, *Progr. in Particle and Nucl. Phys.*, **28** 363 (1992).

118. G.G. Adamian, R.V. Jolos, A.K. Nasirov, Shell effects in the matrix elements of the nucleon transfer in the multinucleon transfer process, *Phys. Atomic Nuclei (Rus)*, **55** 660 (1992).

119. N.V. Antonenko, R.V. Jolos, Inhancement of the light particle emission in the nuclear fusion, *Izv. AN SSSR, (ser. fyz.) (Rus)*, **56** 84 (1992).

120. G.G. Adamian, N.V. Antonenko, R.V. Jolos, A.K. Nasirov, Microscopic driving potential for a dinuclear system, *Nucl. Phys. A*, **551** 321 (1993).

121. A. Zilges, P. von Brentano, R.V. Jolos et al., First identification of dipole excitations to a $2^+ \otimes 3^- \otimes$ particle multiplet in odd-A nucleus, *Phys. Rev. Lett.*, **70** 2880 (1993).

122. R.V. Jolos, P. von Brentano, F. Dönau, Barrier penetration effect on the angular momentum dependence of the parity splitting in actinide nuclei, *Journ. Phys. G*, **19** L1 (1993).

123. G.G. Adamian, N.V. Antonenko, R.V. Jolos, S.P. Ivanova, A.K. Nasirov, Evolution of a dinuclear system formed in heavy ion collisions, *Proc. Int. Conf. on Nucl. Struct. and Nucl. React., Dubna*, **E4–93–58** (1993).

124. R.V. Jolos, A. Gelberg, Analytical approach to particle–rotor model for single j case, *Phys. Lett. B*, **317** 495 (1993).

125. G.G. Adamian, N.V. Antonenko, R.V. Jolos, Mass parameters for dinuclear system, *Dubna, Preprint JINR*, **E4–93–324** (1993).

126. G.G. Adamian, N.V. Antonenko, R.V. Jolos, S.P. Ivanova, O.I. Melnikova, Potential energy of a dinuclear system, *Dubna, Preprint JINR*, **E4–93–377** (1993).

127. G.G. Adamian, R.V. Jolos, A.K. Nasirov, Partition of excitation energy between reaction products in heavy ion collisions, *Dubna, Preprint JINR*, **E4–93–175** (1993).

128. G.G. Adamian, N.V. Antonenko, S.P. Ivanova, R.V. Jolos, W. Scheid, Mechanism of light nuclei production in fusion reactions, *Proc. Int. School–Seminar on Heavy Ions, Dubna, ed. Yu.Ts. Oganessian, Yu.E. Penionzhkevich, R. Kalpakchieva*, **E7–93–274 2** 52 (1993).

129. G.G. Adamian, N.V. Antonenko, R.V. Jolos, A.K. Nasirov, Driving potential for dinuclear system, *Proc. 3rd Int. School on Nucl. Phys., Kiev*, 342 (1993).

130. G.G. Adamian, R.V. Jolos, A.K. Nasirov, Partition of the excitation energy between reaction products in heavy ion collisions, *Z. Phys. A*, **347** 203 (1994).

131. G.G. Adamian, R.V. Jolos, A.K. Nasirov, Excitation energy distribution between fragments of the deep inelastic collision of heavy ions, *Izv. AN SSSR, (ser. fyz.) (Rus)*, **58** 71 (1994).

132. R.V. Jolos, P. von Brentano, On the angular momentum dependence of the parity splitting in nuclei with octupole correlations, *Phys. Rev. C*, **49** R2301 (1994).

133. N.V. Antonenko, R.V. Jolos, S.P. Ivanova, W. Scheid, Application of the Lindblad axiomatic approach to nonequilibrium nuclear processes, *Jour. Phys. G*, **20** 1447 (1994).

134. P.Petkov, R.Krucken, A.Dewald, P.Sala, J.Altman, A.Gelberg, P.von Brentano, W.Andrejtscheff, R.V. Jolos, RDDS measurements of collective E2 transition strength in ^{122}Xe, *Nucl. Phys. A*, **568** 572 (1994).

135. N.V. Antonenko, S.P. Ivanova, R.V. Jolos, W. Scheid, Light nuclei production in fusion of heavy ions, *Phys. Rev. C*, **50** 2063 (1994).

136. G.G. Adamian, N.V. Antonenko, S.P. Ivanova, R.V. Jolos, O.I. Melnikova, Potential energy of a dinuclear system, *Phys. Atomic Nuclei (Rus)*, **57** 1 (1994).

137. R.V. Jolos, P. von Brentano, A. Gelberg, Signature and parity splitting in rotational bands. Double minimum potential model, *Proc. Int. Sym. on the "Frontiers of Nuclear Structure Physics", Tokyo, Japan, World Scientific*, 243 (1994).

138. A. Gelberg, R.V. Jolos, Interacting boson–fermion model for strongly deformed nuclei, *Proc. Int. Conf. "On perspective for the Interacting boson model", Padova, June 13–17, World scientific*, 299 (1994).

139. G.G. Adamian, N.V. Antonenko R.V. Jolos and A.K. Nasirov, Influence of the shell effects on dynamics of deep inelastic heavy ion collision, *Particles and Nuclei*, **25** 1379 (1994).

140. O. Vogel, A. Gelberg, P.von Brentano, R.V. Jolos, Triaxial rotor plus particle description of negative parity states in proton odd Cs nuclides, *Nucl. Phys. A*, **576** 109 (1994).

141. G.G. Adamian, N.V. Antonenko, R.V. Jolos, Increase of coupling between the modes of motion in asymmetric dinuclear system, *Proc. 4th Int. School on Nucl. Phys., Kiev,* 299 (1994).

142. G.G. Adamian, R.V. Jolos, A.K. Nasirov, Effect of the shell structure and N/Z ratio on excitation energy distribution in deep inelastic heavy ion collisions, *Proc. 4th Int. School on Nucl. Phys., Kiev,* 266 (1994).

143. G.G. Adamian, N.V. Antonenko, R.V. Jolos, Inertia tensor in the collective hamiltonian of a dinuclear system, *Phys. Atomic Nuclei (Rus),* **58** 360 (1995).

144. G.G. Adamian, N.V. Antonenko, R.V. Jolos, Mass parameters for dinuclear system, *Nucl. Phys. A,* **584** 205 (1995).

145. R.V. Jolos, P. von Brentano, Rotational spectra and parity splitting in nuclei with strong octupole correlations, *Nucl. Phys. A,* **587** 377 (1995).

146. N.V. Antonenko, S.P. Ivanova, R.V. Jolos, Introduction into theory of the heavy ion reactions, *Dubna, JINR, 95-2,* (1995).

147. G.G. Adamian, R.V. Jolos, A.K. Nasirov, Effect of the shell structure and N/Z ratio of projectile on excitation energy distribution in nuclei in deep inelastic heavy ion collisions, *Proc. LEND-95, S. Peterburg,* 441-444 (1995).

148. G.G. Adamian, N.V. Antonenko, R.V. Jolos, Inertia tensor in the collective hamiltonian of a dinuclear system, *Izv. RAN, (ser. fyz.) (Rus),* **59** 83 (1995).

149. R.V. Jolos, P. von Brentano, R.F. Casten, N.V. Zamfir, An analytic interpretation of universal anharmonic vibrator behavior in the IBA model, *Phys. Rev. C,* **51** R2298 (1995).

150. R.V. Jolos, A. Gelberg, P. von Brentano, Wave functions of the triaxial rotor model in the multiple "Q-excitation" scheme, *Phys. Rev. C,* **53** 168 (1996).

151. G.G. Adamian, N.V. Avtonenko, R.V. Jolos, S.P. Ivanova, O.I. Melnikova, Effective nucleus-nucleus potential for calculations of the potential energy of dinuclear system, *Int. J. Mod. Phys. E,* **5** 191 (1996).

152. G.G. Adamian, R.V. Jolos, A.I. Muminov, A.K. Nasirov, Influence of the N/Z ratio of the projectile on the excitation energy distribution between the products of the deep inelastic heavy ion collisions, *Phys. Atomic Nuclei (Rus),* **59** 89 (1996).

153. G.G. Adamian, R.V. Jolos, A.K. Nasirov, Effect of shell structure and N/Z-ratio of projectile on excitation energy distribution between interacting nuclei in DIC, *Phys. Rev. C,* **53** 871 (1996).

154. R.V. Jolos, A.R. Safarov, Description of the parity splitting in rotational bands of the even-even nuclei in the framework of the one-dimensional model of the octupole vibrations, *Phys. Atomic Nuclei (Rus),* **59** 2136 (1996).

155. R.V. Jolos, P. von Brentano, The absolute value of the static quadrupole moment $Q(2_1^+)$ expressed by $B(E2)$ values", *Phys. Lett. B,* **381** 7 (1996).

156. R.V. Jolos, P. von Brentano, R.F. Casten, N.V. Zamfir, Simple formula for $E(4_1^+) - E(2_1^+)$ correlations and magnification of structural anomalies, *Phys. Rev. C,* **54** R2146 (1996).

157. A.M. Oros, P. von Brentano, L.Trache, G. Graw, G. Gata-Danil, B.D. Valnion, A. Gollwitzer, K. Heyde, R.V. Jolos, New 0^+ states in ^{146}Sm from (p,t) experiment and the particle-core coupling model, *Nucl. Phys. A,* **613** 209 (1997).

158. R.V. Jolos, A.R. Safarov, Parity splitting of doublets in odd nuclei, *Phys. Atomic Nuclei (Rus),* **60** 988 (1997).

159. R.V. Jolos, P. von Brentano, N. Pietralla, I. Schneider, Shape invariants in the multiple "Q excitation" scheme, *Nucl. Phys. A,* **618** 126 (1997).

160. N. Pietralla, O. Beck, J. Besserer, P. von Brentano, R.V. Jolos, The scissors mode and other magnetic and electric dipole excitations in the transitional nuclei ^{178,180}Hf, *Nucl. Phys. A,* **618** 141 (1997).

161. G.G. Adamian, N.V. Antonenko, R.V. Jolos, W. Scheid, Neck dynamics at the approach stage of heavy ion collisions, *Nucl. Phys. A,* **619** 241 (1997).

162. G.G. Adamian, N.V. Antonenko, R.V. Jolos, W. Scheid, Neck radius as a collective variable in heavy ion collisions, *Izv. RAN, (ser. fyz.) (Rus),* **61** 697 (1997).

163. E. Radermacher, M. Wilhelm, P. von Brentano, R.V. Jolos, The gamma-decay of single particle states in ^{205}Pb and ^{207}Pb using an Euroball cluster detector, *Nucl. Phys. A,* **620** 151 (1997).

164. A.M. Oros, P. von Brentano, L. Trache, G. Graw, G. Cata-Danil, B.D. Valnion, A. Gollwitzer, K. Heyde, R.V. Jolos, New 0^+ states in ^{146}Sm in the (p,t) experiment and the particle-core coupling model, *Nucl. Phys. A,* **613** 209 (1997).

165. R.V. Jolos, Yu.V. Palchikov, Cluster properties and strong octupole correlations in medium and heavy nuclei, *Phys. Atomic Nuclei (Rus),* **60** 1202 (1997).

166. G.G. Adamian, R.V. Jolos, A.I. Muminov, A.K. Nasirov, Friction coefficient for deep inelastic collisions, *Phys. Rev. C,* **56** 373 (1997).

167. G.G. Adamian, R.V. Jolos, A.K. Nasirov, Microscopic friction coefficient for deep inelastic collisions of heavy ions, *Izv. RAN, (ser. fyz.) (Rus),* **61** 191 (1997).

168. R.V. Jolos, Yu.V. Palchikov, V.V. Pashkevich, A.V. Unzhakova, Reflection asymmetric deformation and clustering in heavy nuclei, *Nuovo. Cim. A,* **110** 941 (1997).

169. G.G. Adamian, R.V. Jolos, A.I. Muminov, A.K. Nasirov, The energy window of entrance channel and the synthesis of superheavy elements, *Proc. of the VI Int. School-Seminar, Dubna, September 22-27,* (1997).

170. N. Pietralla, T. Mizusaki, P. von Brentano, R.V. Jolos, T. Otsuka, V. Werner, 2_1^+ and 2_2^+ states in collective nuclei as multiple Q-phonon excitations, *Phys. Rev. C,* **57** 150 (1998).

171. Yu.V. Palchikov, P. von Brentano, R.V. Jolos, Universal description of 0_2^+ state in collective even-A nuclei, *Phys. Rev. C*, **57** 3026 (1998).

172. R.V. Jolos, A.K. Nasirov, A.I. Muminov, The role of the entrance channel in the fusion of massive nuclei, *Euro. Phys. Journ. A*, **4** 245 (1998).

173. R.V. Jolos, P. von Brentano, A. Gelberg, K.H. Kim, and T. Otsuka, Supersymmetric operator for the U(6/4) dynamical symmetry, *Phys. Lett. B*, **430** 1 (1998).

174. P. Petkov, A. Dewald, R.V. Jolos, In band M1 and E2 transition rates and collective structure in ^{128}Ba, *Nucl. Phys. A*, **640** 293 (1998).

175. L. Eβer, P. von Brentano, R.V. Jolos, Shell model calculations for ^{146}Gd and ^{147}Tb, *Nucl. Phys. A*, **650** 157 (1999).

176. A. Gelberg, F. Iachello, T. Otsuka, R.V. Jolos, Generation of irreducible representations in the O(6) limit of the IBM, *Prog. Theor. Phys.*, **101** 1261 (1999).

177. R.V. Jolos, P. von Brentano, Parity splitting in the alternating parity bands of some actinide nuclei, *Phys. Rev. C*, **60** 064317 (1999).

178. R.V. Jolos, P. von Brentano, Formal comparison of supersymmetry in the nuclear U(6/2) model and in quantum field theory, *Phys. Rev. C*, **60** 064317 (1999).

179. A.F. Lisetskiy, N. Pietralla, P. von Brentano, R.V. Jolos, Quasideutron configurations in odd-odd nuclei, *Phys. Rev. C*, **60** 064310 (1999).

180. L. Eβer, R.V. Jolos, F. Becker, P. von Brentano, Shell model calculations for ^{144}Sm and ^{145}Eu, *Nucl. Phys. A*, **672** 111 (2000).

181. R.V. Jolos, Yu. V. Palchikov, Relation between E2-transition probabilities for nuclei that are soft with respect to β–vibrations, *Phys. Atomic Nuclei*, **63** 570 (2000).

182. R.V. Jolos, Relation between signature splting in rotational bands of odd nuclei and the amplitude of the Ω=1/2 component, *Phys. Atomic Nuclei*, **63** 191 (2000).

183. I. Schneider, A.F. Lisetskiy, C. Friessner, R.V. Jolos et al., Low–spin structure of the $N = Z$ odd–odd nucleus $^{54}_{27}$Co$_{27}$, *Phys. Rev. C*, **61** 044312 (2000).

184. P. von Brentano, A.F. Lisetskiy, I. Schneider, R.V. Jolos et al., Low–spin structure of odd–odd $N = Z$ nuclei, *Prog. Pat. Nucl. Phys.*, **44** 29 (2000).

185. V. Werner, N. Pietralla, P. von Brentano, R.F. Casten, R.V. Jolos, Quadrupole shape invariants in the Interacting boson model, *Phys. Rev. C*, **61** 021301 (2000).

186. R.V. Jolos, P. von Brentano, U(1/2) supersymmetry without dynamical symmetry, *Phys. Rev. C*, **62** 034310 (2000).

187. A.K. Nasirov, A.I. Muminov, G.G. Adamian, R.V. Jolos, Effect of shell structure on energy dissipation in heavy–ion collisions, *Europ. Phys. J. A*, **8** 115 (2000).

188. A.F. Lisetskiy, P. von Brentano, R.V. Jolos et al., Shell model description of "mixed symmetry" states in ^{94}Mo, *Nucl. Phys. A*, **677** 100–114 (2000).

189. I. Schneider, A.F. Lisetskiy, C. Friessner, N. Pietralla, A. Schmidt, D. Weisshaar, P. von Brentano, R.V. Jolos, Low spin structure of the $N = Z$ odd–odd nucleus $^{54}_{27}$Co$_{27}$, *Phys. Rev. C*, **61** 044312 (2000).

190. R.V. Jolos, P. von Brentano, Partial supersymmetry in particle–rotor model, *Phys. Rev. C*, **63** 024304 (2001).

191. R.V. Jolos, Q–phonon scheme in the collective nuclear model, *Phys. Atomic. Nuclei*, **64** 520 (2001).

192. R.V. Jolos, Supersymmetry in nuclear structure, *Phys. Part. Nucl.*, **32** 113 (2001).

193. R.V. Jolos, Supersymmetry in some nuclear structure models, *Phys. Atomic Nuclei*, **64** 1203 (2001).

194. A.F. Lisetskiy, A. Gelberg, N. Pietralla, P. von Brentano, R.V. Jolos, Quasideutron states with deformed core, *Phys. Lett. B*, **512** 296 (2001).

195. A.F. Lisetskiy, C. Friessner, A. Schmidt, I. Schneider, N. Pietralla, P. von Brentano, R.V. Jolos, T. Otsuka, T. Sebe, Y. Utsuno, Toward isovector M1 transitions in odd–odd $N = Z$ nuclei, *Phys. Atomic. Nuclei*, **64** 1206 (2001).

196. Yu.V. Palchikov, J. Dobes, R.V. Jolos, $T = 0$ and $T = 1$ pairing and the formation of four-particle correlated structures in the ground states of $Z = N$ nuclei, *Phys. Rev. C*, **63** 034320 (2001).

197. A.F. Lisetskiy, C. Friessner, A. Schmidt, I. Schneider, N. Pietralla, P. von Brentano, R.V. Jolos, T. Otsuka, T. Sebe, Y. Utsuno, Approaching rotational collectivity in odd–odd $N = Z$ nuclei in pf–shell, *Prog. Part. Nucl. Phys.*, **46** 197 (2001).

198. V. Werner, P. von Brentano, R.V. Jolos, Simple relations among E2 matrix elements of low-lying collective states, *Physics Letters B*, **521** 146 (2001).

199. T. Klug, A. Dewald, R.V. Jolos, B. Saha, P. von Brentano, J. Jolie, Supersymmetry of identical bands in ^{171,172}Yb supported by lifetime data, *Physics Letters B*, **524** 252 (2002).

200. T.M. Shneidman, G.G. Adamian, N.V. Antonenko, R.V. Jolos, W. Scheid, Cluster interpretation of parity splitting in alternating parity bands, *Physics Letters B*, **526** 322 (2002).

DINUCLEAR SYSTEM PHENOMENA IN NUCLEAR REACTIONS AND IN NUCLEAR STRUCTURE

G.G.Adamian[1,2,3], N.V.Antonenko[1,3], S.P.Ivanova[1,3], A.K.Nasirov[1,2,3] and W.Scheid[3]
[1]*Joint Institute for Nuclear Research, 141980 Dubna, Russia*
[2]*Institute of Nuclear Physics, Tashkent, Uzbekistan*
[3]*Institut für Theoretische Physik der Justus-Liebig-Universität, D-35392 Giessen, Germany*

The dinuclear system model considers a configuration of two touching nuclei which exchange nucleons and/or clusters. Within this concept we explain deep inelastic collisions, fusion of heavy ions to superheavy nuclei and quasifission in collisions of heavy ions, study the production of angular momentum of fission fragments, describe hyperdeformed states formed in heavy ion reactions and interpret the parity splitting of rotational bands observed in the spectra of actinides.

I. INTRODUCTION

Reactions between heavy nuclei, the structure of nuclei and the structure of nuclei with cluster behaviour can be described with the dinuclear system concept [1,2]. A dinuclear system (DNS) is a configuration consisting of two touching nuclei which keep their individuality and exchange nucleons and/or clusters. Other notations for a dinuclear system are quasimolecular configurations, nuclear molecules and bi-cluster configurations. Well known examples with light nuclei are the ^{8}Be configuration built up by two touching α-particles and the nuclear molecular resonances [3] in the reactions ^{12}C on ^{12}C up to ^{58}Ni on ^{58}Ni. Also the fusion of heavy nuclei to superheavy nuclei can be explained by the dinuclear system concept [4]. In this case a dinuclear system is formed in the reaction between two heavy ions and then the touching nuclei exchange nucleons by transfer up to the moment the system crosses the inner fusion barrier and an excited compound nucleus is formed.

The important collective degrees of freedom of the dinuclear system are described by the relative internuclear distance R between the nuclear centers and by the mass asymmetry coordinate defined as $\eta = (A_1 - A_2)/(A_1 + A_2)$ where A_1 and A_2 are the mass numbers of the clusters. Here, $\eta = 0$ means a symmetric configuration ($A_1 = A_2$) and $\eta = \pm 1$ denotes the fused system (A_1 or $A_2 = 0$). The mass asymmetry degree of freedom was used to describe mass distributions in cold fission and to predict suitable target-projectile combinations for producing superheavy nuclei [5].

In this review, which is dedicated to Prof. R.V.Jolos on the occasion of his 60th birthday, we demonstrate the usefulness of the dinuclear system concept for the description of the fusion of heavy ions to superheavy nuclei, of the quasifission, of deep inelastic collisions (DIC), and of special cluster properties in the structure of heavy nuclei. In Section 2 we discuss the fusion of heavy nuclei and justify the DNS concept; in Section 3 we consider the quasifission; we describe the effect of the entrance channel in fusion reactions in Section 4 and investigate the kinetic energy dissipation in DIC in Section 5; in Section 6 we study the role of the bending mode in fission; in Section 7 we interpret hyperdeformed states as dinuclear resonance states and explain the properties of alternating bands in actinides with collective oscillations in the mass asymmetry coordinate.

II. FUSION OF HEAVY NUCLEI

The evaporation residue cross section is factorized as follows [2,4,6–8]

$$\sigma_{ER}(E_{\rm c.m.}) = \sigma_c(E_{\rm c.m.})P_{CN}(E_{\rm c.m.}, J=0)W_{sur}(E_{\rm c.m.}, J=0). \quad (1)$$

The calculations of the evaporation residue cross sections demand an analysis of all three factors in (1). The value of $\sigma_c = \pi\lambda^2(J_{max}+1)^2T(E_{\rm c.m.}, J=0)$ is the effective capture cross section for the transition of the colliding nuclei over the entrance (Coulomb) barrier with the probability T. The contributing angular momenta in the evaporation residue cross section are limited by the survival probability $W_{sur}(E_{\rm c.m.}, J)$ with $J_{max} \approx 10$ when highly fissionable superheavy nuclei are produced for energies $E_{\rm c.m.}$ near the Coulomb barrier. The probability of complete fusion P_{CN} in (1) depends on the competition between complete fusion in η and quasifission (decay of the DNS in R after the capture stage) [6–8].

A. Problems of adiabatic treatment of fusion

Models describing the fusion process as an internuclear melting of nuclei usually use adiabatic potential energy surfaces (PES). We apply the microscopic two-center shell model (TCSM) [3] with the following coordinates: elongation $\lambda = \ell/(2R_0)$, where ℓ is the length of the system and $2R_0$ the diameter of compound system, neck parameter ε with ε=0 showing no neck and $\varepsilon \approx 1$ showing necked-in shapes, mass asymmetry coordinate η and deformation parameters $\beta_i = a_i/b_i$ which are ratios of semiaxes of the clusters i=1 and 2. The adiabatic potential is obtained as

$$V_{ad}(\lambda, \varepsilon, \eta, \eta_z, \beta_i) = V_{LDM} + \delta U_{shell}, \quad (2)$$

where V_{LDM} is the liquid drop potential, δU_{shell} the shell correction part originating from the TCSM. In addition to the PES the masses $M_{q_iq_j} = M^{WW}_{q_iq_j}$ are calculated with the Werner-Wheeler (or hydrodynamic) approximation and the friction coefficients are found with the expression $\gamma_{q_iq_j} = \Gamma M_{q_iq_j}/\hbar$ (Γ is an average width of single particle states).

The fusion takes place with a scenario of the macroscopic dynamical model (including fluctuations): 1) By using the masses $M^{WW}_{q_iq_j}$, the neck fast grows after the nuclei touch each other and the united system falls into the fission-type valley in a short time of $(3-4)\times 10^{-22}$s. 2) The compound nucleus is formed due to the diffusion process to a smaller elongation λ (or relative distance R) in this valley. The necessary condition for the compound nucleus formation is that the fusing system passes inside the fission saddle point at $\lambda = \lambda_{sd}$.

In order to calculate the fusion probability we started from a value of $\lambda = \lambda_v$ in the fission valley obtained from the dynamical calculation of the descent into this valley. The fusion probability is determined by the leakage $\Lambda^{\lambda}_{fus}(t)$ through the barrier in λ which separates the strongly deformed configuration with an equilibrated large neck and the compound nucleus:

$$P_{CN} = \int_0^{t_0} \Lambda^{\lambda}_{fus}(t)dt, \quad (3)$$

where t_0 is the lifetime of the system and $\Lambda^{\lambda}_{fus} \sim \exp(-B^{\lambda}_{fus}/(k\Theta))$ (Kramers expression). Here, $B^{\lambda}_{fus} = V_{ad}(\lambda_{sd}) - V_{ad}(\lambda_v)$ is the barrier for fusion in λ and $k\Theta = \sqrt{12E^*/A}$ the local thermodynamic temperature with the excitation energy E^* of the system. For nearly symmetric reactions ^{100}Mo+^{100}Mo, ^{100}Mo+^{110}Pd, ^{110}Pd+^{110}Pd and others, the fusion probabilities in λ are much larger [6] than the values found from experimental data. While the experimental fusion probability decreases with mass asymmetry in the entrance channel [9], the calculated data give the opposite tendency (Fig. 1). Experimental evidence for a hindrance of fusion has been raised mainly by the impossibility to produce fermium evaporation residues with nearly symmetric projectile-target combinations. The adiabatic treatment of fusion in λ mostly gives the wrong dependence of the fusion probability on the isotope composition of the colliding nuclei [6]. The qualitative and quantitative contradictions obtained with the adiabatic scenario of the fusion point to the existence of an additional hindrance for the fast growth of the neck and the motion to smaller λ.

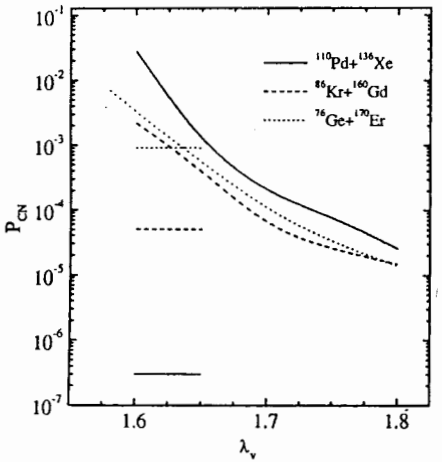

FIG. 1. Fusion probabilities depending on the starting value λ_v in the adiabatic PES for various reactions leading to the same compound nucleus ^{246}Fm. The values extracted from experimental data are given by horizontal lines

B. Reasons for a breakdown of adiabatic treatment

Microscopic inertia tensor

The hydrodynamical mass for the neck coordinate is small and allows to increase the neck of the DNS rapidly to a shape of a strongly deformed compound nucleus. However, crossings of single particle levels lead to a large inertia of the system which hinders the growth of the neck. Using the single-particle spectrum ϵ_α and wave functions $|\alpha>$ of both the adiabatic and diabatic TCSM [10], one can obtain the mass parameters with an extended cranking formula [6,11]

$$M^{cr}_{ij} = \hbar^2 \sum_{\alpha,\beta} \frac{<\alpha|\frac{\partial \hat{H}}{\partial q_i}|\beta><\beta|\frac{\partial \hat{H}}{\partial q_j}|\alpha>}{(\epsilon_\beta - \epsilon_\alpha)^2 + \frac{1}{4}(\Gamma_\beta + \Gamma_\alpha)^2} \frac{n_\alpha - n_\beta}{\epsilon_\beta - \epsilon_\alpha}, \qquad (4)$$

where Γ_α and Γ_β are the widths of the single particle states. The main contributions to M^{cr}_{ij} arise from the diagonal elements at $\epsilon_\beta \to \epsilon_\alpha$. Comparing our results with M^{WW}_{ij} obtained in the Werner-Wheeler approximation for a touching configuration with excitation energy 30 MeV (Θ=1.3 MeV), we find $M^{cr}_{\lambda\lambda} = M^{WW}_{\lambda\lambda}$, $M^{cr}_{\varepsilon\varepsilon} \approx$ (20-30)$M^{WW}_{\varepsilon\varepsilon}$ and $M^{cr}_{\lambda\varepsilon} \approx$ 0.4 $M^{WW}_{\lambda\varepsilon}$, practically independent of the mass number of the system [6,11]. As result we conclude that the initial neck coordinate is nearly kept fixed due to the large microscopical mass parameter for a time comparable with the reaction time. Since the mass of the neck degree of freedom is large, the neck parameter can be taken approximately fixed ($\varepsilon = 0.75$) during the fusion. As in the previous case, the adiabatic treatment of fusion in λ (at the fixed neck parameter) yields fusion probabilities P_{CN} which are considerably overestimated in comparison to the experimental data. The reason of this overestimate is clearly seen in Fig. 2. In contrast to experiment the hindrance of fusion in these potentials is practically absent ($P_{CN} \approx 1$) because there is no internal fusion barrier for the motion to smaller elongations. So, fusion probabilities will be considerably overestimated in any model of fusion in λ where only the neck parameter is taken fixed.

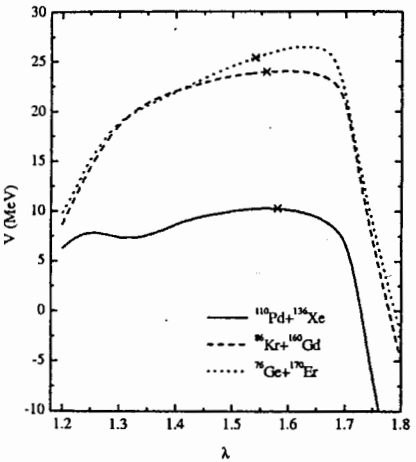

FIG. 2. Adiabatic potential in different reactions leading to ^{246}Fm as a function of λ for a fixed $\varepsilon = 0.75$. The crosses denote the touching configurations

Effect of structural forbiddenness of fusion in λ

Since the adiabatic PES (with and without fixed neck parameter) is not adequate for the description of fusion, we have to answer how fast is the transition between an initially diabatic (sudden or frozen density) and adiabatic regimes during the fusion process. The main question is the validity of the use of an adiabatic PES from the beginning of the fusion process.

a) Algebraic description. Let us first consider an algebraic description. After the formation of the DNS there is large structural forbiddenness effect for the motion to smaller elongations (melting) in the heavy cluster system [12]. This effect arises from the difference,created by the Pauli principle, between the compound state and the dinuclear cluster state. For the fusion channel $A_1 + A_2 \to A$, the wave function can be written

$$\Psi_{A_1+A_2} = \hat{A}_{as}\{\Psi_{A_1}\Psi_{A_2}\phi(R)\}, \qquad (5)$$

where Ψ_{A_i} are the cluster wave functions with the lowest oscillator quanta numbers N_{A_i} allowed by the Pauli principle, $\phi(R)$ the function of their relative motion along the collision axis z and $\hat{A}_{as}$ the operator of antisymmetrization. The minimal number of oscillator quanta $N_{A_1+A_2}$ of $\Psi_{A_1+A_2}$ is determined by application of the SU(3) group theory. The cluster wave function $\Psi_{A_1+A_2}$ and the compound nucleus wave function Ψ_A belong to different SU(3) (or Sp(2,R) for deformed nuclei A_1 and A_2) representations. We have to construct the U(3) irreducible representation $[f_x f_y f_z]$ for $\Psi_{A_1+A_2}$ which possesses the minimal sum $f_x + f_y + f_z$ and does not vanish with antisymmetrization. The proper procedure for the construction of the vector of highest weight of this representation is the use of the vector of highest weight for the wave function of the relative motion and the vectors of lowest weights for the wave functions of the fragments which possess the maximal value of the sum $f_x^{(1)} + f_y^{(1)} + f_x^{(2)} + f_y^{(2)}$ (upper index denotes the fragment). The resulting $N_{A_1+A_2}$ value turns out to be essentially larger than N_A if the mass of the lighter fragment is rather large. Therefore, we obtained the generalization of the Talmi-Moshinsky rule for heavy ion physics. The minimal difference $q = N_{A_1+A_2} - N_A$ is referred to the degree of structural forbiddenness for the fusion channel $A_1 + A_2 \to A$. The wave function $\Psi_{A_1+A_2}$ of the DNS has a nonvanishing overlap integral with the wave function Ψ_A of the compound nucleus if $N_{A_1+A_2} \geq N_A + q$.

The forbiddenness effect is model-independent and the SU(3) approach is only a simple method to determine it. With the pole-to-pole orientation of the DNS consisting of deformed nuclei, the values of q are larger than those of the DNS with spherical nuclei. The quantity $B^{\lambda}_{fus} = \hbar\omega q$ ($\hbar\omega = 41\mathrm{MeV}A^{-1/3}$) is a qualitative estimate of the minimal energy thresholds for the fusion in the relative distance degree of freedom at fixed mass asymmetry η.

Table 1. Experimental and calculated minimal values of the energy thresholds ΔE_{min}, at which fusion is possible, are compared with the degree q of forbiddenness and B^{λ}_{fus} (see text)

System	ΔE_{min} (MeV) exp. [9]	ΔE_{min} (MeV) DNS model [8,12,13]	q	B^{λ}_{fus} (MeV)
^{40}Ar+^{206}Pb	-0.5±3	0	16	105
^{76}Ge+^{170}Er	10±5	8	22	144
^{86}Kr+^{160}Gd	≥15.7	11.5	20	131
^{110}Pd+^{136}Xe	≥23.5	15	26	170
^{96}Zr+^{124}Sn	6.5±3	5	28	183
^{90}Zr+^{90}Zr	0.0	0.0	30	196
^{100}Mo+^{100}Mo	7.2	6.0	30	196
^{110}Pd+^{110}Pd		12.0	30	196

If the excitation energy of the system is much smaller than the value of B^{λ}_{fus}, the fusion in λ is strongly forbidden. The dependence of q on η is not monotonic, the q-value is maximal for almost symmetric combinations and decreases with increasing η. For very asymmetric combinations, the structural forbiddeness practically disappears. The structural forbiddenness in the λ-channel is weakened by the coupling between cluster channels with different mass asymmetries. Since the absolute values of q (or B^{λ}_{fus}) are large

for not very asymmetric DNS, there is a strong hindrance for the evolution of these DNS to smaller λ due to the large energy barrier between the initial DNS and the compound shapes (Table 1) [12].

b) Dynamical diabatic description. It is important to study whether the system has time for destroying the "memory" on the structural forbiddenness and reorganizing the density of the system for the transition from the sudden or diabatic potential $V_{di}(\lambda)$ to the adiabatic potential $V_{ad}(\lambda)$ [14]:

$$V(\lambda,t) = V_{di}(\lambda)\exp(-\int_0^t \frac{dt}{\tau(\lambda,t)}) + V_{ad}(\lambda)[1-\exp(-\int_0^t \frac{dt}{\tau(\lambda,t)})]. \quad (6)$$

The diabatic potential can be written

$$V_{di}(\lambda,\varepsilon) = V_{ad}(\lambda,\varepsilon) + \delta V_{di}(\lambda,\varepsilon), \quad (7)$$

where $\delta V_{di} = \sum_\alpha \epsilon_\alpha^{di} n_\alpha^{di} - \sum_\alpha \epsilon_\alpha^{ad} n_\alpha^{ad}$. Here, ϵ_α^{di}, ϵ_α^{ad} and n_α^{di}, n_α^{ad} are the single-particle energies and occupation numbers of the diabatic and adiabatic levels, respectively. The initial occupation probabilities n_α^{di} are determined by the configuration of the separated nuclei. They depend on time since the excited diabatic levels get deexcited:

$$\frac{dn_\alpha^{di}(\lambda,\varepsilon,t)}{dt} = -\frac{1}{\tau(\lambda,\varepsilon,t)}(n_\alpha^{di}(\lambda,\varepsilon,t) - n_\alpha^{ad}(\lambda,\varepsilon)), \quad (8)$$

where τ is a relaxation time determined by a mean single particle width depending on the diabatic occupation numbers, $\tau(\lambda,\varepsilon,t) = 2\hbar\sum_\alpha n_\alpha^{di}/\sum_\alpha n_\alpha^{di}\Gamma_\alpha$.

Diabatic potentials show a strong increase with decreasing elongation λ. The dynamical diabatic potential $V(\lambda,t)$ is the relevant tool to measure the structural forbiddenness. Their repulsive character screens smaller values of the elongation and hinders the DNS to melt into the compound nucleus. Fig. 3 shows the diabatic potential for the system ^{110}Pd+^{110}Pd as a function of the elongation λ for the initial time and the lifetime t_0 of the DNS. The decay process in λ determines the lifetime $t_0 \approx 10^{-20}$ of the DNS which mainly depends on the quasifission barrier B^{λ}_{qf}.

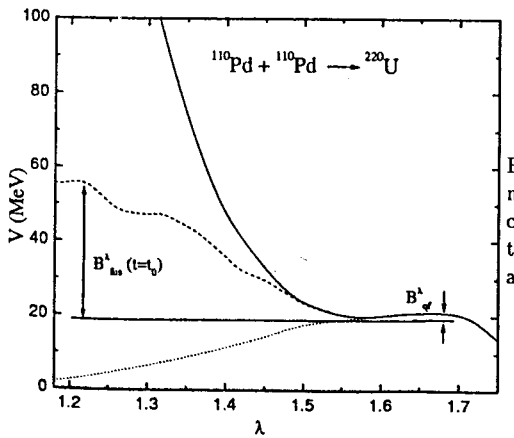

FIG. 3. The diabatic ($t = 0$) and final ($t = t_0$) potentials (solid and dashed curves, respectively) and the adiabatic potential (dotted curve) for ^{110}Pd+^{110}Pd as a function of λ

The dynamical diabatic potential at the the lifetime t_0 of the initial DNS (Fig. 4) has a very large fusion barrier in λ and, correspondingly, the fusion probability in λ is negligible for combinations leading to ^{246}Fm. It should be noted that these dynamical potentials were calculated by using the smallest possible relaxation time for the transition between diabatic and adiabatic potentials [11,14]. The calculated energy thresholds for the complete fusion in the λ- and η-channels lead to the conclusion that the DNS evolution to the compound nucleus proceeds in the mass asymmetry degree of freedom. For example, the average fusion barriers B_η^{fus} in mass asymmetry are about 10, 12 and 15 MeV for the reactions ^{76}Ge+^{170}Er (η=0.4), ^{86}Kr+^{160}Gd (η=0.3) and ^{110}Pd+^{136}Xe (η=0.1), respectively [8]. The fusion barrier B_λ^{fus} in λ is about 3–4 times larger than the fusion barrier B_η^{fus} in mass asymmetry. As shown in Fig. 5, the fusion probability P_{CN} in η strongly increases with mass asymmetry in the entrance channel. The same behaviour was experimentally established [9]. For the reactions ^{40}Ar+^{206}Pb and ^{76}Ge+^{170}Er, the values of P_{CN} in η are in good agreement with experimental data from evaporation residue cross sections.

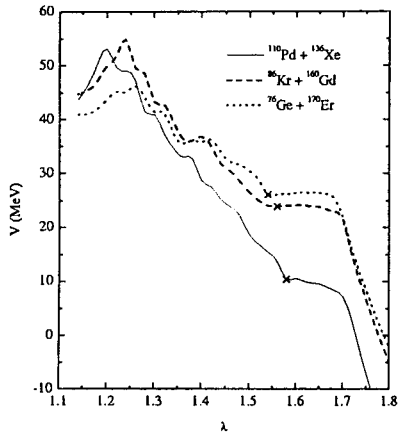

FIG. 4. Dynamical diabatic potential. The notations are the same as in Fig. 2

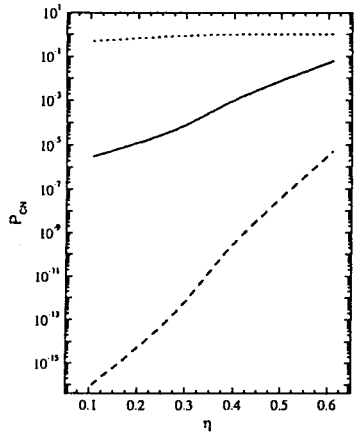

FIG. 5. Fusion probability P_{CN} in the reactions leading to ^{246}Fm with excitation energy 30 MeV as a function of the mass asymmetry in the entrance channel. The result of the adiabatic treatment of the fusion in λ is presented by the dotted line. The upper limit of the fusion probability in λ in the dynamical diabatic treatment is presented by the dashed line. The fusion probability in the η channel with a closed fusion channel in λ is presented by the solid line

In compound systems heavier than ^{246}Fm the difference between the fusion barriers and fusion probabilities in both λ- and η- channels is even larger [14]. Our analysis with

the diabatic dynamics demonstrates that a structural forbiddenness exists for a direct motion of the nuclei to smaller internuclear distances during the fusion process. Fusion of heavy nuclei along the internuclear distance in the coordinates R or λ is practically impossible. These facts strongly support our standpoint that the correct model of fusion of heavy nuclei is the dinuclear system model where fusion is described by the transfer of nucleons, i.e., by a motion in η.

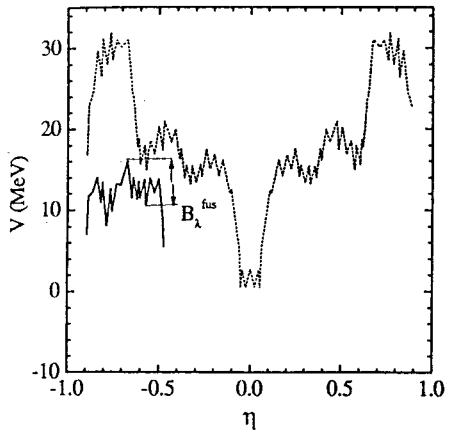

FIG. 6. Driving potential of the dinuclear system in the ^{54}Cr + ^{208}Pb $\rightarrow$ ^{262}Sg reaction as a function of η for $L = 0$. The dotted curve is calculated for spherical shapes of the nuclei, the solid curve for deformed shapes in pole-to-pole orientations. Experimental binding energies are used

C. Fusion to superheavy nuclei

Fusion probability P_{CN}

After the system is captured in a dinuclear configuration, the relative kinetic energy is transferred into potential and excitation energy. The dinuclear system develops in time by diffusion in the mass asymmetry coordinate and in the relative coordinate (a decay of the DNS). The fusion probability P_{CN} gives the probability that the dinuclear system crosses the inner fusion barrier B_η^{fus} in η and forms the compound nucleus. This probability can be calculated by solving a diffusion equation in the coordinates η and R with approximations [7,8]. The probability P_{CN} depends on the competition between complete fusion in η and quasifission (decay of the DNS in R) [8] and is expressed as follows

$$P_{CN} = \frac{\lambda_\eta^{Kr}}{\lambda_R^{Kr}+\lambda_\eta^{Kr}} - \frac{\lambda_\eta^{Kr}\lambda_R^{Kr}}{\lambda_R^{Kr}+\lambda_\eta^{Kr}}\frac{\tau_\eta-\tau_R}{1.72}. \qquad (9)$$

The second term in (9) is related to the transient times τ_R and τ_η to reach the quasi-stationary rates along the R and η coordinates ($\tau_R^{-1}, \tau_\eta^{-1} > \lambda_R^{Kr}, \lambda_\eta^{Kr}$). In the case that the fusion barrier is much higher than the quasifission barrier, $B_\eta^{fus} \gg B_{qf}$, i.e. if the transient time τ_η in η is larger (or equal) than the lifetime t_0 of the initial DNS, we obtain [4,7,8] $P_{CN} = \frac{\lambda_\eta^{Kr}}{1.72}[\tau_\eta(\exp[t_0/\tau_\eta]-1)-t_0]$. For very shallow quasifisson barriers ($B_{qf} \approx 0$) in reactions with large $Z_1 \times Z_2$, the value of P_{CN} in this expression is smaller than the one in the quasi-stationary regime, given by Eq. (9), which can not be reached due to the small value of t_0.

As in Ref. [8] for the quasi-stationary rates of fusion λ_η^{Kr} and quasifission λ_R^{Kr} through the fusion barrier ($B_\eta = B_\eta^{fus}$) in η and quasifission barrier ($B_R = B_{qf}$) in R, respectively, we use a two-dimensional Kramers-type expression

$$\lambda_k^{Kr} = \frac{1}{2\pi}\frac{\omega_k\omega_{\bar{k}}}{\omega_R^{B_k}\omega_\eta^{B_k}}\left(\sqrt{\left[\frac{\Gamma}{2\hbar}\right]^2 + (\omega_k^{B_k})^2} - \frac{\Gamma}{2\hbar}\right)^{1/2} \exp\left[-\frac{B_k}{(k\Theta)}\right]. \qquad (10)$$

The frequencies $\omega_k^{B_i}$ $(k, i = R, \eta)$ are calculated in the harmonic oscillators approximation of the potential in the variables R and η around the tops of the barriers B_η^{fus} and B_{qf}, and ω_k, $\omega_{\bar{k}}$ $(k \neq \bar{k})$ are the frequencies of the harmonic oscillators approximating the potential of the initial DNS. Since the oscillator approximation of the potential energy surface is suitable for the reactions considered, we neglect the nondiagonal components of the curvature tensor in (10). As was shown in [4,7,8], the friction coefficients obtained with $\Gamma = 2$ MeV have the same order of magnitude as the ones calculated within other approaches. B_η^{fus} is the barrier with respect to the potential $V(\eta_i, R_t)$ of the entrance dinuclear configuration with the initial mass fragmentation η_i at the touching radius R_t. The height of this barrier is strongly influenced by shell and deformation effects as shown in Fig. 6.

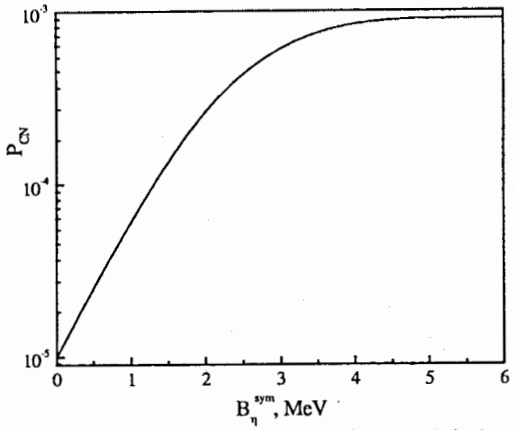

FIG. 7. Fusion probability for the reaction ^{54}Cr+^{208}Pb→^{262}Sg as a function of the barrier height B_η^{sym} in the η-coordinate. This barrier is assumed beside the lead minimum in the potential energy surface in the direction to more symmetric cluster configurations. A realistic value is $B_\eta^{sym} \approx$ 4MeV

The minima in the potential $V(\eta, R = R_t)$ give a sensitive effect on the fusion probability and can be used in selecting optimum target and projectile combinations for producing superheavy elements. This idea goes back to Sandulescu *et al* [15,16] who argued that the nuclei can fuse with higher probabilities along the valleys in an adiabatic potential in the R-coordinate and point to the experimentally successful choice of target-projectile combinations with the Pb-nucleus as target as proof for their hypothesis. The potential at the touching distance of two nuclei is an adiabatic-type potential and naturally shows the same structure of minima as the potential energy surface of Sandulescu *et al* [15,16]. We interpret these minima as follows: A certain initial system in a minimum is hindered by the barrier of the potential in η to change fast to a more symmetric system. A more symmetric system has a much smaller probability of fusion and a much higher probability for quasifission because of the larger Coulomb repulsion which leads to a dissolution of the DNS. Therefore, an asymmetric dinuclear system in a potential minimum has a

longer lifetime with respect to its decay by quasifission than outside of a minimum and hence a larger chance to fuse by diffusion via nucleon transfer into the compound nucleus. This point is clarified by an example for the reaction ^{54}Cr+^{208}Pb → ^{262}Sg. In Fig. 7 we show the calculated fusion probability as a function of the height B_η^{sym} of an assumed barrier in η beside the lead minimum in the direction to a more symmetric cluster configuration of the system. One recognizes that the fusion probability increases over two orders of magnitude with growing barrier height B_η^{sym} up to a saturation value. The latter value is reached when B_η^{sym} is equal to the quasifission barrier B_{qf} which is 2.7 MeV for ^{54}Cr+^{208}Pb. Then the fusion probability can no more rise because the initial system directly decays by quasifission.

Survival probability W_{sur}

The compound system is formed in an excited state and mainly decays by fission. If only one neutron is emitted, the survival probability is roughly the ratio

$$W_{sur}(1 \text{ neutron emission}) \sim \frac{\Gamma_n}{\Gamma_f}, \qquad (11)$$

where Γ_n is the neutron emission width and Γ_f the fission width. The widths and the probability are obtained with a statistical model [14] and vary moderately with the shell structure of the compound nucleus between 10^{-4} and 10^{-2} for lead-based fusion with the evaporation of one neutron as shown in Fig. 8.

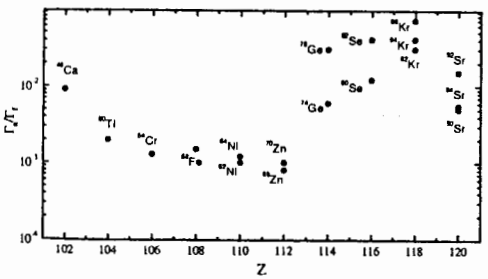

FIG. 8. Calculated Γ_n/Γ_f values for the neutron-evaporation in the fusion reactions ^AZ + ^{208}Pb. The calculations with Fermi-gas model were done for $J = 0$ using the code GROGIF [17]

Results for lead (bismuth) - based reactions ^AZ + ^{208}Pb (^{209}Bi)→ superheavy nucleus + 1n

a) Optimal excitation energies: To get the largest cross section for producing a compound nucleus by fusion, one has to choose an incident energy which is sufficiently high that the system is able to cross the inner fusion barrier B_η^{fus}. Since the potential $V(\eta, R)$ counts the energy above the ground state energy of the compound nucleus, the optimal, i.e., smallest excitation energy of the compound nucleus is given by

$$E_{CN}^* = V(\eta_i, R_t) + B_\eta^{fus}. \qquad (12)$$

In Fig. 9 we compare calculated optimal excitation energies with the experimental ones. The calculated values depend sensitively on the deformation effects.

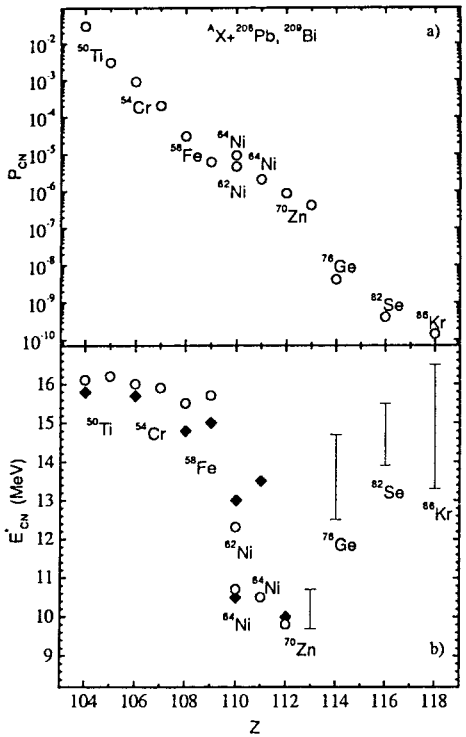

FIG. 9. a) Calculated fusion probabilities P_{CN} for cold fusion in (HI,1n) reactions for the projectiles indicated (open circles). For the compound nuclei with Z=104-112, the calculations were performed with Q-values from Ref. [18]. b) Optimal excitation energies of the compound nuclei. For the nuclei with Z=113,114,116 and 118, the lower and upper limits of bars were calculated with Q-values from Ref. [18] and Ref. [19], respectively. The experimental data [20] are shown by solid diamonds

b) Capture cross section, fusion probability, survival probability and evaporation cross section: In Table 2 we list the capture cross section, fusion probability, survival probability and evaporation cross section for selected reactions (see Ref. [4] for further reactions). Whereas the capture cross section is nearly constant, the fusion probability is exponentially decreasing with increasing projectile mass (Fig. 9). The reason for this strong decrease is that the mass asymmetry of the initial DNS gets smaller with growing projectile mass which means an increase of the inner fusion barrier B_{η}^{fus} and, therefore, an exponential decrease of P_{CN} according to Eq.(9). Since the variation of the survival probability is moderate, the evaporation cross section drops from nb over pb to fb because of the exponential decrease of P_{CN}. The calculated evaporation residue cross sections agree with the experimental data in about a factor of 2 as shown in Fig. 10.

In Pb-based reactions with neutron-rich nuclei ^{70,74,78}Ni, ^{80}Zn,^{86}Ge and ^{92}Se a decrease of P_{CN} can be compensated by W_{sur} increasing with the number of neutrons (Fig. 11). For example, in the ^{62}Ni+^{208}Pb reaction the yield of the Z=110 element is comparable with the yields in the ^{70,74}Ni+^{208}Pb reactions. The calculated values of P_{CN} in the cold fusion reactions are maximal when the neutron number of the projectile is a magic number [4]. As follows from our model, intensive beams of neutron-rich nuclei will be useful for producing heavy actinides, for example Fm as listed in Table 2. In the Pb-based reactions the use of neutron-rich projectiles leads to values of σ_{ER} comparable with evaporation residue cross sections for reactions with stable projectiles.

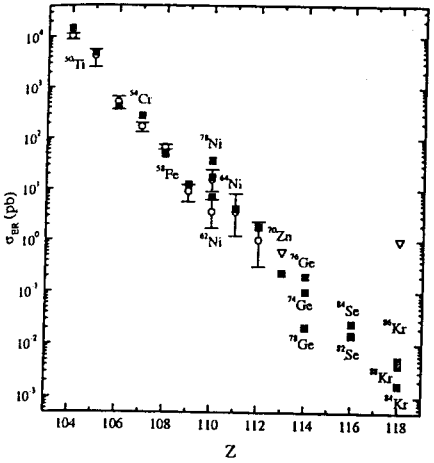

FIG. 10. Evaporation residue cross sections for ^{208}Pb- and ^{209}Bi-based fusion. The full squares and the open circles are calculated and experimental data [20], respectively. The open triangles give experimental upper limits (GSI)

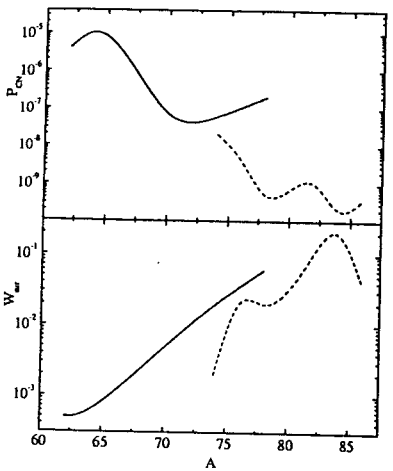

FIG. 11. Fusion (P_{CN}) and survival (W_{sur}) probabilities as functions of mass number A of the projectile in reactions ^{A}Ni+^{208}Pb (solid lines) and ^{A}Ge+^{208}Pb (dashed lines)

Results for actinide - based reactions

The actinide-based fusion reactions ^{48}Ca + ^{238}U, ^{242,244}Pu and ^{248}Cm were used at JINR in Dubna to synthesize the elements 112, 114 and 116 [21]. The theoretical and experimental evaporation residue cross sections with the emission of 3 and 4 neutrons are of the order of 1pb. Table 3 shows the various cross sections and probabilities for reactions with ^{48}Ca. Since in these reactions the DNS are more asymmetric then in the lead-based reactions, the fusion probability is larger. However, the survival probability is diminished because the compound nucleus has an excitation energy of about 30–35 MeV and, therefore, 3 to 4 neutrons have to be emitted to reach the ground state.

Table 2. Excitation energy, probabilities and cross sections for selected reactions

Reaction	E^*_{CN} (MeV)	σ_{cap} (mb)	P_{CN}	W_{sur}	σ^{th}_{1n}	σ^{exp}_{1n}
^{66}Zn+^{174}Yb→^{238}Fm+2n	26.0	9.6	4×10^{-2}	8×10^{-7}	0.3 nb	
^{76}Zn+^{174}Yb→^{248}Fm+2n	23.0	8.8	2×10^{-3}	6×10^{-4}	10.6 nb	
^{76}Ge+^{170}Er→^{244}Fm+2n	24.6	8.4	5×10^{-4}	3×10^{-4}	1.3 nb	$1.6^{+1.3}_{-1.6}$ nb
^{62}Ni+^{208}Pb→^{269}110+1n	12.3	3.5	4.5×10^{-6}	5×10^{-4}	7 pb	$3.5^{+2.7}_{-1.8}$ pb
^{64}Ni+^{208}Pb→^{271}110+1n	10.7	3.4	1×10^{-5}	5×10^{-4}	17 pb	15^{+9}_{-6} pb
^{70}Ni+^{208}Pb→^{277}110+1n	13.5	3.1	7×10^{-8}	5×10^{-3}	1.1 pb	
^{74}Ni+^{208}Pb→^{281}110+1n	15.0	3.0	6×10^{-8}	2×10^{-2}	3.6 pb	
^{78}Ni+^{208}Pb→^{284}110+2n	17.5	3.0	2×10^{-7}	6×10^{-2}	36 pb	
^{64}Ni+^{209}Bi→^{272}111+1n	10.5	3.4	2×10^{-6}	6×10^{-4}	4.1 pb	$3.5^{+4.6}_{-2.3}$ pb

Table 3. Calculated evaporation residue cross sections in the actinide-based reactions leading to the nuclei with Z =110, 112, 114, 116 and 118 are compared with available experimental data [21]

Reaction	E^*_{CN} (MeV)	xn	σ_{xn}	σ^{exp}_{xn}
^{48}Ca+^{232}Th	32	3n	1.4 pb	$2^{+4.6}_{-1.7}$ pb
^{48}Ca+^{238}U	33	3n	1.7 pb	5^{+6}_{-3} pb
^{48}Ca+^{244}Pu	35.5	4n	1.0 pb	$\sim$ 1 pb
^{48}Ca+^{242}Pu	32	3n	1.0 pb	$2.5^{+3.3}_{-1.6}$ pb
^{48}Ca+^{248}Cm	32	3n	0.2 pb	
^{48}Ca+^{248}Cm	35	4n	0.2 pb	$\sim$ 0.5 pb
^{48}Ca+^{249}Cf	30	3n	0.02 pb	

III. QUASIFISSION

A. Mass and charge distributions

Quasifission means no formation of a compound nucleus but the decay of the dinuclear system over the quasifission barrier B_{qf}. The time-development of the dinuclear system includes the transfer of nucleons changing the mass asymmetry coordinate and the quasifission described by the internuclear coordinate [22]. Both processes are strongly coupled and have to be treated simultaneously. We use master equations in order to calculate the probability $P_{Z,A}(t)$ for finding the dinuclear system at time t in a configuration where the

light fragment-nucleus has charge and mass numbers $Z_1 = Z$ and $A_1 = A$, respectively, and the heavy fragment-nucleus $Z_2 = Z_{total} - Z$ and $A_2 = A_{total} - A$.

$$\begin{aligned}\frac{dP_{Z,A}(t)}{dt} &= \Delta^{(-,0)}_{Z+1,A+1}P_{Z+1,A+1}(t) + \Delta^{(+,0)}_{Z-1,A-1}P_{Z-1,A-1}(t) \\ &+ \Delta^{(0,-)}_{Z,A+1}P_{Z,A+1}(t) + \Delta^{(0,+)}_{Z,A-1}P_{Z,A-1}(t) \\ &- (\Delta^{(-,0)}_{Z,A} + \Delta^{(+,0)}_{Z,A} + \Delta^{(0,-)}_{Z,A} + \Delta^{(0,+)}_{Z,A} + \Lambda^{qf}_{Z,A})P_{Z,A}(t). \qquad (13)\end{aligned}$$

Here, the transport coefficients $\Delta^{(\pm,0)}_{Z,A}$ and $\Delta^{(0,\pm)}_{Z,A}$ are probability rates for transfer of a proton and neutron, respectively, and $\Lambda^{qf}_{Z,A}$ the decay rate in the coordinate R for quasifission. The transfer rates are calculated microscopically, the decay rate is approximated by the Kramers rate which is proportional to $\exp(-B_{qf}/(k\Theta))$. The measurable charge and mass yields for quasifission are obtained from

$$Y_{Z,A}(t_0) = \Lambda^{qf}_{Z,A}\int_0^{t_0} P_{Z,A}(t)dt, \qquad (14)$$

where the reaction time t_0 is determined by solving the equation

$$\sum_{Z,A}\Lambda^{qf}_{Z,A}\int_0^{t_0} P_{Z,A}(t)dt = 1 - P_{CN}. \qquad (15)$$

Fig. 12 shows the mass yield as a function of the mass number of the light fragment for the hot fusion reaction ^{48}Ca + ^{244}Pu → ^{292}114 in comparison with experimental data [23]. We note that near the initial masses, the quasifission events overlap with the products of deep inelastic collisions and were taken out in the experimental analysis since they are difficult to discriminate from the deep inelastic events. Maxima in the mass yield arise from minima in the driving potential which are caused by shell effects in the dinuclear system.

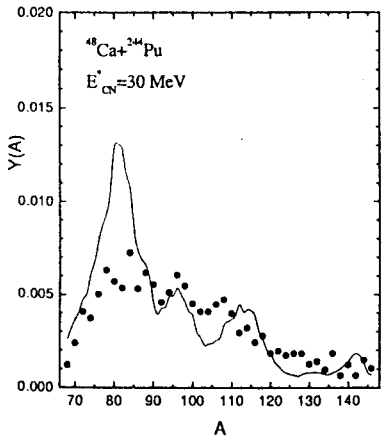

FIG. 12. Mass yield $Y(A) = \sum_Z Y_{Z,A}(t_0)$ of the quasifission products as a function of A of the light fragment for the hot fusion reaction ^{48}Ca+^{244}Pu →^{292}114 at a bombarding energy 230 MeV corresponding to an excitation energy of the compound nucleus of 30 MeV. The experimental data [23] are shown by solid points

B. Total kinetic energy distribution

In order to calculate the average total kinetic energy (TKE) of the quasifission products and its dispersion, one has to regard the deformation of the fragments in addition. The distribution of the fragments in charge, mass and deformation can be written as

$$P = P(Z_1, A_1, \beta_1, Z_2, A_2, \beta_2) = Y_{Z_1,A_1}(t_0) P_{\beta_1}(Z_1, A_1) P_{\beta_2}(Z_2, A_2). \quad (16)$$

Here, $P_\beta(Z, A)$ is a distribution in deformation at fixed values of Z and A. It can be taken as

$$P_\beta(Z, A) = \frac{1}{\sqrt{2\pi\sigma_\beta^2}} \exp(-(\beta - <\beta>)^2/(2\sigma_\beta^2)) \quad (17)$$

with $\sigma_\beta^2 = \frac{\hbar\omega_{vib}}{2C_{vib}} \coth(\hbar\omega_{vib}/(2k\Theta))$, where $\omega_{vib}(Z, A)$ and $C_{vib}(Z, A)$ are the frequency and stiffness parameter of quadrupole vibrations, respectively, and $\Theta(Z, A)$ is the temperature of the dinuclear system. Applying the distribution (16) we calculate the average total kinetic energy as a function of the mass number A_1 of light fragment:

$$< TKE(A_1) >= \int\int d\beta_1 d\beta_2 \sum_{Z_1} TKE \cdot P / (\int\int d\beta_1 d\beta_2 \sum_{Z_1} P)$$
$$\approx \sum_{Z_1} TKE|_{\beta_i = <\beta_i>} Y_{Z_1,A_1}(t_0) / \sum_{Z_1} Y_{Z_1,A_1}(t_0), \quad (18)$$

with $TKE = V_{nucl}(R_b) + V_{Coul}(R_b)$, where the radius $R_b = R_b(Z_1, A_1, \beta_1, Z_2, A_2, \beta_2)$ is the position of the Coulomb barrier. The variance of TKE can be written as a sum of the contributions of variances from the exchange of nucleons and from the deformations:

$$\sigma_{TKE}^2(A_1) \approx \sum_{Z_1} TKE^2|_{\beta_i = <\beta_i>} Y_{Z_1,A_1}(t_0) / \sum_{Z_1} Y_{Z_1,A_1}(t_0) - < TKE(A_1) >^2$$
$$+ (\sigma_{TKE}^{def}(A_1))^2_{\text{light nucleus 1}} + (\sigma_{TKE}^{def}(A_1))^2_{\text{heavy nucleus 2}}, \quad (19)$$

where

$$(\sigma_{TKE}^{def}(A_1))_j^2 = \sum_{Z_1} \left(\frac{\partial TKE}{\partial \beta_j} \right)^2 \Bigg|_{\substack{\beta_1 = <\beta_1> \\ \beta_2 = <\beta_2>}} \sigma_{\beta_j}^2 Y_{Z_1,A_1}(t_0) / \sum_{Z_1} Y_{Z_1,A_1}(t_0). \quad (20)$$

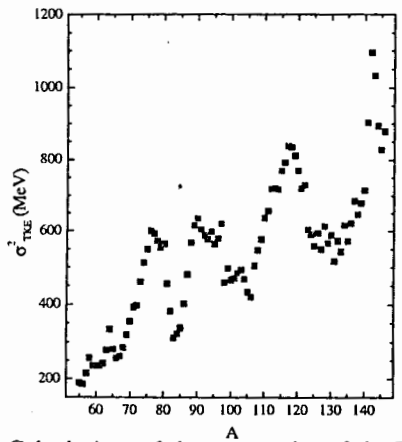

FIG. 13. Calculated variance of the total kinetic energy of quasifission products in the reaction ^{48}Ca+^{244}Pu as a function of the mass number of light fragment. The incident energy 230 MeV corresponds to an excitation energy of 30 MeV of the compound nucleus

Calculations of the mean value of the TKE yield $< TKE > = 260$ MeV of quasifission products for $A = A_1 = 146 \pm 20$ in the reaction ^{48}Ca + ^{244}Pu at an incident energy 230

MeV which corresponds to an excitation energy of the compound nucleus of 30 MeV. Fig. 13 shows the variance of the TKE as a function of the mass number $A = A_1$ of the light fragment. The minima in σ_{TKE}^2 appear at mass numbers where one of the fragments is a very stable nucleus, namely Pb, Zr and Sn. The ratio between both kinds of contributions to the variance, $r(A_1) = (\sigma_{TKE}^{exchange})^2/(\sigma_{TKE}^{def})^2$, is in the same reaction $r(76) = 30/570$, $r(110) = 27/610$ and $r(144) = 1/893$, which shows the high importance of the fluctuations in the deformation for the variance of the TKE. Further investigations and comparison with experimental data are presently carried out.

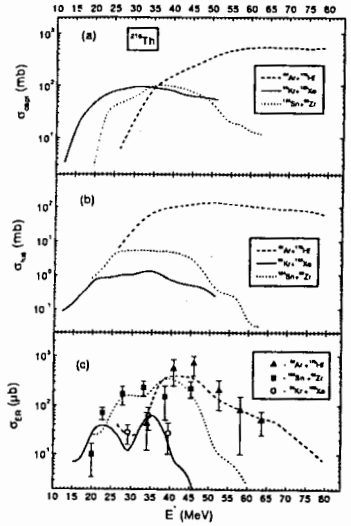

FIG. 14. Comparison of the calculated capture (a) and fusion excitation function (b) as well as calculated total excitation functions of evaporation residues with the experimental data (c) for the ^{40}Ar+^{176}Hf [25], ^{124}Sn + ^{92}Zr [27], and ^{86}Kr + ^{130}Xe [24] reactions leading to ^{216}Th

IV. EFFECT OF ENTRANCE CHANNEL IN COMPLETE FUSION REACTIONS

Differences between fusion excitation functions of reactions leading to the same compound nucleus allow us to analyze the effect of the shell structure on the fusion mechanism. Experimental data [24–27] reveal that the maximum value of the evaporation residue (ER) cross sections in the ^{40}Ar+^{176}Hf (I) reaction is twelve times larger than in the ^{86}Kr + ^{130}Xe (II) reaction and three times larger than in the ^{124}Sn + ^{92}Zr (III) reaction. Since the ^{40}Ar+^{176}Hf reaction has the largest initial charge asymmetry ($\eta_Z = (Z_2 - Z_1)/(Z_1 + Z_2)$) in comparison with the two other reactions (II,III), the height of the inner fusion barrier (B_η^{fus}) is smaller than those in (II,III). The excitation functions for capture and fusion calculated within the DNS model [28] for these reactions are presented in Fig. 14. The calculated excitation functions of the ER are in good agreement with the experimental data. Taking into account the deformation effects in the calculation of the DNS potential energy as a function of η or η_Z, one can explain that the maximum value of the ER cross section for ^{124}Sn + ^{92}Zr is four times larger than for ^{86}Kr + ^{130}Xe at nearly the same value of E_{CN}^*.

The ER cross section in the ^{86}Kr + ^{136}Xe reaction is about 500 times larger than in reaction (II) (Fig. 15c). This result is related to the two characteristics of the fusion-fission mechanism. First, the fusion cross section calculated with the approach given in Ref. [28] is larger for the reaction ^{86}Kr+^{136}Xe than that for ^{86}Kr+^{130}Xe (Fig. 15b). Second, the survival probability [29] of ^{222}Th is larger than the one of ^{216}Th because the fission barrier is larger for the isotope $A = 222$ than for the isotope $A = 216$ and the neutron separation energy of ^{222}Th (S_n = 7.808 MeV) is smaller than that of ^{216}Th (S_n = 8.701 MeV). Therefore, the Γ_n/Γ_f ratio is larger for ^{222}Th than for ^{216}Th.

V. DEEP INELASTIC COLLISIONS

Dissipation of a large amount of the kinetic energy in deep inelastic heavy ion collisions (DIC) is a fundamental time-dependent process [30–37] that has attracted theoretical interest since the discovery of this class of reactions. At an earlier stage of investigations it was assumed that the excitation energy is distributed between reaction partners in proportion to their masses. However, after a series of experiments, it became clear that a large part of the excitation energy is concentrated in the light fragments for a wide range of total kinetic energy losses. Various models have been proposed to explain this phenomenon, taking into account the coupling of the relative motion to intrinsic degrees of freedom. The simple macroscopic models with phenomenological friction forces can not be used to treat this problem. The important aspect of the description of the nucleon transfer and kinetic energy dissipation is connected with an influence of the peculiarities of the shell structure of the interacting nuclei on the correlations between the kinetic energy loss and the width of the fragment charge distribution. Indeed, it was demonstrated by analysing experimental data of different reactions that these correlations are sensitive to the projectile–target combination.

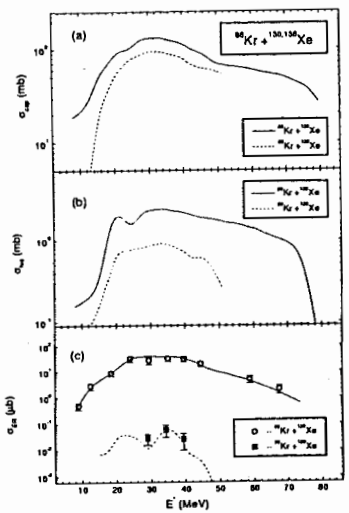

FIG. 15. Comparison of the calculated capture (a), fusion (b) and evaporation residue (c) excitation functions as well as the measured excitation functions of evaporation residue cross section (c) for the ^{86}Kr + ^{136}Xe (solid curve, open circles) [24] and ^{86}Kr + ^{130}Xe (dashed curve, solid squares) [24] reactions

The present microscopical model is based on the assumption that the colliding nuclei

moving approximately along the classical trajectories conserve mainly their individual properties at the kinetic energies under consideration. Each nucleus is described by nucleons captured in a potential well (Woods-Saxon potential). During the interaction time both potential wells act on the nucleons in each nucleus causing transitions of nucleons between single-particle states. The transitions taking place in every nucleus are particle-hole excitations while those occurring between partner-nuclei are nucleon exchanges. Thus, in the proposed model the single-particle mechanism is considered as the main mechanism of excitation and dissipation. Although easily excited surface vibrations can contribute to the dissipation, the adiabaticity of the relative motion with respect to these vibrations decreases their effect.

The total Hamiltonian of a dinuclear system $\hat{H}$ is taken in the form

$$\hat{H} = \hat{H}_{rel} + \hat{H}_{in} + \hat{V}_{int} \tag{21}$$

The Hamiltonian $\hat{H}_{rel} = \hat{\mathbf{P}}^2/2\mu + U(\hat{\mathbf{R}})$ of the relative motion in R consists of the kinetic energy and the nucleus-nucleus interaction potential $U(\hat{\mathbf{R}})$. The last two terms in (21) describe the intrinsic motion of nuclei and the coupling between the relative and intrinsic motions. Employing the Ehrenfest theorem it is easy to obtain the classical limit of equations of motion in the collective variable $\mathbf{R}$ from (21):

$$\dot{\mathbf{R}} = \nabla_P(H_{rel} + < t|\hat{V}_{int}|t >), \tag{22}$$

$$\dot{\mathbf{P}} = -\nabla_R(H_{rel} + < t|\hat{V}_{int}|t >), \tag{23}$$

where $< t|...|t >$ means an average over the intrinsic state at the time t. It is clear that the relative motion of the nuclei additionally depends on the nonconservative and nonstationary coupling potential $< t|\dot{\hat{V}}_{int}|t >$ which can be calculated by solving the equation of motion for the single-particle density matrix $\hat{n}$.

The single-particle basis is constructed from the asymptotic single-particle state vectors of noninteracting nuclei: for projectile $"P"$ $|P >$ and target $"T"$ $|T >$ in the form $|\tilde{P} >= |P > -\frac{1}{2}\sum_T |T >< T|P >$, $|\tilde{T} >= |T > -\frac{1}{2}\sum_P |P >< P|T >$. The orthogonality condition for the given basis is fulfilled up to the second order of the overlapping integral $< P|T >$.

The single-particle Hamiltonian of a dinuclear system $\hat{\mathcal{H}}$ is as follows

$$\hat{\mathcal{H}}(\mathbf{R}(t)) = \sum_{i=1}^{A}\left(\frac{-\hbar^2}{2m}\Delta_i + \hat{U}_P(\mathbf{r}_i - \mathbf{R}(t)) + \hat{U}_T(\mathbf{r}_i)\right), \tag{24}$$

where m is the nucleon mass, $A = A_P + A_T$ is the total number of nucleons in the system. The average single-particle potentials of projectile U_P and target U_T include both the nuclear and Coulomb fields.

In the second quantization form the Hamiltonian (24) can be rewritten as

$$\begin{aligned}
&\hat{\mathcal{H}}(\mathbf{R}(t)) = \hat{H}_{in}(\mathbf{R}(t)) + \hat{V}_{int}(\mathbf{R}(t)),\\
&\hat{H}_{in}(\mathbf{R}(t)) = \sum_i \tilde{\varepsilon}_i(\mathbf{R}(t))\mathrm{a}_i^+\mathrm{a}_i = \sum_P \tilde{\varepsilon}_P(\mathbf{R}(t))\mathrm{a}_P^+\mathrm{a}_P + \sum_T \tilde{\varepsilon}_T(\mathbf{R}(t))\mathrm{a}_T^+\mathrm{a}_T,\\
&\hat{V}_{int}(\mathbf{R}(t)) = \sum_{i\neq i'} V_{ii'}(\mathbf{R}(t))\mathrm{a}_i^+\mathrm{a}_{i'}\\
&= \sum_{P\neq P'} \chi^{(T)}_{PP'}(\mathbf{R}(t))\mathrm{a}_P^+\mathrm{a}_{P'} + \sum_{T\neq T'} \chi^{(P)}_{TT'}(\mathbf{R}(t))\mathrm{a}_T^+\mathrm{a}_{T'} + \sum_{T,P} \mathrm{g}_{PT}(\mathbf{R}(t))(\mathrm{a}_P^+\mathrm{a}_T + \mathrm{a}_T^+\mathrm{a}_P).
\end{aligned} \tag{25}$$

Up to the second order in $< P|T > \tilde{\varepsilon}_P(\mathbf{R}(t)) = \varepsilon_P + < P|U_T(\mathbf{r})|P >$, $\tilde{\varepsilon}_T(\mathbf{R}(t)) = \varepsilon_T + < T|U_P(\mathbf{r}-\mathbf{R}(t))|T >$, $\chi^{(T)}_{PP'}(\mathbf{R}(t)) = < P|U_T(\mathbf{r})|P' >$, $\chi^{(P)}_{TT'}(\mathbf{R}(t)) = < T|U_P(\mathbf{r}\text{-}\mathbf{R}(t))|T' >$, $g_{PT}(\mathbf{R}(t)) = \frac{1}{2} < P|U_P(\mathbf{r}\text{-}\mathbf{R}(t)) + U_T(\mathbf{r})|T >$. Here, $\varepsilon_{P(T)}$ are single-particle energies of nonperturbed states in the projectile (target) nucleus. These states are characterized by the set of quantum numbers $P \equiv (n_P, j_P, l_P, m_P)$ and $T \equiv (n_T, j_T, l_T, m_T)$. The diagonal matrix elements $< P|U_T|P >$ and $< T|U_P|T >$ determine the shifts of the single-particle energies of the projectile nucleus caused by the target mean field. The corresponding nondiagonal matrix elements $\chi^{(T)}_{PP'}$ and $\chi^{(P)}_{TT'}$ generate particle-hole transitions in the same nucleus. The matrix elements g_{PT} induce the nucleon exchange between the reaction partners due to the nonstationary mean field of the dinuclear system. The contributions of noninertial recoil effects to the matrix elements are neglected since they are small.

Since a residual interaction requires extensive calculations, it is customary to take the two-particle collision integral into account in a linearized form (τ-approximation) in the equation for the single-particle density matrix:

$$i\hbar\frac{\partial\hat{n}(t)}{\partial t} = [\hat{\mathcal{H}}, \hat{n}(t)] - \frac{i\hbar}{\tau}[\hat{n}(t) - \hat{n}^{eq}(\mathbf{R}(t))], \tag{26}$$

where τ is the relaxation time, $n^{eq}(\mathbf{R}(t))$ is a local quasi-equilibrium density matrix at fixed value of $\mathbf{R}(t)$ which is determined by the excitation energy of each nucleus.

The present model allows us to calculate the average number of protons $< Z_{P(T)} > = \sum_{P(T)}^{Z} n_{P(T)}(t)$ or neutrons $< N_{P(T)} > = \sum_{P(T)}^{N} n_{P(T)}(t)$, their variances $\sigma^2_{Z(N)} = \sum_{P}^{Z(N)} n_P(t)[1 - n_P(t)]$ and to determine the intrinsic excitation energies $E^*_{P(T)}(t) = \sum_{P(T)}[\varepsilon_{P(T)}(\mathbf{R}(t)) - \varepsilon_{F_P(F_T)}(\mathbf{R}(t))][n_{P(T)}(t)]$, for every nucleus. Here, $\varepsilon_{F_P(F_T)}(\mathbf{R}(t))$ is the Fermi energy of a projectile-like nucleus "P" or target-like nucleus "T". The top index $Z(N)$ at the sums restricts the summation over the proton(neutron) single-particle levels.

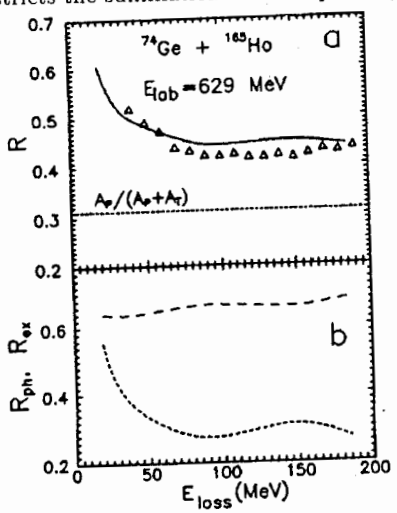

FIG. 16. a) Ratio R_P of the projectile-like fragment excitation energy (E^*_P) to the total excitation energy for the reaction ^{74}Ge(629 MeV) + ^{165}Ho as a function of the total excitation energy $E_{loss} = E^*_P + E^*_T$. Triangles mark the experimental data. Solid line presents the theoretical result of our model. Dotted line corresponds to thermal equilibrium ($E^*_P/E_{loss} = A_P/(A_P + A_T)$).
b) Calculated ratios $R^{(ex)}_P = E^{*(ex)}_P/(E^{*(ex)}_P + E^{*(ex)}_T)$, $R^{(ph)}_P = E^{*(ph)}_P/(E^{*(ph)}_P + E^{*(ph)}_T)$ as a function of E_{loss} are presented by long-dashed and short-dashed lines, respectively

The model described is capable to explain both the multinucleon transfer data (the values of charge (mass) drift and variances of charge (mass) distributions) and the distribution of the excitation energy between the primary fragments in DIC for a wide range

of total energy losses (Figs. 16–18). The results obtained show that a redistribution of the excitation energy takes place during the whole interaction time, not only at the initial stage. Nucleon exchange, particularly, neutron exchange is a dominant mechanism of energy dissipation. However, for the heavy DNS ($A_{P,T} > 100$) the $p-h$ excitation energies $E^{*(ph)}_{P,T}$ become equally important as the nucleon exchange energies $E^{*(ex)}_{P,T}$. Influence of the shell structure of the interacting nuclei on the nucleon transfer and the partition of excitation energy is significant. The density of the single-particle levels of the proton and neutron subsystems near the Fermi surface determines the ratio between the excitation energies of the products of the collision. The shell structure strongly influences the correlations between the width of the charge distributions and the total kinetic energy losses.

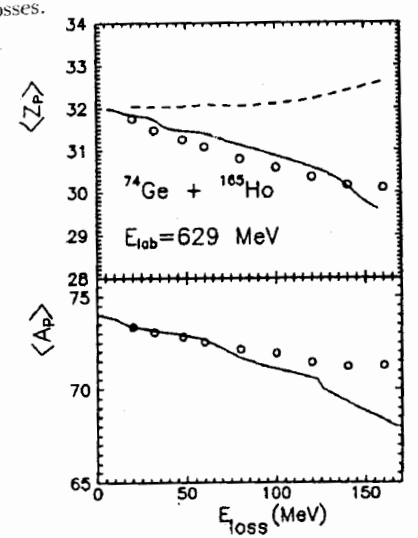

FIG. 17. Centroids of the Z_P, A_P distributions for projectile-like fragments of the reaction ^{74}Ge(629 MeV) + ^{165}Ho as a function of the total excitation energy E_{loss}. Circles give the primary values [38], dashed lines present results of the nucleon exchange transport model [39] and solid lines are predictions of the primary distributions with our model

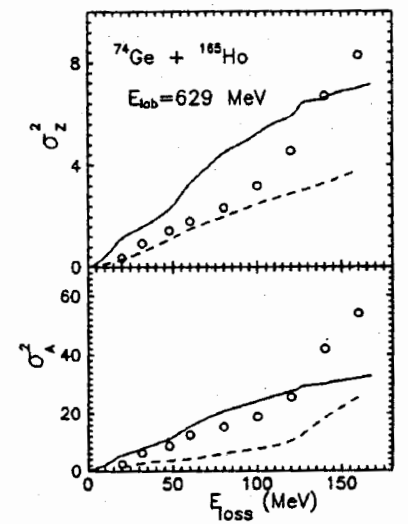

FIG. 18. Variances of the Z_P, A_P distributions for projectile-like fragments of the reaction ^{74}Ge(629 MeV) + ^{165}Ho as a function of energy loss E_{loss}. Symbols are the same as in Fig. 17

VI. APPLICATION TO FISSION

At the scission point, a fissioning system can be approximately considered as a DNS whose intrinsic degrees of freedom are in thermal equilibrium. However, the shape of the DNS is not equilibrated. We assume [40] that the angular momenta of fission fragments are generated by small bending vibrations of DNS nuclei around the pole-to-pole orientation. This model [40] describes quite well the measured angular momenta of fission fragments as a function of the total number of evaporated neutrons ν for the fragmentation Mo+Ba of ^{252}Cf [41] as shown in Fig. 19. The DNS excitation was estimated for the standard fission mode by assuming a small deformation energy of the nuclei.

For $\nu > 5$, the calculated values of the angular momenta of the fragments, obtained by neglecting a possible formation of an alpha particle chain in the neck, deviate from the experimental ones. However, the higher values of the neutron multiplicity are connected to the second mode of fission which could have a different cluster composition which is more complicated than that of the DNS. The system ^{102}Zr+^{4}He+^{4}He+^{142}Xe which supplies the experimental TKE is assumed for the second fission mode. The calculation for this mode is done for $\nu \geq 8$ by assuming a rigid coupling between the alpha particles and heavy nuclei. The calculations for the cluster configuration give a better agreement with the experimental data for $\nu \geq 8$ than the calculations with the DNS used for the standard fission mode.

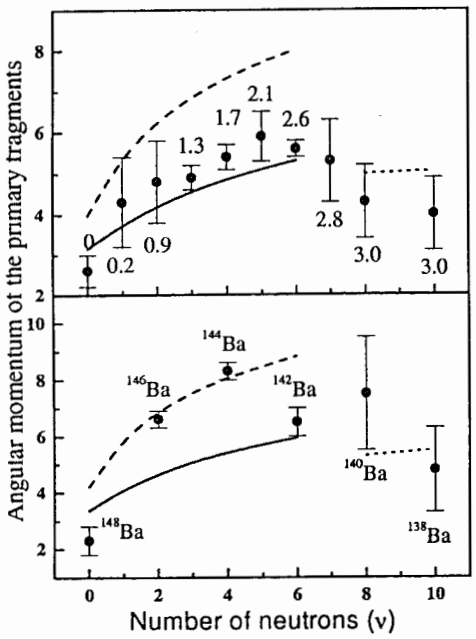

FIG. 19. Calculated and experimental [41] (solid circles) angular momentum (unit $\hbar$) of fission fragments as a function of the total number of evaporated neutrons ν. The secondary fragment pairs involve ^{104}Mo with different Ba isotopes. The numbers in the upper figure are the adjusted numbers of emitted neutrons from the primary Mo fragments. The calculations for the first fission mode performed with experimental and rigid body moments of inertia are shown by solid and dashed lines, respectively. The calculations for the second fission mode performed with experimental moments of inertia are shown by the short-dashed lines

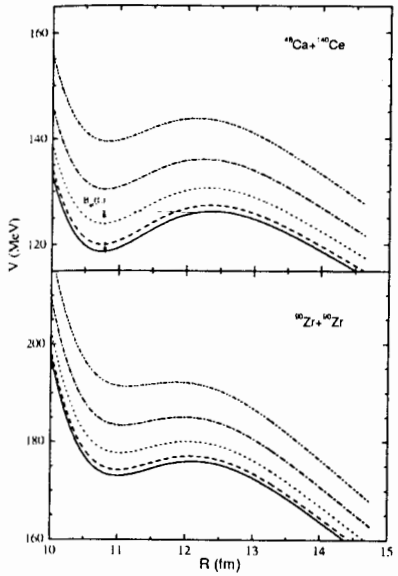

FIG. 20. The potential $V(R, L)$ for the systems ^{48}Ca + ^{140}Ce and ^{90}Zr + ^{90}Zr as a function of R for $L = 0, 20, 40, 60, 80\hbar$ presented by solid, dashed, dotted, dashed-dotted, dashed-dotted-dotted curves, respectively

VII. APPLICATION TO NUCLEAR STRUCTURE

Dinuclear configurations are also important for the explanation of special nuclear structure effects. In this section we report on states of the dinuclear system in the relative and mass asymmetry motions and therewith explain hyperdeformed states and the parity splitting in alternating parity bands of actinides.

A. Hyperdeformed nuclei as dinuclear configurations

Hyperdeformed (HD) nuclei are usually assumed as strongly deformed nuclear systems with an ratio of axes of about 3 : 1. For such large ratios a neck could be formed and a dinuclear configuration could be thought. Under the assumption that HD states can be explained as states with a dinuclear configuration, we consider their direct formation in collisions of heavier nuclei [42]. As example we choose the reactions ^{48}Ca + ^{140}Ce and ^{90}Zr + ^{90}Zr.

The potential for dinuclear configurations has a depression around the touching distance as shown in Fig. 20 in which quasi-bound states are situated. In the examples of Fig. 20 we find one to three quasi-bound states with $\hbar\omega \approx 2.2$ MeV for angular momenta $L > 40\hbar$. The escape width through the fission barrier is about 10 eV. The absolute energy values at $L = 0$, the quadrupole moments of (70 - 80)$\times 10^2$ efm^2 and moments of inertia (160-190) $\hbar^2$/MeV of these dinuclear configurations are close to those estimated for HD states. Quasi-bound states are also known in reactions of light heavy ions, e.g. in the ^{12}C + ^{12}C reaction, where they show up as quasimolecular resonances.

We propose to form HD states with heavy ion reactions in which quasi-bound states are occupied [42]. In order that this can happen, the DNS must be formed nearly cold which

means that the nuclei are captured into a quasi-bound state via a quantum tunneling through the potential barrier. The target and projectile nuclei should be magic or double magic, i.e. they should be stiff against nucleon transfer which has as consequence that the potential energy is in a minimum with respect to the mass asymmetry coordinate. The quasi-bound dinuclear state can decay by γ-transitions to energetically deeper dinuclear states, i.e. HD states, with lower angular momenta in coincidence with fragments of the DNS decay. The lifetime against DNS decay is of the order of 10^{-16}s.

Optimum conditions for the considered reactions are

^{48}Ca + ^{140}Ce:	$E_{c.m.} = 147$ MeV,	$90\hbar < L < 100\hbar$,
^{90}Zr + ^{90}Zr:	$E_{c.m.} = 180$ MeV,	$40\hbar < L < 50\hbar$.

The estimated cross section for the formation of a HD nucleus is about 1 μb.

Heavy ion experiments with coincidences of γ-rays and quasifission could verify whether the cluster interpretation is suitable for hyperdeformed nuclear states. In principle, this means the search of nuclear molecular resonances in heavier systems.

B. Parity splitting in alternating parity bands of actinides

The actinide isotopes of Ra, Th and U have a ground state band with positive parity and a related first excited band with negative parity. In comparison with the positive parity states the negative parity states are shifted which is denoted as parity splitting. This parity splitting is characterized by two quantities: the energy of parity splitting at the beginning of the bands and the critical spin value when the effect vanishes. The parity splitting can be explained by octupole vibrations superimposed on the rotation spectrum of a quadrupole-deformed intrinsic shape. Here, we apply the dinuclear model for the description of the parity splitting [43].

Calculating the binding energy of the dinuclear system for the actinide nuclei Ra, Th and U, we find an alpha-cluster configuration mixed to the ground state wave function:

$$^{A}Z \rightarrow ^{(A-4)}(Z-2) + \alpha.$$

The united (compound) system has an higher binding energy than the alpha-cluster configuration. The potential is schematically depicted as a function of the mass asymmetry coordinate in Fig. 21, where also the reflection-asymmetric shapes of the alpha-cluster configuration are shown. The mass asymmetry coordinates of the later configurations are $\eta_\alpha = \pm(1 - 8/A)$. The deformation parameters of the dinuclear ground-state shape of ^{226}Ra are $\beta_2 = 0.17$ and $\beta_3 = 0.09$ in agreement with the measured octupole deformation of $\beta_3 \approx 0.1$.

According to quantum mechanics the dinuclear system oscillates in the potential $V(\eta)$ (see Fig. 21), which is a two-center potential in the coordinate $x = \eta - 1$ for $\eta > 0$ and $x = \eta + 1$ for $\eta < 0$. The ground state in this potential is split in a lower positive parity state and a higher negative parity state where the difference in energies (splitting) decreases with an increase of the barrier at $\eta = 1$ ($x = 0$). This splitting is interpreted as the parity splitting observed in experiment. With increasing nuclear spin I the splitting approaches zero because the moment of inertia in the rotational energy $V_{rot} = \hbar^2 I(I+1)/(2J(\eta, R))$

which is added to the potential $V(\eta)$ lets increase the barrier at $\eta = 0$ with increasing nuclear spin.

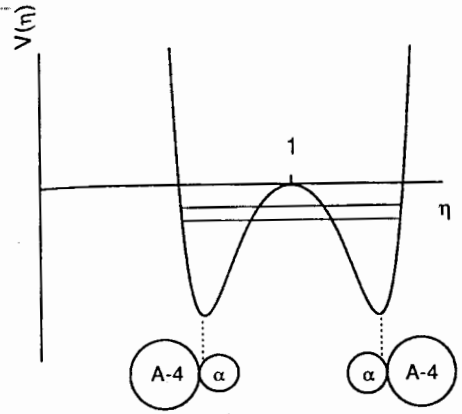

FIG. 21. Schematic picture of the potential in the mass asymmetry and of the two states with different parities (parallel lines, lower state with positive parity, higher state with negative parity)

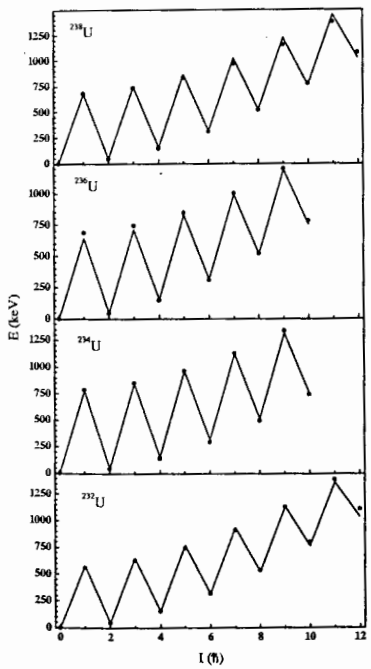

FIG. 22. Experimental (points) and theoretical rotational spectra for ^{238,236,234,232}U

For the application of this model to the spectra of the isotopes of the actinides Ra,

Th and U, we calculated the eigenvalues of the Hamiltonian

$$H = -\frac{\hbar^2}{2M_\eta}\frac{d^2}{dx^2} + \sum_{k=1}^{4} a_{2k}(I)(x^{2k} - x_\alpha^{2k}), \tag{27}$$

where M_η are chosen as a constant mass for all the considered nuclei: $M_\eta = 20 \times 10^4 m$ fm^2. The parameters $a_{2k}(I)$ are obtained by fitting the calculated potential values for $|\eta| = 1$, $|\eta_\alpha| = 1 - 8/A$ and $|\eta_{Li}| = 1 - 14/A$. Fig. 22 shows the results for U - isotopes in comparison with experimental data. Similar agreement with the experimental spectrum is found for the isotopes of Ra and Th [43].

VIII. SUMMARY AND CONCLUSIONS

The dinuclear system concept assumes two touching nuclei which can exchange nucleons by transfer. In this concept one describes the fusion of heavy nuclei to superheavy nuclei, the competing quasifission, fission and nuclear structure phenomena connected with cluster structures. The dynamics of the dinuclear system has essentially two degrees of freedom: the mass asymmetry degree of freedom and the relative motion of the nuclei.

The fusion is described by nucleon transfer between touching nuclei. The potential energy surface is diabatic and forbids a direct melting of the nuclei. The transfer process proceeds by diffusion. Available experimental data for fusion and quasifission of superheavy systems formed in lead- and actinide-based reactions can be well reproduced. This large set of data gives a strong experimental support for the usefulness of the dinuclear system concept.

HD nuclear states and the parity splitting observed in the spectra of actinides are explainable by clusters within the dinuclear model. In heavier nuclei HD states are interpreted as dinuclear resonance states which can be formed in heavy ion reactions. These configurations have very similar properties as the well-known quasimolecular resonances in light heavy ion systems, e.g. in the $^{12}C + ^{12}C$ system.

The properties of alternating parity bands in actinides can be described with collective oscillations in the mass asymmetry. The octupole-deformed reflection-asymmetric shapes near the ground state are thought as dinuclear configurations with a large component of an alpha-cluster configuration.

The fusion and quasifission proceed at excitation energies and level densities of the dinuclear states where statistical methods can be used. The nuclear structure phenomena are explainable by selected states of the dinuclear system, quasi-bound or bound states in the relative and mass asymmetry coordinates, respectively. So, the dinuclear system concept has a large variety of applications to heavy ion scattering, fission and bound nuclear systems, and is astonishing which large part of nuclear structure physics and dynamics can be described within this model. Future experimental and theoretical studies will settle down further details of the basic principles of this concept.

ACKNOWLEDGEMENTS

Large parts of the presented results were obtained in collaboration with Prof. R.V. Jolos. We are very thankful to him for his exciting ideas and contributions. We also thank our collaborators Profs. G. Giardina, A.I. Muminov, Yu.M. Tchuvil'sky and V.V. Volkov, Drs. E.A. Cherepanov, A. Diaz-Torres and N. Nenoff, and Mr. T.M. Shneidman. Further we thank Profs. W. Greiner, S. Hofmann, G. Münzenberg, J. Peter, A. Sobiczewski, Drs. H. Hofmann and Yu.V. Palchikov for fruitful discussions and suggestions. This work was supported by DFG, RFBR, BMBF, DAAD, Humboldt- and VW-Stiftung, and STCU.

[1] V.V. Volkov, *Izv.AN SSSR ser.fiz.* **50**, 1879 (1986).

[2] N.V. Antonenko, E.A. Cherepanov, A.K. Nasirov, V.B. Permjakov, V.V. Volkov, *Phys. Lett.* B **319**, 425 (1993); *Phys. Rev.* C **51** 2635 (1995).

[3] W. Greiner, J.Y. Park, W. Scheid, *Nuclear Molecules* (World Scientific, Singpore, 1995).

[4] G.G. Adamian, N.V. Antonenko, W. Scheid, *Nucl. Phys.* A **678**, 24 (2000).

[5] J. Maruhn, W. Greiner, W. Scheid, in *Heavy Ion Collisions*, Vol. 2, ed. R. Bock (North Holland Publ. Comp., Amsterdam, 1980) p. 399.

[6] G.G. Adamian, N.V. Antonenko, S.P. Ivanova, W. Scheid, *Nucl. Phys.* A **646**, 29 (1999).

[7] G.G. Adamian, N.V. Antonenko, W. Scheid, *Nucl. Phys.* A **618**, 176 (1997).

[8] G.G. Adamian, N.V. Antonenko, W. Scheid, V.V. Volkov, *Nucl. Phys.* A **627**, 361 (1997).

[9] H. Gäggeler *et al.*, *Z. Phys.* A **316**, 291 (1984).

[10] A. Diaz-Torres, N.V. Antonenko, W. Scheid, *Nucl. Phys.* A **652**, 61 (1999).

[11] G.G. Adamian, N.V. Antonenko, A. Diaz-Torres, W. Scheid, *Nucl. Phys.* A **671**, 233 (2000).

[12] G.G. Adamian, N.V. Antonenko, Yu.M. Tchuvil'sky, *Phys. Lett.* B **451**, 289 (1999).

[13] R.V. Jolos, A.K. Nasirov, A.I. Muminov, *Eur. Phys. J.* B **4**, 245 (1999).

[14] A. Diaz-Torres, G.G. Adamian, N.V. Antonenko, W. Scheid, *Phys. Lett.* B **481**, 228 (2000).

[15] A. Sandulescu, R.K. Gupta, W. Scheid, W. Greiner, *Phys. Lett.* B **60**, 225 (1976).

[16] W. Greiner, *Nuov. Cim.* **110A**, 1237 (1997).

[17] G.G. Adamian, N.V. Antonenko, S.P. Ivanova, W. Scheid, *Phys. Rev.* C **62**, 064303 (2000).

[18] P. Möller, R. Nix, *At. Data Nucl. Data Tables* **39**, 213 (1988).

[19] P. Möller *et al.*, *At. Data Nucl. Data Tables* **59**, 185 (1995).

[20] S. Hofmann, G.Münzenberg, *Rev. Mod. Phys.* **72**, 733 (2000).

[21] Yu.Ts. Oganessian, M.G. Itkis, A.G. Popeko, V.K. Utyonkov, A.V. Yeremin, *Nucl. Phys.* A **682**, 108c (2001).

[22] A. Diaz-Torres, G.G. Adamian, N.V. Antonenko, W. Scheid, *Phys. Rev.* C **64**, 024604 (2001).

[23] M.G. Itkis *et al.*, *Proc. 7th Int. Conf. on Clustering Aspects of Nuclear Structure and Dynamics* (Rab, Croatia, 1999), ed. M. Korolija, Z. Basrak, R. Caplar (World Scientific, Singapore, 2000) p.386; *preprint JINR*, E15-99-248 (1999).

[24] Yu.Ts. Oganessian *et al.*, *JINR FLNR Scientific Report 1995–1996. Heavy Ion Physics*, B.I. Pustylnik ed., p. 62 (JINR, E7-97-206, Dubna) (1997).

[25] D. Vermeulen *et al.*, *Z. Phys.* A **318**, 157 (1984).

[26] H.-G. Clerc *et al.*, *Nucl.Phys.* A **419**, 571 (1984).

[27] C.-C. Sahm *et al.*, *Nucl.Phys.* A **441**, 316 (1985).

[28] G. Giardina, S. Hofmann, A.I. Muminov, A.K. Nasirov, *Eur. Phys. J.* A **8**, 205 (2000).

[29] A. D'Arrigo *et al.*, *J. Phys.* G **20**, 365 (1994).

[30] V.V. Volkov, *Nuclear Reactions of Deep Inelastic Transfers* (Energoizdat, Moscow, 1982).

[31] W.U. Schröder and J.R. Huizenga, in *Treatise on Heavy-Ion Science*, ed. D.A. Bromley, v. 2 (Plenum Press, New York, 1984) p.115.

[32] G.G. Adamian, A.K. Nasirov, N.V. Antonenko, R.V. Jolos, Phys. Part. Nucl. **25**, 583 (1994).

[33] G.G. Adamian, R.V. Jolos, A.K.Nasirov, *Phys. Rev.* C **53**, 871 (1996).

[34] G.G. Adamian, R.V. Jolos, A.I. Muminov, A.K. Nasirov, *Phys. Rev.* C **56**, 171 (1997).

[35] G.G. Adamian, R.V. Jolos, A.K. Nasirov, *Physics of Atomic Nuclei* **55**, 366 (1992).

[36] G.G. Adamian, N.V. Antonenko, R.V. Jolos, A.K. Nasirov, *Nucl. Phys.* A **551**, 321 (1993).

[37] G.G. Adamian, R.V. Jolos, A.K. Nasirov, *Z. Phys.* A **347**, 203 (1994).

[38] J. Toke *et al.*, *Phys. Rev.* C **44**, 390 (1991).

[39] J. Randrup, *Nucl. Phys.* A **307**, 319 (1978); *Nucl. Phys.* A **327**, 490 (1979).

[40] T.M. Shneidman *et al.*, *Physics of Atomic Nuclei* (in print).

[41] G.S. Popeko *et al.*, *Proc. Int. Conf. Fission and Properties of neutron-rich nuclei*, ed. J. H. Hamilton and G. S. Ramayya (World Scientific, 1998) p.645.

[42] G.G. Adamian, N.V. Antonenko, N. Nenoff, W. Scheid, *Phys. Rev.* C **64**, 014306 (2001).

[43] T.M. Shneidman *et al. Phys. Lett.* B (in print).

Q-phonons and Q-invariants

P. von Brentano, N. Pietralla, and V. Werner

Institut für Kernphysik, Universität zu Köln, 50937 Köln, Germany

T. Otsuka

Department of Physics, University of Tokyo, Hongo, Tokyo 113-0033, Japan

(Dated: November 27, 2001)

The paper discusses the concept of Q-invariants and its connection to the Q-phonon scheme and the shape parameters of nuclei. It will also discuss the simple relations among Q-invariants, many of them discovered in seminal work by R.V. Jolos.

PACS numbers: 21.60.Fw, 21.60.Ev, 21.10.Re
Keywords: Collective states, Q-phonons and Q-invariants, shape parameters

I. INTRODUCTION

This paper is dedicated to the scientific work of Professor R.V.Jolos on the occasion of his sixtieth birthday. We had the pleasure to work with him on many projects. On this occasion we remember many fruitful discussions and the discussion of science is very much at the heart of science.

The paper will discuss the concept of Q-invariants and its connection to the Q-phonon scheme and the shape parameters. It will also discuss the simple relations among the Q-invariants, many of them discovered in seminal work by R.V. Jolos. These relations allow one to determine crucial nuclear observables, like the quadrupole moment, $Q(2_1^+)$, in future measurements with rare isotopes beams.

After a brief survey over collective models we will introduce the concept of Q-phonon excitations. The Q-phonons serve as a basis to the concept of Q-invariants that lead us to the dimensionless K-invariants, K_n. These K-invariants serve as a suitable generalization to the shape parameters beta and gamma, which work only for rigid rotors. Finally we discuss the determination of the K-invariants from accessible observables and simple relations among these observables, which were proposed by Prof. Jolos.

The low lying excitations of nuclei can be described by a few nucleon Shell Model [1] near the magic shells and by the collective model [2] nearly everywhere else. In recent years the technology of Shell Model has made marvellous progress in the hands of Tokyo, Tübingen, and Madrid groups (cf. [3–5] and references therein) so even the heavy nuclei may become accessible. At present the collective models are still the centre of our understanding of non-magic heavy nuclei.

In the geometrical model of Bohr and Mottelson [2] the low-lying excitations are described in terms of three different Hamiltonians for vibrators, rigid deformed and gamma soft rotors [2, 6, 7]. The different models clearly led to a search for unification. This was achieved in the seventies by various models such as the Bohr Hamiltonian [2], the Greiner Gneuss model (also called GCM model) [8], the quadrupole boson model [9, 10], and the Interacting Boson Model (IBM) [11–14]. Of these models the quadrupole boson model is by Jansen, Dönau,

and Jolos. They are right to be proud of it. The most developed and used model is of course the IBM. Although these models differ in various aspects they all achieve the unification of the three separate collective Hamiltonians.

From this unification one may surmise that there is an underlying similarity of the wave functions of the various modes. This similarity is put in evidence by the so called Q-phonon scheme. This scheme was suggested for the O(6) dynamical symmetry by Otsuka and Kim [15] and was developed by the Cologne, Dubna, Tokyo, Yale collaborations [16-23].

II. WAVEFUNCTIONS OF THE 2_1^+ AND 2_2^+ STATES IN THE Q-PHONON SCHEME

In the Q-phonon scheme one exploits the fact that there are comparably simple, approximate relations between the wave functions of different collective states, including the ground state. These relations stay the same for a wide range of values for the Hamiltonian parameters. The wave functions of some excited states can be described by successive actions of one-body operators on the ground state wave function with good accuracy. In even-even nuclei, where the ground state is a 0^+ state, the wave function of the 2_1^+ state is given by the quadrupole operator, Q, acting on the ground state. The generalization of this concept has been named the Q-phonon scheme [15–23]. In this approach one describes the low-lying collective positive parity states of even-even nuclei in the basis of multiple Q-phonon excitations of the ground state, $|0_1^+\rangle$,

$$|L^+, n\rangle = N^{(L,n)} \underbrace{(Q...Q)}_{n}{}^{(L)} |0_1^+\rangle \ . \tag{1}$$

In the IBM-1 the Q operator of the Q-phonon scheme is the isoscalar electric quadrupole operator, which is also the $E2$ transition operator in the Extended Consistent Q Formalism (ECQF) [24, 25],

$$T(E2) = Q = e_B \, Q^{\rm IBM} \ , \tag{2}$$

where $Q^{\rm IBM}$ is the quadrupole operator in the IBM

$$Q^{\rm IBM} = Q^\chi = s^+\tilde{d} + d^+ s + \chi [d^+ \tilde{d}]^{(2)} \tag{3}$$

and e_B is the effective boson quadrupole charge which is fixed for a given nucleus.

In the framework of the IBM-1 [12, 13] it has been shown over the whole parameter space of the Casten triangle [26] of the ECQF (Extended Consistent Q Formalism) Hamiltonian [24, 25] that each of the wave vectors of the yrast states can be described by only one multiple Q-phonon configuration with good accuracy [16, 17, 19]. This finding has been recently supported by the results of microscopic calculations in terms of the shell model done by the Tokyo group [27]. The Q-phonon scheme suggests the existence of selection rules for the matrix elements of the Q operator. These selection rules may not always be exact since the Q-phonon excitations do not form an orthogonal basis in general. But indeed, one finds that $E2$ transitions between Q-phonon configurations, that differ by more than one Q-phonon, are weak compared to transitions between those configurations that differ by only one Q-phonon. During the last years much data on γ-soft nuclei has been collected, especially in the $A = 130$ mass region [28], which support these selection rules, *e.g.* [16, 18, 29, 30].

Since single Q-phonon excitations generally exhaust large portions of the wave function of a collective state, they can be used as an alternative basis with a faster convergence (few important terms). In the O(6) dynamical symmetry of the IBM, which describes γ-soft nuclei, all low-lying states with the O(6) quantum number $\sigma = N$ can be described as multiple Q-phonon excitations of the ground state [15]. The 2_1^+ and 2_2^+ states in the $O(6)$ dynamical symmetry are represented exactly by only one individual multiple Q-phonon excitation. In general, however, multiple Q-phonon excitations may not be eigenstates of the Hamiltonian. The wave vectors of the lowest-lying eigenstates may then be approximated by series expansion in multiple Q-phonon excitations of the ground state

$$|L_i^+\rangle \approx \left[\sum_{k \geq L/2} a_{i,k} (Q_1 \dots Q_k)^{(L)} \right] |0_1^+\rangle \ . \tag{4}$$

It has been shown that, for the ECQF Hamiltonian of the IBM, and for the Davidov Fillipov model of a rigid triaxial core, the convergence of this series is fast. This makes the Q-phonon scheme a useful concept for semi-analytical descriptions outside the dynamical symmetries of the IBM.

To be specific we will now give the Q-phonon wave functions for the first and second 2^+ states in nuclei. These wave functions are generically valid for collective nuclei, *e.g.*, for nuclei with a ratio $R_{4/2} = E(4_1^+)/E(2_1^+) > 2$, *i.e.*, for which the 4_1^+ state has at least double the excitation energy of the 2_1^+ state [26].

The wavefunctions of the first two 2^+ states are well approximated by the expressions [23]:

$$|2_Q^+\rangle = \mathcal{N}_Q \, Q \, |0_1^+\rangle \tag{5}$$

and

$$|2_{QQ}^+\rangle = \mathcal{N}_{QQ} \left[(QQ)^{(2)} - v \, Q \right] |0_1^+\rangle \tag{6}$$

in large regions of the Hamiltonian parameter space. The quantity v is obtained from the orthogonality condition

$$\langle 2_Q^+ | 2_{QQ}^+ \rangle = 0 \tag{7}$$

The value of v is

$$v = \frac{\langle 0_1^+ | (QQQ)^{(0)} | 0_1^+ \rangle}{\langle 0_1^+ | (QQ)^{(0)} | 0_1^+ \rangle} \ . \tag{8}$$

The normalization constants $\mathcal{N}_Q$ and $\mathcal{N}_{QQ}$ are obtained from

$$\langle 2_Q^+ | 2_Q^+ \rangle = 1 = \langle 2_{QQ}^+ | 2_{QQ}^+ \rangle \tag{9}$$

yielding the expressions

$$\frac{1}{\mathcal{N}_Q} = \sqrt{\langle 0_1^+ | (QQ)^{(0)} | 0_1^+ \rangle} \tag{10}$$

and

$$\frac{1}{\mathcal{N}_{QQ}} = \sqrt{\frac{1}{\sqrt{5}} \left[\langle 0_1^+ | ((QQ)^{(2)} (QQ)^{(2)})^{(0)} | 0_1^+ \rangle - \frac{\langle 0_1^+ | (QQQ)^{(0)} | 0_1^+ \rangle^2}{\langle 0_1^+ | (QQ)^{(0)} | 0_1^+ \rangle} \right]} \ . \tag{11}$$

These "wave functions" are, of course, implicit as nothing is said about the structure of the ground state which is highly complex, in general. The "wave functions" depend further on the structure of the Q operator, *e.g.*, on the χ parameter of the quadrupole operator

in the IBM as is shown in Eq.(3). In the Davidov Fillipov model of a rigid triaxial rotor [7] with $\gamma = 30°$ expressions for the wavefunctions in the Q-phonon scheme were obtained by Jolos [31]. The normalization constants, $\mathcal{N}$ are expectation values of multiple moments of the quadrupole operator $\langle 0_1^+|Q^n|0_1^+\rangle$ up to $n = 4$. These quantities were discussed and extensively used first by Kumar and Cline [32, 33], who called them quadrupole shape invariants. We will refer to them mostly as Q-invariants. They can be calculated from a few $B(E2)$ values between low-lying states [21].

III. Q-INVARIANTS

Following Kumar [32] and Cline [33, 34] we define [35] Q-invariants up to fourth order of the quadrupole operator:

$$q_2 = \langle 0_1^+|(Q \cdot Q)|0_1^+\rangle \tag{12}$$

$$q_3 = \sqrt{\frac{35}{2}}|\langle 0_1^+|[QQQ]^{(0)}|0_1^+\rangle| \tag{13}$$

There are three possibilities to couple the quadrupole operators to obtain fourth order scalars,

$$q_4^{(0)} = \langle 0_1^+|(Q \cdot Q)(Q \cdot Q)|0_1^+\rangle \ , \tag{14}$$

$$q_4^{(2)} = \frac{7\sqrt{5}}{2} \langle 0_1^+| \left[[QQ]^{(2)}[QQ]^{(2)}\right]^{(0)} |0_1^+\rangle \ , \tag{15}$$

$$q_4^{(4)} = \frac{35}{6} \langle 0_1^+| \left[[QQ]^{(4)}[QQ]^{(4)}\right]^{(0)} |0_1^+\rangle \ , \tag{16}$$

The notation $[\ldots]^{(L)}$ abbreviates the tensor coupling of two operators to rank L, the dot denotes scalar product, and $[QQQ]^{(0)}$ abbreviates the unique tensor coupling to rank zero.

These three scalars are equal according to Dobaczewski, Rohoziński and Srebrny [36], if the Q-operators commute.

$$q_4^{(0)} = q_4^{(2)} = q_4^{(4)} \equiv q_4 \ . \tag{17}$$

In the IBM-1 the Q-operators do not commute. The effect of the non-commutativity of the quadrupole operators scales, however, with $1/N$ and is, therefore, neglected in first order.

With the Q-invariants (12–16) we define [35] the dimensionless K-invariants by normalizing relative to an appropriate power of q_2

$$K_n = \frac{q_n}{{q_2}^{n/2}} \text{ for } n \in \{3, 4, 5, 6\} \ . \tag{18}$$

The quantities K_n do not depend on the effective boson charge e_B. The shape invariants K_n differ slightly from earlier definitions of Jolos *et al.* [21] by normalization constants and tensor coupling. We stress again that we neglect in this work the non-commutativity of the Q operators implying interesting ambiguities for the tensor coupling scheme in the definition of the K-invariants that we will exploit below. All K-invariants are exactly equal to unity in the limit of the rigid symmetric rotor and in the SU(3) limit of the IBM.

In the rigid rotor the shape invariants are functions of the fixed deformation parameters β and γ. If we do not stipulate a rigid deformation, we can give expressions for the shape

invariants as

$$q_2 = \left(\frac{3ZeR^2}{4\pi}\right)^2 \langle\beta^2\rangle \equiv \left(\frac{3ZeR^2}{4\pi}\right)^2 {\beta_{\text{eff}}}^2 \tag{19}$$

$$K_3 = \frac{\langle\beta^3 \cos 3\gamma\rangle}{\langle\beta^2\rangle^{3/2}} \equiv \cos 3\gamma_{\text{eff}} \tag{20}$$

$$K_4 = \frac{\langle\beta^4\rangle}{\langle\beta^2\rangle^2} \tag{21}$$

explicitly using expectation values of β and $\cos 3\gamma$. We can define effective values of the deformation parameters β_{eff} and γ_{eff} by Eqs. (19,20).

The shape invariants are measures of effective deformation parameters and their fluctuations. This is made more explicit by defining the following quantities as measures of the fluctuations of β and $\cos 3\gamma$

$$\sigma_\beta = \frac{\langle\beta^4\rangle - \langle\beta^2\rangle^2}{\langle\beta^2\rangle^2} = K_4 - 1 \tag{22}$$

$$\sigma_\gamma = \frac{\langle\beta^6 \cos^2 3\gamma\rangle - \langle\beta^3 \cos 3\gamma\rangle^2}{\langle\beta^2\rangle^3} = K_6 - {K_3}^2 \ . \tag{23}$$

We note that in the large N limit of the IBM-1 the theoretical values for the K_4 are 1 for the SU(3) and the O(6), and 1.4 for the U(5) dynamical symmetry limit, distinguishing between β-rigid and vibrational nuclei, respectively.

The invariant K_4, as well as the fluctuation $\sigma_\gamma = K_6 - K_3^2$, are of special interest as they differ clearly between rigid and soft potentials in β and γ, respectively, which can be difficult otherwise, *e.g.*, for the O(6) and U(5) symmetries. Q-invariants have been studied in the GCM, as well [37]. Finally we note that the values of σ_γ change most rapidly [35] for IBM-1 Hamiltonians that show shape coexistence [38, 39].

IV. SIMPLE RELATIONS AMONG E2 MATRIX ELEMENTS BETWEEN COLLECTIVE STATES

From the Q-invariants one can deduce information about nuclear deformations. The value of the K's can be obtained from a complete set of $E2$ matrix elements. Shape invariants were first introduced by Kumar [32] and Cline [33] in the discussion of a large set of $E2$ matrix elements obtained in Coulomb excitation experiments. Calculating shape invariants in the geometrical model shows their connection to the deformation parameters β and γ introduced by Bohr and Mottelson. Actually the K-invariants generalize the deformation parameters β and γ to soft nuclei. In this case we can define effective parameters, β_{eff} and γ_{eff}, and the fluctuations of those.

For the determination of the shape invariants from experimental data it is convenient to write the expressions for the Q-invariants as sums over $E2$ matrix elements. The tensor properties of the quadrupole operator are taken into account and the unit operator $\mathbf{1} = \sum_{J_i,i,M} |J_i M\rangle\langle J_i M|$ is inserted between every pair of quadrupole operators. Using the Wigner-Eckhardt theorem and the unitarity relation of Clebsch-Gordan coefficients one obtains

$$q_2 = \sum_i \langle 0_1^+ \parallel Q \parallel 2_i^+\rangle\langle 2_i^+ \parallel Q \parallel 0_1^+\rangle \tag{24}$$

$$q_3 = \sqrt{\frac{7}{10}}\,|\sum_{i,j}\langle 0_1^+ \parallel Q \parallel 2_i^+\rangle\langle 2_i^+ \parallel Q \parallel 2_j^+\rangle\langle 2_j^+ \parallel Q \parallel 0_1^+\rangle| \tag{25}$$

$$q_4^{(0)} = \sum_{i,j,k}\langle 0_1^+||Q||2_i^+\rangle\langle 2_i^+||Q||0_j^+\rangle\langle 0_j^+||Q||2_k^+\rangle\langle 2_k^+||Q||0_1^+\rangle\ , \tag{26}$$

$$q_4^{(2)} = \frac{7}{10}\sum_{i,j,k}\langle 0_1^+||Q||2_i^+\rangle\langle 2_i^+||Q||2_j^+\rangle\langle 2_j^+||Q||2_k^+\rangle\langle 2_k^+||Q||0_1^+\rangle\ , \tag{27}$$

$$q_4^{(4)} = \frac{7}{18}\sum_{i,j,k}\langle 0_1^+||Q||2_i^+\rangle\langle 2_i^+||Q||4_j^+\rangle\langle 4_j^+||Q||2_k^+\rangle\langle 2_k^+||Q||0_1^+\rangle \tag{28}$$

that involve reduced matrix elements between 0^+ , 2^+ and 4^+states only. Equations (24 – 28) allow the calculation of the Q-invariants in all nuclear structure models able to predict $E2$ transition matrix elements.

We note that q_2 is equal to the total absolute $E2$ excitation strength from the ground state

$$q_2 = \sum_j B(E2; 0_1^+ \rightarrow 2_j^+)\ . \tag{29}$$

Thereby, q_2 is the only quantity in the set of ivariants q_2, K_n where an absolute value of the effective quadrupole charge (e_B in the IBM) appears.

In view of the (approximate) selection rules of the Q-phonon scheme, the sums (24 – 28) can be reduced drastically in first approximation. If, for instance, $E2$ transitions between states with $\Delta Q > 1$ are neglected [15], the set of $E2$ matrix elements necessary for the calculation of $q_4^{(n)}$ $(n = 0, 2, 4)$ reduces to the matrix elements

$$\langle 2_1^+||Q||4_i^+\rangle \longrightarrow i = 1\ , \tag{30}$$

$$\langle 2_1^+||Q||2_i^+\rangle \longrightarrow i = 1, 2\ , \tag{31}$$

$$\langle 2_1^+||Q||0_i^+\rangle \longrightarrow i = 1, 2, 3\ . \tag{32}$$

The first three 0^+ states are taken into account, because the $0^+_{2,3}$-eigenstates of the ECQF Hamiltonian are mixtures of two- and three-Q-phonon 0^+ configurations for a wide range of parameter values. Of course, if there are low-lying non-collective 0^+ states, the ECQF $0^+_{2,3}$ eigenstates may refer to higher lying physical states.

We will show now how one can obtain simple relations [40] between matrix elements of $E2$ operators from the above. As an example we consider fourth order scalars obtained by coupling the four quadrupole operators in different ways. One obtains several different expressions for the fourth order quadrupole shape invariants in terms of only a few $E2$ matrix elements. The approximate identity of these expressions can be used to derive approximate relations between various observables, *e.g.*, for the quadrupole moment of the first 2^+ state or the lifetime of the first excited 0^+ state, and more easily accessible nuclear data. Such information is very desirable for nuclei where complete experimental information about low-lying states is not – or not yet – available as, *e.g.*, nuclei which are produced using rare isotope beams.

From Eqs. (17,26 – 32) one obtains a relation for the quadrupole moment of the 2_1^+ state:

$$\langle 2_1^+||Q||2_1^+\rangle^2 + \langle 2_1^+||Q||2_2^+\rangle^2 = \frac{5}{9}\langle 2_1^+||Q||4_1^+\rangle^2 \tag{33}$$

or

$$Q^2_{2_1^+} = \frac{32\pi}{35}\left[B(E2; 4_1^+ \rightarrow 2_1^+) - B(E2; 2_2^+ \rightarrow 2_1^+)\right]. \tag{34}$$

If we define $B(E2; 2_1^+ \rightarrow 2_1^+) \equiv 1/5\langle 2_1^+||Q||2_1^+\rangle^2$, we can rewrite expression (33) in an intuitively appealing way:

$$B(E2; 2_1^+ \rightarrow 2_1^+) + B(E2; 2_2^+ \rightarrow 2_1^+) = B(E2; 4_1^+ \rightarrow 2_1^+)\ . \tag{35}$$

We stress that this relation is exactly valid in the ECQF for the O(6) limit, for the whole $O(6) \rightarrow U(5)$ transition path and for the U(5) limit with $\chi = 0$. Its approximate validity for all U(5) and SU(3) like nuclei was already well known, while now it can be extended also to transitional nuclei. The predictive power of relation (34) is tested for several nuclei with dramatically different structure in Table I. A relation similar to (34) for $N \rightarrow \infty$ has been obtained earlier by Jolos et al. [20].

Applying the above results leads to an important approximation formula for K_4 that has already been obtained by Jolos [21]

$$K_4 \approx \frac{7}{10}\frac{B(E2; 4_1^+ \rightarrow 2_1^+)}{B(E2; 2_1^+ \rightarrow 0_1^+)} \equiv K_4^{\text{appr.}}\ . \tag{36}$$

Combining Eqs.(34,36) one finds

$$q(2_1^+) \equiv \frac{35}{32\pi}\frac{Q^2_{2_1^+}}{B(E2; 2_1^+ \rightarrow 0_1^+)} = \left[\frac{10}{7}\ K_4 - \frac{B(E2; 2_2^+ \rightarrow 2_1^+)}{B(E2; 2_1^+ \rightarrow 0_1^+)}\right]\ . \tag{37}$$

Eq.(37) connects in a remarkably simple way three fundamental quantities of nuclear quadrupole collectivity: the quadrupole moment of the 2_1^+ state, and the relative quadrupole transition strengths within the yrast cascade and to off-yrast states. This relation can well be used to demonstrate key signatures for structure changes. We note that $K_4 \in [1, 1.4]$. Let us consider the O(6) to SU(3) transition for which $K_4 = 1$. In the SU(3) limit $[B(E2; 2_2^+ \rightarrow 2_1^+)/B(E2; 2_1^+ \rightarrow 0_1^+) \approx 0]$ the relative quadrupole moment, $q(2_1^+)$, is 10/7. In the O(6) limit $[q(2_1^+) = 0]$ one finds $B(E2; 2_2^+ \rightarrow 2_1^+)/B(E2; 2_1^+ \rightarrow 0_1^+) = 10/7$. In the transition from O(6) to SU(3) the value of $q(2_1^+)$ rises from zero to 10/7, while the value of $B(E2; 2_2^+ \rightarrow 2_1^+)/B(E2; 2_1^+ \rightarrow 0_1^+)$ drops from 10/7 to zero in leading order. Thus, these ratios characterize nicely the change of structure.

To summarize, the Q-phonon scheme and the concept of Q-invariants is reviewed. This concept offers a simple method to derive sets of relations between experimental observables for the quadrupole operator, including quadrupole moments and reduced transition matrix elements. This approach is based on the use of the quadrupole shape invariants, the approximate selection rules of the Q phonon scheme and the fact that corrections from non-commutativity of the components of the quadrupole moment operator in the IBM-1 are small. As an example of the general scheme, up to fourth order Q-invariants of the ground state are given. A satisfactory agreement between data and theoretical relations has been obtained in many cases, but some exceptions clearly need further study.

ACKNOWLEDGMENTS

It is our particular pleasure to thank Professor Jolos for innumerable clarifying discussions on nuclear structure physics and for years of very fruitful collaboration. For further discussions we thank Prof. R.F. Casten, Dr. A Dewald, Dr. A. Gade, Prof. A. Gelberg, Prof. J.

Jolie. This work has been partly supported by the Deutsche Forschungsgemeinschaft under Contracts No. Br 799/9-3, Br 799/10-1, and Pi 393/1-2.

TABLE I: Comparison of the experimental value for the quadrupole moment of the 2_1^+ state with the relations obtained from the Q-phonon scheme for various nuclei.

	$Q^2_{2_1^+}$ [e^{2}b^2]	[e^{2}b^2]
	Eq. (34)	exp.
^{156}Gd	3.79(11)	3.72(15)
^{158}Gd	4.19(11)	4.04(16)
^{160}Gd	4.20(10)	4.33(17)
^{164}Dy	4.09(22)	4.12(81)
^{186}Os	1.97^{+14}_{-29}	1.76^{+26}_{-44}
^{188}Os	1.80^{+7}_{-21}	1.72^{+10}_{-38}
^{190}Os	1.14^{+15}_{-30}	0.90^{+19}_{-32}
^{192}Os	0.56^{+6}_{-19}	0.84^{+24}_{-8}
^{194}Pt	0	0.20^{+2}_{-7}
^{196}Pt	0.26(9)	0.24(18)
^{106}Pd	0.28^{+8}_{-22}	0.30^{+5}_{-6}
^{108}Pd	0.20^{+9}_{-20}	0.38^{+4}_{-8}
^{112}Cd	0.43(6)	0.14(3)
^{114}Cd	0.31(4)	0.13(6)

[1] J.H.D. Jensen, H. Suess and O. Haxel, Die Naturwissenschaften **36** (1949) 155.
[2] A. Bohr and B.R. Mottelson, *Nuclear Structure* **II**, (Benjamin, Reading, 1975).
[3] T. Otsuka, M. Honma, and T. Mizusaki, Phys. Rev. Lett. **81** (1998) 1588.
[4] A. Petrovici, K. W. Schmid, and A. Faessler, Nucl. Phys. **A665** (2000) 333.
[5] A.Poves, J.Sanchez-Solano, E.Caurier, F.Nowacki, Nucl. Phys. **A694** (2001) 157.
[6] J. Wilets and M. Jean, Phys. Rev. **102**, (1956) 788.
[7] A.S. Davydov and G.F. Fillipov, Nucl. Phys. **8** (1958) 237.
[8] G. Gneuss, W. Greiner, Nucl. Phys. **171**, (1971) 449
[9] D. Janssen ,R. V. Jolos,F. Dönau, Yad. Fiz. **A 22** (1974) 965.
[10] R. V. Jolos, F. Dönau , D. Janssen Nucl. Phys. **A 224** (1974) 740.
[11] A. Arima and F. Iachello, Phys. Rev. Lett. **35**, (1975) 1069.
[12] F. Iachello and A. Arima, *The Interacting Boson Model*, (Cambridge University Press, Cambridge, 1987).
[13] F. Iachello, P. Van Isacker, *The Interacting Boson-Fermion Model*, (Cambridge University Press, Cambridge, 1987).
[14] T. Otsuka, A. Arima,F. Iachello, I. Talmi , Phys. Lett. **B76** (1978) 139.
[15] T. Otsuka and K.-H. Kim, Phys. Rev. C **50** (1994) R1768.
[16] G. Siems, U. Neuneyer, I. Wiedenhöver, S. Albers, M. Eschenauer, R. Wirowski, A. Gelberg, P. von Brentano, T. Otsuka, Phys. Lett. **320B** (1994) 1.
[17] N. Pietralla, P. von Brentano, R.F. Casten, T. Otsuka, N.V. Zamfir, Phys. Rev. Lett. **73**, (1994) 2962.
[18] P. von Brentano, O. Vogel, N. Pietralla, A. Gelberg, I. Wiedenhöver in: *Perspectives for the Interacting Boson Model*, Padova, Italy, 1994, edt. R.F. Casten *et al.* (World Scientific, Singapore, 1994).
[19] N. Pietralla, P. von Brentano, T. Otsuka, R.F. Casten, Phys. Lett. **B 349**, (1995) 1.
[20] R.V. Jolos, P. von Brentano, Phys. Lett. **B 381** (1996) 7.
[21] R.V. Jolos, P. von Brentano, N. Pietralla, I. Schneider, Nucl. Phys. **A 618** (1997) 126.
[22] Yu.V. Palchikov, P. von Brentano, and R.V. Jolos, Phys. Rev. C **57**, 3026 (1998).
[23] N. Pietralla, T. Mizusaki, P. von Brentano, R.V. Jolos, T. Otsuka, and V. Werner, Phys. Rev. C **57**, 150 (1998).
[24] D.D. Warner and R.F. Casten, Phys. Rev. Lett. **48**, (1982) 1385.
[25] P.O. Lipas, P. Toivonen, and D.D. Warner, Phys. Lett. **B 155**, (1985) 295.
[26] R.F. Casten, *Nuclear structure from a simple perspective*, (Oxford University Press, 2000).
[27] N. Shimizu, T. Otsuka, T. Mizusaki, M. Honma, Phys. Rev. Lett. 86, 1171 (2001).
[28] R.F. Casten and P. von Brentano, Phys. Lett. **152** (1985) 22.
[29] A. Gade, I. Wiedenhöver, M. Luig, A. Gelberg, H. Meise, N. Pietralla, V. Werner and P. von Brentano, Nucl. Phys. A **673** (2000) 45.
[30] V. Werner, H. Meise, I. Wiedenhöver, A. Gade and P. von Brentano, Nucl. Phys. A **692** (2001) 451.
[31] R.V. Jolos, A. Gelberg, P. von Brentano, Phys. Rev. C **53** (1996) 163.
[32] K. Kumar, Phys. Rev. Lett. **28** (1972) 249.

[33] D. Cline, Ann. Rev. Nucl. Part. Sci. **36** (1986) 683, and references therein.
[34] D. Cline, Acta Phys. Pol. B **30** (1999) 1291.
[35] V. Werner, N. Pietralla, P. von Brentano, R.F. Casten and R.V. Jolos, Phys. Rev. C **61** (2000) 021301.
[36] J. Dobaczewski, S.G. Rohoziński and J. Srebrny, Nucl. Phys. A **462** (1987) 72.
[37] J.-Y.Zhang, R.F.Casten, N.V.Zamfir, Phys.Rev. C **60** (1999) 021304.
[38] R.F. Casten, M. Wilhelm, E. Radermacher, N.V. Zamfir, and P. von Brentano, Phys. Rev. C **57**, R1553 (1998).
[39] N.V. Zamfir, R.F. Casten, M.A. Caprio, C.W. Beausang, R. Krücken, J.R. Novak, J.R. Cooper, G. Cata-Danil, and C.J. Barton, Phys. Rev. C **60**, 054312 (1999).
[40] V. Werner, P. von Brentano, and R.V. Jolos, Phys. Lett. **B521** (2001) 146.

Phase Transitions and Critical Behavior in Nuclei

R. F. Casten

WNSL, Yale University, New Haven, CT 06520, USA

The origin of shape transitions in finite nuclei is discussed, focusing on the conditions under which finite nuclei undergo shape changes with nucleon number in a way which closely resembles phase transitional behavior. Evidence for such behavior has led to the proposal, and discovery, of a new class of critical point symmetries that provides new paradigms for structure.

I. INTRODUCTION

Traditionally, the concept of phase transitions has been reserved for infinite, many-body, systems in which some observable (the order parameter) changes rapidly as a function of a control parameter (typically the temperature in macroscopic systems). However, in recent years, the idea of finite system phase transitions has also been much discussed [1].

Nuclei play a unique role in many-body physics, being composed of two interacting "fluids" (protons and neutrons) interacting under the strong and electroweak forces. They have sufficiently many constituents that many-body methods are essential for the microscopic calculation of their properties. Yet, as finite systems, one would not expect them to exhibit sharp phase transitions. On the other hand, the conceptual separation of their constituent nucleons into closed shells and valence nucleons means that their structure is usually, in fact, determined by just a few nucleons and, therefore, the variation of nucleon number by small amounts can often alter structure dramatically. Thus, the irony that finite nuclei can display phase transitional behavior, reminiscent of many-body systems, as a function of nucleon number *precisely because* so few nucleons determine structure and, hence, a small change in the number of such key constituents is fractionally significant.

Thus, a key question is what is it about nuclei that allows phase transition-like behavior to occur? Why are just a few nucleons so potent as to induce major, and often sudden, equi-

librium shape changes? This is not such an easy question and has been the subject of much discussion [2]. It is the purpose of the present paper to try to put together some comments on this issue and to briefly summarize recent experimental results on phase transitions, phase coexistence, critical points, and critical point symmetries in nuclei.

This paper is dedicated to Slava Jolos to commemorate his many major contributions to nuclear physics over decades of prominence in the field. Despite his quiet and unassuming manner, he has played a pivotal role in so many aspects of nuclear structure ranging from fundamental work on the collective building blocks of nuclei [3,4], to simple models [5,6] of octupole correlations, parity splitting and octupole deformation, important insights into the Q-phonon structure [7-10] of collective modes, and elucidation of concepts of nuclear supersymmetry [11,12]. He has also played a significant role for me personally, as an admired collaborator, as one who can explain difficult ideas simply [13], and, in general, as a friend and colleague for many years.

II. BEHAVIOR OF SHAPE TRANSITION REGIONS

In trying to understand why nuclei become deformed and how phase transitional behavior can result with the addition of just a couple of nucleons, it is useful to first inspect the phenomenology of different transitional regions. The most obvious fact is that some regions are gradual and smooth, while others are extremely rapid. The actinides, and the region around A$\sim$120-130 with N<82, are examples of the former. The A=100 and 150 regions are extraordinary paradigms for the latter.

Of course, with *integer* nucleon number as the control parameter, one cannot, even in principle, discuss real phase transitional behavior, which involves concepts of discontinuous derivatives of some observable against the control parameter. However, we have shown [14] that a change in variables to a control parameter that is potentially continuous can obviate this dilemma. The energy of the first 2^+ state, $E(2_1^+)$, serves this purpose. Figure 1 illustrates this with 2-nucleon separation energies in the N<82 and N>82 regions. For N<82,

there are gradual changes reflecting a gradual onset of collectivity. For N>82, though, the behavior of S_{2n} resembles that of a classic phase transition with a sharp kink – nearly a discontinuity – at $E(2_1^+)$ $\sim$100 keV, where deformation is indeed known to set in.

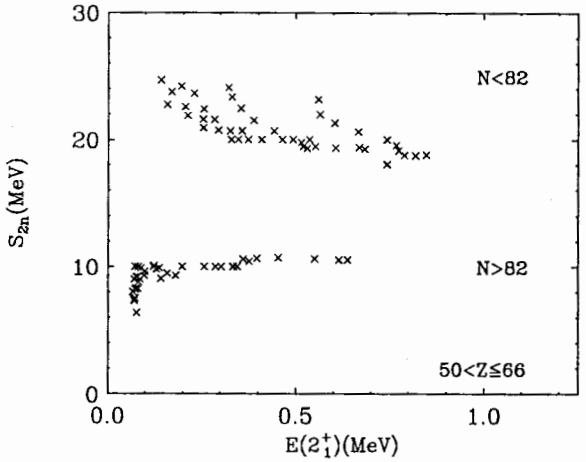

FIG. 1. Two nucleon separation energies against $E(2_1^+)$ for two regions. From ref. [14]

Deformation depends on the buildup of correlations and configuration mixing and therefore on a certain abundance of valence nucleons. However, singly magic nuclei (such as Sn) do not deform regardless of the number of valence neutrons. Their level schemes resemble more those of the single-j seniority scheme. The like-nucleon interaction is strong but it is strongly attractive primarily only in the $J=0^+$ pairing channel which favors spherical shapes.

Rather, it is generally accepted that deformation arises primarily because of valence proton-neutron interactions. The competition between these and the like-nucleon pairing interaction determines how structure evolves. Since the latter scales with total valence nucleon number, $N_p + N_n$, it will invariably lose out [15] to p-n correlations, which go as N_pN_n [ref. 16], if there are sufficient valence nucleons of both types. How quickly this will happen depends on the strengths of the p-n and pairing interactions, which depends on which orbits are being filled. A useful guideline [16] is the parameter $P=N_pN_n/(N_p+N_n)$.

When $P \gtrsim 5$, nuclei become deformed, reflecting the fact that p-n interactions (which individually are on the order of 200 keV) achieve structural control over pairing interactions (~1 MeV) when there are about 5 p-n interactions for each like-nucleon pairing interaction. However, as noted, there are variations from region to region. To understand how and where phase transitional behavior can occur in nuclei, it is necessary to understand the origins of these variations, in particular the relation of the p-n interaction to shell structure, and the relative importance of deformation-driving quadrupole correlations involving normal and unique parity orbitals.

Since ($J \neq 0^+$)configuration mixing is tantamount to deformation, and since the multi-j environment of normal parity orbits offers more opportunity for configuration mixing [17], then, everything else being equal, the normal parity orbits should be dominant in promoting spherical-deformed transition regions. However, not everything else is, in fact, equal. Residual interactions depend on the nl quantum numbers of the independent particle model orbits occupied by the valence nucleons. The smaller the differences Δn and Δl are between two interacting orbits, the larger the interaction [18]. In typical major shells in heavy nuclei there is a wide range of principal quantum numbers and of orbital angular momenta (e.g., n=1-3, l=1-5 for N=82-126). Hence, many p-n interactions will be rather weak. However, interactions between particles in the highest j orbits (e.g., $1h_{11/2p}$ and $1i_{13/2n}$) or between spin-orbit partner (SOP) pairs (e.g., $1h_{11/2p}$ and $1h_{9/2n}$) are enhanced, and further augmented since high-j orbits can contain larger numbers of nucleons than low j orbits.

So, what then, is the relation of normal and unique parity configuration mixing in the development of deformation? The answer depends on the mass region. In some regions (e.g., A~120-130: see Fig. 1 (top)), where deformation sets in gradually, interactions involving protons and neutrons in both types of orbits are important. The abundance of J$\neq 0^+$ pairs that can be made from the normal parity orbits controls the development of collectivity. Here the quadrupole interaction (especially the quadrupole p-n interaction) is paramount.

However, in other regions, where there are significant sub-shell gaps, it is the monopole

p-n interaction that plays a key role. This is the renowned Federman-Pittel mechanism [15,19] and is illustrated in Fig. 2. In the ^{90}Zr region, the 28-40 proton shell is too small and has too low degeneracy to develop enough quadrupole correlations for the development of deformation. Moreover, the proton-neutron correlations are relatively weak with Δn=1 and/or Δl=1. However, above N=56, when neutrons begin filling the $1g_{7/2n}$ orbit, the strong *monopole* p-n interaction with the $1g_{9/2p}$ orbit leads to a lowering of the proton $1g_{9/2}$ *single particle energy* [15,18,19] and to the obliteration of the Z=40 shell gap. This immediately increases the "gene pool" of proton configurations that can contribute to correlated $J \neq 0$ configurations and leads to the sudden onset of deformation.

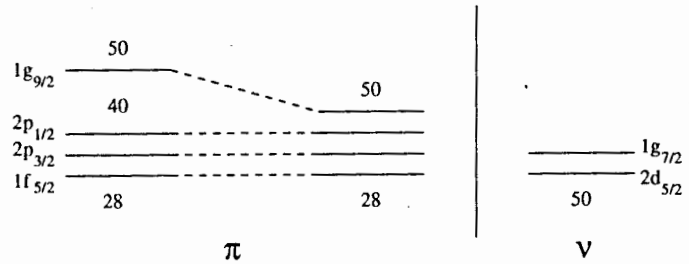

FIG. 2. Evolution of proton single particle energies, due to effects of the monopole p-n interaction [18], as the neutron $1g_{7/2}$ orbit is filling in the A~100 region. The p-n interaction leads to a rapid dissolution of the Z=40 mid-shell gap [19]. Other p-n interactions among high-j orbits, such as $1g_{9/2p} - 1h_{11/2n}$, also play key roles [20]

Thus, it is the effect of the monopole p-n interaction in modifying the effective *space* in which quadrupole p-n and like-nucleon interactions operate that allows this extremely rapid transitional region to occur. A similar explanation applies to the A~150 region [21] and accounts for the very different "trajectories" of nuclei like Ba and Gd through the spherical-deformed transition region.

A related way to look at this is directly in terms of the kind of level crossing phenomenon that underpins the idea of a first-order phase transition and the Jahn-Teller effect [20]. As

long as the Z=40 gap is pronounced, configuration mixing involving the $1g_{9/2p}$ orbit will lead to highly excited deformed configurations. However, when the SOP $1g_{9/2p} - 1g_{7/2n}$ or other large, monopole p-n interactions, reduce the Z=40 gap, this deformed configuration is lowered in energy. At some point - the critical point - its energy "crosses" that of the spherical ground state (whose proton configurations are composed primarily of orbits in the 28-40 shell) and deformation immediately ensues [18-20] as in a true phase transition.

III. PHASE TRANSITIONS AND CRITICAL POINT SYMMETRIES

Having seen how, under appropriate circumstances of shell structure and proton and neutron orbits near the Fermi surface, phase transitions can develop in finite nuclei, we now turn to the description of nuclei undergoing such phase transitions, that is, at the critical point (or configuration crossing point). Such nuclei have traditionally been considered the most difficult to treat, precisely because of the competition between such different (i.e., spherical and deformed) degrees of freedom.

Thus it is all the more remarkable that Iachello has recently been able to develop [22] a new class of symmetry that describes critical point nuclei *analytically* and in a parameter-free way (except for scale). The idea is the essence of simplicity. Before the phase transition, the potential has a global minimum for quadrupole deformation β=0 and an excited minimum at finite β. After the phase transition, the energies of the two minima are reversed. At the critical point the two minima are degenerate, with a small barrier between them. If one assumes that the "walls" of this potential are very steep (that is, the nuclear oscillations in β are strongly confined), and if we ignore the small internal barrier between the minima, we can approximate the potential by a square well in β. This is the ansatz leading to the E(5) and X(5) critical point symmetries that describe the second order vibrator to γ-soft rotor [U(5)→O(6)] and the first order vibrator to symmetric rotor [U(5)→SU(3)] critical points, respectively. The main difference between these two cases is that, for X(5), the potential is not γ-flat so that a change of the potential in γ is involved as well. Of course, to describe

actual nuclei, the problem must be solved in 5 dimensions (β, γ and the three Euler angles). In the important β degree of freedom, the resulting wave functions are simply Bessel functions. However, their order is half-integer for E(5) and *irrational* for X(5), and the eigenvalues are given by the zeros of these Bessel functions. The essential point is that the predictions are completely characteristic of the critical points – that is, they are completely analytic, and parameter-free (except for energy and transition rate scales). We stress that these two new critical point symmetries are solutions to a differential equation in β and γ (i.e., the Bohr Hamiltonian). They are not symmetries of the IBA [although the IBA can be used to numerically simulate E(5) and X(5)].

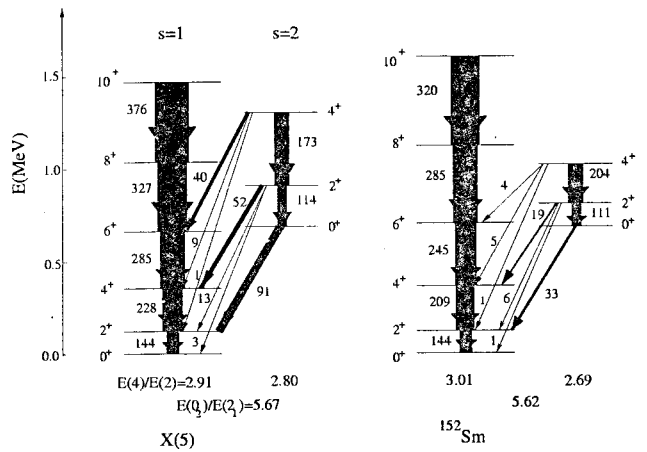

FIG. 3. Comparison of X(5) [see ref. 22] with the data for ^{152}Sm. From ref. [23]

As soon as Iachello developed the E(5) and X(5) symmetries [22], empirical examples were found [23] – in ^{134}Ba and ^{152}Sm – and, subsequently, an additional candidate for X(5) has been found in ^{150}Nd [24]. Figure 3 shows a comparison of X(5) with the data for ^{152}Sm, The overall agreement is superb, and discussed in detail in the literature [22], as have the discrepancies seen in Fig. 3. E(5) and X(5) provide two new paradigms of structure as illustrated in the symmetry triangle of Fig. 4. These are the first wholly new, analytic,

paradigms in half a century, since the development of the vibrator, axial rotor, and γ-soft rotor in the 1950's.

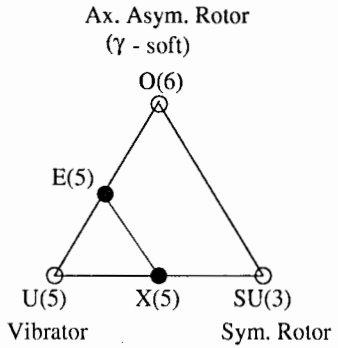

FIG. 4. New structural triangle for nuclei showing the three historic benchmarks of structure at the vertices. The new critical point symmetries E(5) and X(5) are noted along two transition legs. The line connecting X(5) and E(5) is a region of first order transitions (rigorously, the line has small but finite width) culminating at the second order phase transition point E(5)

IV. CONCLUSIONS

We have discussed the origins of deformation and shape transitions as a function of nucleon number in nuclei, with emphasis on understanding how phase transitional behavior can occur in finite systems, especially in systems whose structure is dominated by the effects of only a few valence nucleons. One conclusion, perhaps ironic when expressed this way, is that it is precisely *because of* the dominance of a few nucleons that small changes in particle number can induce sudden structural changes in many-body nuclear systems so that their systematics resembles the phase transitional behavior of larger systems. This resemblance is not accidental since the origin of such rapid structural changes is in fact a crossing of spherical and deformed configurations with nucleon number, a characteristic feature of a first-order phase transition.

Such phase transitions develop in regions where the evolution of shell structure fosters rapid changes, namely regions with significant sub-shell gaps, whose obliteration by the

effects of the monopole p-n interaction in modifying single particle energies can suddenly alter the size of the valence space available for deformation-inducing configuration mixing.

We then discussed the development by Iachello of a new class of symmetry [developed in two manifestations, E(5) and X(5)] that gives analytic descriptions of nuclei at the critical points of first and second order phase transitions, respectively. Finally, we discussed the discovery of empirical manifestations of these critical point symmetries and we showed the comparison of X(5) with the data for ^{152}Sm.

I am grateful to Slava Jolos for wonderful collaborations and for many enlightening discussions over the years. I am also grateful to Victor Zamfir for help in preparing this paper and to he, Peter von Brentano, Stu Pittel, Alejandro Frank, Witek Nazarewicz, and Kris Heyde for discussions of these issues in recent years that have helped me in putting together some of the ideas here that they understand far better than I. Work supported by USDOE Grant Number DE-FG02-91ER-40609.

---

[1] Trento Meeting on Phase Transitions in Finite Systems, Sept. 11-22, 2000, ECT*, Trento, Italy.

[2] See the excellent series of papers in: Int. J. Mod. Phys. **E2**, Supplement (1993).

[3] D. Janssen, R. V. Jolos, and F. Dönau, Yad. Fiz. **A22**, 965 (1974).

[4] R. V. Jolos, F. Dönau, and D. Janssen, Nucl. Phys. **A224**, 740 (1974).

[5] R. V. Jolos, P. von Brentano, and F. Dönau, J. Phys. **G19**, L151 (1993).

[6] R. V. Jolos and P. von Brentano, Phys. Rev. **C60**, 064317 (1999).

[7] R. V. Jolos, A. Gelberg, and P. von Brentano, Phys. Rev. **C53**, 168 (1996).

[8] V. Werner, N. Pietralla, P. von Brentano, R. F. Casten, and R. V. Jolos, Phys. Rev. **C61**, 021301 (2000).

[9] Yu. V. Palchikov, P. von Brentano, and R. V. Jolos, Phys. Rev. **C57**, 3026 (1998).

[10] R. V. Jolos, P. von Brentano, R. F. Casten, and N. V. Zamfir, Phys. Rev. **C51**, R2298 (1995).

[11] R. V. Jolos and P. von Brentano, Phys. Rev. **C60**, 064318 (1999).

[12] R. V. Jolos and P. von Brentano, Phys. Rev. **C63**, 024304 (1999).

[13] For example, it is only through discussions with Slava that I finally understood after many years the seemingly simple idea of why the γ-vibrational mode has K=2.

[14] R. F. Casten, Dimitri Kusnezov, and N. V. Zamfir, Phys. Rev. Letts. **82**, 5000 (1999).

[15] See S. Pittel and P. Federman, in ref. 2, p. 3.

[16] R. F. Casten, Phys. Rev. Letts. **54**, 1991 (1985); R. F. Casten, Phys. Letts. **152B**, 145 (1985); R. F. Casten, D. S. Brenner, and P. E. Haustein, Phys. Rev. Lett. **58**, 658 (1987).

[17] M. Guidry and C. L. Wu, in ref. 2, p. 17.

[18] K. Heyde et al., Phys. Lett. **155B**, 303 (1985).

[19] P. Federman and S. Pittel, Phys. Letts. **69B**, 385 (1977).

[20] W. Nazarewicz, in ref. 2, p. 51; J. Dobaczewski et al., Phys. Rev. Letts **60**, 2254 (1988).

[21] R. F. Casten et al., Phys. Rev. Letts. **47**, 1433 (1981).

[22] F. Iachello, Phys. Rev. Letts. **85**, 3580 (2000), and **87**, 052502 (2001).

[23] R. F. Casten and N. V. Zamfir, Phys. Rev. Letts. **85**, 3584 (2000), and **87**, 052503 (2001).

[24] R. Krücken et al., Phys. Rev. Letts., in press.

Nuclear clusterization and dynamical symmetries*

J. Cseh

Institute of Nuclear Research of the Hungarian Academy of Sciences, Debrecen, Pf. 51, Hungary-4001, cseh@atomki.hu

A variety of dynamical symmetries related to nuclear clusterization is discussed.

I. INTRODUCTION

Clusterization is an important phenomenon of nuclear structure, covering a broad range of mass number, excitation energy, angular momentum, deformation, and cluster types. Its theoretical description is a fairly complex problem, and symmetry-considerations can help in finding the solutions.

Different symmetries may show up in cluster configurations, here we concentrate on the dynamical symmetries. Even they have remarkable variety, and we discuss them in the sequence of increasing complexity.

We pay more attention to the method, than to the details of the phenomenon; and the physical examples mentioned below simply illustrate, how the concept of dynamical symmetry can contribute to our understanding of nuclear cluster structure.

II. EXACT SYMMETRIES

A quantum mechanical system is said to have a continuous symmetry described by a Lie group G, if its Hamiltonian (H) commutes with all the group-generators ($X_i^{\{G\}}$):

$$[H, X_i^{\{G\}}] = 0. \tag{1}$$

The algebraic properties of the group is defined by the corresponding Lie-algebra:

$$[X_i^{\{G\}}, X_j^{\{G\}}] = \sum_k c_{i,j}^{\{G\}k}, X_k^{\{G\}}, \tag{2}$$

where $c_{i,j}^{\{G\}k}$ denote the structure constants. In such a case H can depend on the generators only through the Casimir-invariants of the group.

If both the potential and the total energy is invariant, the symmetry is called geometrical, contrary to the dynamical symmetry which leaves invariant only the total energy [1]. Well-known examples are the $O(4)$ dynamical symmetry of the Coulomb problem, and the $U(3)$ dynamical symmetry of the harmonic oscillator problem. In both cases $O(3)$ is a geometrical symmetry.

If an exact symmetry holds, then several important consequences follow.

i) Good quantum numbers specify the energy-eigenstates. In other words: the eigenvectors

*It is a pleasure to dedicate this paper to Professor R. V. Jolos, an expert of clusterization and symmetries, on the occasion of his 60th birthday.

are symmetric in the sense that they transform according to irreducible representations (irreps) of the symmetry group and its subgroups:

$$G \supset G' \supset G'' \supset \dots . \tag{3}$$

ii) The states have a multiplet structure (defined by the relations of irreps of groups in (3)).
iii) The eigenvalue-problem has an analytical solution.
iv) The multiplets are degenerate.
v) Selection rules are available.

It is worth stressing that some of the consequences [i), ii), iv), v)] apply even if the exact Hamiltonian is not given explicitly, only its symmetry is known.

In short, we can say that an exact symmetry holds, if both the (Hamilton) operator and its eigenvectors are symmetric.

Familiar exact (geometrical) symmetry of nuclear structure is the three-dimensional rotation, giving rise to the conservation of angular momentum. When applied to a cluster-decay of a parent nucleus (P) into two daughter nuclei (C_1 and C_2) it reads:

$$J^{\{P\}} = J^{\{C_1\}} \otimes J^{\{C_2\}} \otimes J^{\{R\}}, \tag{4}$$

where J indicates the angular momentum of the nuclei (P, C_1, C_2), R stands for relative motion, $\otimes$ denotes direct product (vector coupling), and the $'='$ sign says that $J^{\{P\}}$ is supposed to match with one of the results of the products on the right hand side.

The exact dynamical symmetries, as discussed here, hold only for very special forces, therefore, in this strict form they are not very helpful in building up models of few- and many-body systems.

III. DYNAMICAL(ALLY BROKEN) SYMMETRIES

It is a generalized version of the dynamical symmetry that proved to be very successful in various areas of physics: when the Hamiltonian can be expressed in terms of Casimir-invariants of a chain of nested subgroups (3) (see e.g. [2,3]).

From the presence of such a dynamically broken symmetry consequences i) ii) iii) and v) still follow. The degeneracy, however, which corresponds to an exact G symmetry splits up. The Hamiltonian with this kind of dynamical symmetry contains more general interactions than the one with an exact G symmetry. The symmetry-breaking interaction does not have to be week (perturbative), it can be very strong, but it needs to be very special, expressed in terms of the invariant operators of the subalgebras.

In case of this kind of general dynamical symmetry (or as it is called sometimes dynamically broken symmetry) the operator is not symmetric, yet its eigenvectors are symmetric.

Dynamical symmetries (in its general form) are very important in nuclear structure. The isospin $U^T(2)$, Wigner's $U^{ST}(4)$ spin-isospin symmetry [4], and Elliott's $U(3)$ (space) symmetry [5] are well-known examples.

When applied to the cluster-decay of the previous section the $U(3)$ and $U^{ST}(4)$ selection rules read:

$$[n_1^{\{P\}}, n_2^{\{P\}}, n_3^{\{P\}}] = [n_1^{\{C_1\}}, n_2^{\{C_1\}}, n_3^{\{C_1\}}] \otimes [n_1^{\{C_2\}}, n_2^{\{C_2\}}, n_3^{\{C_2\}}] \otimes [n_1^{\{R\}}, 0, 0], \tag{5}$$

$$[f_1^{\{P\}}, f_2^{\{P\}}, f_3^{\{P\}}, f_4^{\{P\}}] = [f_1^{\{C_1\}}, f_2^{\{C_1\}}, f_3^{\{C_1\}}, f_4^{\{C_1\}}] \otimes [f_1^{\{C_2\}}, f_2^{\{C_2\}}, f_3^{\{C_2\}}, f_4^{\{C_2\}}], \tag{6}$$

where $[n_1, n_2, n_3]$ and $[f_1, f_2, f_3, f_4]$ denote irreps of the $U(3)$ and $U^{ST}(4)$ groups, respectively.

The $U(3)$ and $U^{ST}(4)$ symmetries turned out to be relevant for light nuclei, therefore, the application of these selection rules provide us with interesting information on the possible cluster structure, and consequently, on the possible decay modes of states of light nuclei.

In [6] the relation of special deformed states and cluster configurations were investigated. Special deformation includes spherical, superdeformed, hyperdeformed, etc shapes; in general: any ellipsoidal shape with the ratios of main axes expressed as ratios of integer numbers. Alpha-like light nuclei were considered from ^{12}C to ^{44}Ti, and alpha-like binary and multicluster configurations were taken into account.

In [7] the allowed and forbidden binary cluster-configurations were determined for the ground-state-like configurations of the *sd*-shell nuclei. They are considered to be important in the fission studies of light nuclei [8], as well as in elastic transfer reactions [9].

A further interesting study can investigate the structural influence on the mass-distribution of cold binary fission (as a function of the quadruple deformation of the parent nucleus) [10].

Similar questions are even more interesting concerning heavy nuclei, due to the fact that fission can take place from their ground-state (contrary to similar procedures in light nuclei, which are energetically forbidden). Unfortunately, however, the $U(3)$ symmetry is not valid for heavy nuclei (in its original form), due to the strong spin-orbit and other symmetry-breaking interactions; therefore, one can not apply the $U(3)$ selection rule, as it is done for light nuclei. Nevertheless, it seems that an even more general symmetry, as discussed in the next section, may work, and enable us to formulate a selection rule based on the microscopic structure.

IV. EFFECTIVE SYMMETRIES

Is there any way for a quantum mechanical symmetry to act, when neither the (Hamilton) operator, nor its eigenvectors are symmetric? Surprisingly enough, the answer is yes. This kind of symmetry is called effective symmetry, and its consequences are as remarkable, as its appearance is.

The effective symmetry is more general, than the dynamically broken symmetry of the previous section in the sense that the symmetry-breaking interactions of the Hamiltonian in this case mix the basis vectors of different irreps, thus the energy-eigenstates are given in terms of linear combinations.

In order to illustrate the situation, let us consider a case characterized by a simple group-chain:

$$G \supset G', \tag{7}$$

$$| \alpha \ , \ \beta \rangle , \tag{8}$$

where we have indicated the representation labels as well, and in general α and β may denote several indices. The matrix elements for a representation are:

$$\langle \alpha', \beta' | \Gamma(X_i^{\{G\}}) | \alpha'', \beta'' \rangle = f(\alpha, \beta), \tag{9}$$

where the $\Gamma(X_i^{\{G\}})$ operator represent the $X_i^{\{G\}}$ generator, and f stands for a function of the representation labels, which is well-defined for the group G. We take the linear combinations:

$$\psi_\beta = \sum_\alpha c_\alpha |\alpha, \beta\rangle. \tag{10}$$

Let us assume that this kind of expansion is available for several β's, and the coefficients c_α are the same for each β. We can calculate the matrix elements between the ψ_β states:

$$\langle \psi_{\beta'} | \Gamma(X_i^{\{G\}}) | \psi_{\beta''} \rangle. \tag{11}$$

If the $f(\alpha, \beta)$ function is linear in the α quantum numbers (which is the case for some physically important groups), then the equations (9) hold also for the linear combinations (10). Then, supposed that there is enough ψ_β's, (9) is again a representation of G. This kind of representation is called embedded representation [11], and the states (10) are said to form a soft band. A soft band is an intermediary between the extremes of pure bands (belonging to a single irrep) and arbitrarily mixed states. An embedded representation behaves like a representation of its own.

If the $f(\alpha, \beta)$ function is not linear in the α quantum numbers, then we can make a series expansion, and the linear approximation may still prove to be reasonable in some domain of the parameters (which is the case for some other, physically important groups) [11–13].

A couple of remarks seems to be appropriate here, concerning the physical applications of the embedded representation (i.e. effective symmetry). The approximation that gives rise to its appearance in physical terms corresponds to the assumption of adiabaticity [11]. Since it is the basis of many models, the effective symmetry opens up new territories for symmetry-considerations. Once, however, the presence of a symmetry seems to follow from the experimental data, attention has to be paid to the distinction between real or effective symmetry (i.e. simple band structure, or the presence of soft bands).

The very general nature of the effective symmetry explains, why some models are successful, when seemingly they do not have any right (due to their assumptions) to be so.

Shell model studies of heavy nuclei revealed the important role of the effective $SU(3)$ symmetries [13]. On the one hand side experimental data gave evidence for the soft $SU(3)$ band, and furthermore, microscopic shell-model configuration could be assigned to the intrinsic state of a soft band. These essential findings inspired the application of the effective symmetry in cluster studies of heavy nuclei.

A novel feature of nuclear clusterization was found by the recent multiple gamma-coincidence measurements of spontaneous fission [14]. Cold binary fission processes were detected from the ground state of the ^{252}Cf nucleus. The results indicate the presence of very exotic (e.g. ^{154}Ba + ^{108}Mo) cluster-configurations. The relative importance of these

kind of very exotic clusterization in the ground state of the parent nucleus is, therefore, an interesting question.

The relative preference of the Ba+Mo configurations were studied from the viewpoint of nuclear structure in [15], based on the concept of effective $U(3)$ symmetry. The main point of this work is, that both the Pauli-principle, and the deformation of the nuclei (parent and daughters) are taken into account, as well as the possible relative orientation of the deformed clusters. The calculated relative forbiddenness characterizes the overlap of the ground-state wavefunction of the parent nucleus (with its well-defined normal deformation) with the possible exotic cluster configurations. Further studies are in progress [16], considering other nuclei, as well as the question of the deformation-dependence of the mass-distributions.

We note here, that somewhat similar firbiddenness-calculations have been carried out, based on the real $SU(3)$ scheme [17,18]. There are, however also important differences between the two methods. One of them is the use of the real or effective $SU(3)$ symmetries, and the other is the way how the forbiddenness is defined. In [17,18] it is calculated on the basis of the number of oscillator quanta, making no difference between different nuclear shapes, and orientations, while in [15] these effects were taken into account, and proved to be important.

V. BEYOND THE SYMMETRIES: SPECTRUM-GENERATION

In light of the usefulness of the algebraic methods in the description of (exact or broken) symmetries, one may wonder, if similar techniques could be used for generating the excitation spectrum of the system as well. We may try to look for an algebra, which can describe not only the symmetries of the system, but also generates its energy-spectrum, and accounts for the transitions between its states as well, in such a way, that all states belong to a single irrep. Such an algebra is called dynamical algebra [19] (sometimes it is called spectrum generating algebra [2]). Obviously, the dynamical algebra has to be a bigger algebra, than the symmetry algebra, and the latter needs to be its subalgebra. If a dynamical algebra can be found, then several of the fruitful consequences discussed in Section 2. are still valid. We illustrate the situation with the example of a dynamical algebra for the two-body-problem, which is important (among others) in the description of the relative motion of clusters.

The relative motion of a two-body system reduces to a one-body problem after removing the center-of-mass-motion. We can apply a harmonic oscillator basis, thus we start from the single-particle harmonic oscillator problem in three dimension. It has an exact $U(3)$ dynamical symmetry [1], and the generators of the symmetry group are the particle number conserving bilinear products of the oscillator quantum creation ($a_i^\dagger$, $i = x, y, z$) and annihilation (a_i) operators: $A_{ij} = a_i^\dagger a_j$. They close under the commutation relations:

$$[A_{ij}, A_{kl}] = \delta_{jk} A_{il} - \delta_{il} A_{jk}. \tag{12}$$

If we introduce a fourth dimension (s) and associate a boson to this direction as well (which is called scalar boson, as opposed to the vector-bosons a) then we can generate the spectrum in the following way. The s boson is supposed to have a lower-lying single-particle state, than the vector boson. Then the ground state of the system corresponds to the case when there are only s bosons. The oscillator spectrum is obtained by creating

a bosons and annihilating s bosons: $a_i^\dagger s$. Now we have four creation and annihilation operators, they give 4x4=16 bilinear products, which close under the commutation relation, exactly like (12), except that the indices run over four coordinates: $i = s, x, y, z$. The resulting algebra is $U(4)$, and a possible algebra-chain is:

$$U(4) \supset U(3) \supset O(3). \tag{13}$$

One can introduce symmetry-breaking interactions, expressed in terms of the invariant operators of (13), and the result is a dynamical symmetry starting with a dynamical (spectrum-generating) algebra. Thus, one has again good quantum numbers, multiplet-structure, analytical solution, and selection rules.

The $U(4)$ algebraic model of the two-body problem is called vibron model [20], and it is applied in molecular physics, hadron spectroscopy, and nuclear structure, as well. The physical operators of the model are expressed in terms of the $U(4)$ generators, the model states belong to an $U(4)$ irrep, therefore, the matrix elements can be calculated with group-theoretical methods.

Similar (spectrum-generating) procedure can be applied for the description of other degrees of freedom. E.g. the (five dimensional) quadruple collectivity is essential in nuclear physics which has a $U(5)$ symmetry-group. A possible dynamical algebra is $U(6)$ [21,2].

VI. SYMMETRIES OF THE SEMIMICROSCOPIC ALGEBRAIC CLUSTER MODEL

The basic assumption of the cluster models is that the relevant degrees of freedom of the atomic nucleus are the relative motion of the clusters, and their internal structure. The vibron model can be applied for the algebraic description of the former one, in case of a multicluster configuration one $U(4)$ model for each independent relative motion. As for the internal structure of the clusters, they can be accounted for by the $U(3)$ shell model, or by the $U(6)$ collective model.

One further aspect has to be considered. A nucleus consists of protons and neutrons, which are fermions, therefore, the total wavefunction should be antisymmetric. Thus, in a cluster picture one has to take into account the Pauli-exclusion principle not only between nucleons in the same cluster, but also between nucleons sitting in different clusters. When it is appreciated, we talk about a microscopically constructed model space, and the model is called fully microscopic, or semimicroscopic, depending on the fact whether or not the applied interactions are microscopic (effective two-nucleon forces), or they are treated phenomenologically. If the exclusion principle is not taken into account, the model is called phenomenological. The latter one has the advantage of being simpler, and in some cases, when the antysimmetrization is not important, e.g. in highly excited molecular states of nuclei, it can be very fruitful, too.

Algebraic cluster models can be formulated both on the phenomenological, and on the semimicroscopic level. Here the adjective 'algebraic' is meant in the strict sense that not only the basis states of the model are characterized by the irreps of an algebra, but the physical operators as well. Thus the matrix elements can be calculated by algebraic methods. (Group-theoretical techniques are very useful also in fully microscopic models,

but they are not algebraic in the strict sense used here.) We summarize briefly the basic concepts of the semimicroscopic algebraic cluster model (SACM) [22] which can be applied both in the ground-state region, and at the high excitation energies.

The internal structure of the clusters are described by Elliott's shell model, and the relative motions by the vibron model. For a configuration of k clusters the model has a group-structure:

$$U_{C_1}^{ST}(4) \otimes U_{C_1}(3) \otimes ... U_{C_k}^{ST}(4) \otimes U_{C_k}(3) \otimes U_{R_1}(4) \otimes ... U_{R_{k-1}}(4), \tag{14}$$

where $U_{C_i}^{ST}(4)$ stands for the spin-isospin symmetry of the C_i cluster, $U_{C_i}(3)$ is its space-symmetry-group, and the $U_{R_j}(4)$ are the dynamical groups of the vibron models, associated to the $k-1$ independent relative motion.

The physical operators are given (phenomenologically) as expansions of the generators of this direct-product group. The Pauli-exclusion principle requires a truncation of the corresponding model space (otherwise we end up with a phenomenological cluster model). The exclusion of the Pauli-forbidden states can be done by different methods, one of them requires a matching between the model space of the (not antisymmetrised cluster model (14)), and the fully antisymmetric $U(3)$ shell-model space of the whole nucleus.

Several dynamical symmetries of this model can be constructed. A very important one is obtained by the coupling on the $U(3)$ level:

$$\begin{aligned}
&U_{C_1}^{ST}(4) \otimes U_{C_1}(3) \otimes ... U_{C_k}^{ST}(4) \otimes U_{C_k}(3) \otimes U_{R_1}(4) \otimes ... U_{R_{k-1}}(4) \supset ... \\
&\supset U_C^{ST}(4) \otimes U_C(3) \otimes U_R(3) \supset ... \\
&\supset U_C^T(2) \otimes U_C^S(2) \otimes U(3) \\
&\supset U_C^T(2) \otimes U_C^S(2) \otimes O(3) \\
&\supset U^T(2) \otimes U(2).
\end{aligned} \tag{15}$$

When the Hamiltonian is expressed in terms of the invariant operators of the groups in this chain, an analytical solution of the energy-eigenvalue problem is available. This circumstance makes the application fairly easy and the model can be applied for the unified description of the clusterization in the ground-state region together with the very high-lying molecular resonances (observed in resonant reactions of heavy ions). Low and high-spin states and different clusterizations can be calculated in this way. Spherical, and deformed (including triaxial deformation) can be accounted for, as well as the different relative orientation of the deformed clusters [23].

A special case of the model reduces to a simple vibron model, as far as the operators are considered. It happens when we consider a binary configuration of two closed-shell clusters, and there is no need to involve coupling between the relative motion and the internal cluster degrees of freedom. The model space, however, is different even in this case from that of the simple vibron model; the Pauli-exclusion requires the truncation of the $U(3)$ basis from the low-lying side.

Due to the break-down of the $U(3)$ symmetry in the heavy nuclei, as mentioned in Section 3, this dynamical symmetry is applicable only for light nuclei. One of the spectroscopic features of heavy nuclei, which calls for a detailed description in terms of cluster

configurations is the appearance of low-lying negative-parity bands [24]. For problems, like this the SACM and its dynamical symmetry has to be extended. A possible way is offered by the effective symmetry of Section 4, or the application [25] of pseudo $U(3)$ symmetry [26].

VII. DYNAMICAL SUPERSYMMETRIES

Supersymmetric (SUSY) schemes, in general, give a unified treatment of bosonic and fermionic degrees of freedom. In a supersymmetry model of nuclear cluster systems the bosonic sector of the superalgebra describes the relative motion of the clusters, while its fermionic sector is associated with their internal structure. Supersymmetry connects similar cluster configurations of different nuclei.

An example is the core+α configurations. The relative motion is described by the vibron model with a $U_R(4)$ (dynamical) group-structure, while the dynamical group for the fermionic sector, when restricted to the p shell, is $U_C(12)$. This latter group contains the $U^{ST}(4) \otimes U(3)$ symmetry-group, mentioned in Section 6. A supersymmetric model is obtained by embedding the $U_R(4) \otimes U_C(12)$ direct-product group into a supergroup: $U(4|12)$. In order to embed the bosonic and fermionic algebras in a superalgebra, one has to define generators which create a fermion and annihilate a boson, or *vice verse*. This problem has been discussed in detail in [27].

As an application for the cluster supersymmetric model, the α-cluster states of the nuclei ^{20}Ne and ^{19}F were analyzed and correlations between their spectra, electric quadruple transitions, and one-nucleon transfer reactions were interpreted in terms of $U(4|12)$ supersymmetry.

The relevant classification is

$$\begin{aligned} & U(4|12) \supset U_R(4) \times U_C(12) \\ & \supset SU_R(3) \times SU_C(3) \times U_C^{ST}(4) \\ & \supset SU(3) \times SU_C^S(2) \times SU_C^T(2) \\ & \supset SO(3) \times SU_C^S(2) \times SU_C^T(2) \\ & \supset SU(2) \times U_F^T(1)\ , \end{aligned} \tag{16}$$

which is the group structure of the SACM for core+α cluster systems, embedded in $U(4|12)$.

The unified description of the core-plus-alpha-particle states of the two nuclei showed the presence of the dynamical supersymmetry with an accuracy, which is comparable to the that found in the application of the dynamical supersymmetry of the quadruple collectivity to heavy nuclei [28].

VIII. MULTICHANNEL DYNAMICAL SYMMETRIES

Multichannel dynamical symmetry (MUSY) may describe different cluster configurations of the same nucleus in a unified framework [29,30]. The basic concept can be formulated as follows.

For the sake of simplicity we consider two different binary clusterizations of an atomic nucleus:

$$c : C_1 + C_2, \quad d : D_1 + D_2. \tag{17}$$

(E. g. the ^{28}Si nucleus may have, and in fact has, some important contributions from the ^{16}O+^{12}C and ^{24}Mg+^{4}He configurations.)

The relation of these different binary cluster configurations can be established by considering an underlying three-cluster configuration. Then we have two independent relative motions, both of them are described by a vibron model with $U(4)$ group structure.

Let us suppose that the relation of the mass-numbers of the clusters are:

$$A_{C_1} \geq A_{C_2},\ A_{D_1} \geq A_{D_2},\ A_{D_1} \geq A_{C_1}, \tag{18}$$

what can be done without any loss of generality. (In the example of the ^{28}Si nucleus, mentioned before, C_1:^{16}O, C_2:^{12}C, D_1:^{24}Mg, D_2:^{4}He.) Let us consider the three-cluster configuration

$$(C_1) + (CD) + (D_2),\ \ (CD) = (C_2 - D_2) = (D_1 - C_1). \tag{19}$$

(In the example: ^{16}O + ^{8}Be + ^{4}He.)

We choose the following two sets of Jacobi-coordinates:

$$\begin{aligned} & \mathbf{t}_c = \mathbf{r}_{D_2} - \mathbf{r}_{CD},\ \mathbf{s}_c = \mathbf{r}_{C_1} - (M_{D_2}\mathbf{r}_{D_2} + M_{CD}\mathbf{r}_{CD})/(M_{D_2} + M_{CD}), \\ & \mathbf{t}_d = \mathbf{r}_{C_1} - \mathbf{r}_{CD},\ \mathbf{s}_d = \mathbf{r}_{D_2} - (M_{C_1}\mathbf{r}_{C_1} + M_{CD}\mathbf{r}_{CD})/(M_{C_1} + M_{CD}), \end{aligned} \tag{20}$$

where M is the mass and $\mathbf{r}$ is the space vector of the corresponding cluster. Then, obviously, the clusterization $C_1 + C_2$, corresponds to the coordinate set c with some restriction on $\mathbf{t}_c$, while clusterization $D_1 + D_2$ corresponds to the coordinate set d with some restriction on $\mathbf{t}_d$.

Since we are interested in the transformations which connect the different binary configurations (different Jacobi-coordinates of the three cluster system), instead of applying a $U_1(4) \otimes U_2(4)$ model, we embed it into the larger group of $U(8)$.

The transformation from the clusterization $C_1 + C_2$ to that of $D_1 + D_2$ amounts to a transformation between the two sets of Jacobi-coordinates: $\mathbf{t}_c, \mathbf{s}_c$ and $\mathbf{t}_d, \mathbf{s}_d$, known as the Talmi-Moshinsky-Smirnov (TMS) transformation [31,32]. These transformations are known to have a $U_q(2)$ group structure [31], where q refers to the quasispin group, which acts in the particle index space [33].

Thus the multichannel symmetry is described by the group-chain:

$$U(8) \supset\ U(6) \supset \{U_q(2) \supset SU_q(2) \supset SO_q(2)\} \otimes \{U(3) \supset SU(3) \supset SO(3)\} \tag{21}$$

and the Hamiltonian of the system is obtained in terms of the invariant operators of these algebras [30].

The multichannel symmetry establishes a strict correlation between the observables of different clusterizations. In this sense it is a very restrictive symmetry, however, because of the same feature it has a very strong predictive power as well. For example, the Hamiltonian of one cluster configuration may completely determine the energy spectrum

of another cluster configuration, without any free parameter (and without any ambiguity in the model space, due to its microscopic construction).

Some applications of this kind have been carried out [29,34]. In [29] e.g. the ^{24}Mg + ^{4}He, and ^{16}O + ^{12}C spectra were described with the same Hamiltonian in a wide energy range. Furthermore, the density of α-particle (scattering or capture) resonances were predicted by this Hamiltonian, without any parameter fitted in the relevant energy region, and the result turned out to be in good agreement with the experimental observation.

IX. ON THE COMPOSITE DYNAMICAL SYMMETRIES

Both the dynamical supersymmetry and the multichannel dynamical symmetry deal with composite systems consisting of two different sectors. Therefore, they are called composite symmetries. Their logical structure show remarkable similarities, and it was discussed in detail in [35].

In addition to the similarities, however, one can realize considerable differences as well. Here we mention one, which has to do with the physical nature of the transformations between the two sectors (supertransformations in SUSY, and TMS transformations in MUSY).

In the case of SUSY the dynamical breaking of the symmetry is (usually) carried out in such a way the invariance with respect to the super transformations is not required, because already in the first step only classical Lie algebras (not super algebras) appear in the algebra-chain.

In the multichannel symmetry, however, the situation is different. Here the dynamic symmetries of the two different cluster configurations are combined with the $U_q(2)$ transformations of the cluster indices. This requires real invariance with respect to some extra transformations (i.e. the generator of $SO_q(2)$).

In this respect the situation is similar to the SUSY models typical in field theory, and exceptional in nuclear physics [36].

X. SUMMARY AND CONCLUSIONS

Nuclear clusterization offers a rich laboratory for the study of symmetries. Dynamical symmetries of different complexity seem to appear in cluster configurations:
- simple dynamical symmetry in the relative motion of two clusters,
- dynamical symmetries in the coupling of the relative motion and internal cluster degrees of freedom,
- effective symmetries in heavy nuclei,
- spectrum-generating dynamical symmetry in light nuclei,
- dynamical supersymmetry, connecting odd and even nuclei,
- multichannel dynamical symmetries, describing different cluster configurations of a nucleus.

This work was supported by the OTKA Grant (No. T22187).

[1] L.I. Schiff, *Quantum Mechanics* (McGraw-Hill, New York, 1968).

[2] F. Iachello and A. Arima, *The interacting boson model* (Cambridge University Press, Cambridge, 1987).

[3] P. Van Isacker, *Rep. Prog. Phys.* **62**, 1661 (1999).

[4] E. P. Wigner, *Phys. Rev.* **51**, 106 (1937).

[5] J. P. Elliott, *Proc. Roy. Soc.* **A245**, 128 and 562 (1958).

[6] J. Cseh and W. Scheid, *J. Phys.* **G18**, 1419 (1992).

[7] J. Cseh, *J. Phys.* **G19**, L97 (1993).

[8] B. R. Fulton and W. D. M. Rae, *J. Phys.* **G16**, 333 (1990).

[9] A. Lépin-Szily et. al., *Phys. Rev. Lett.* **82**, 3972 (1999).

[10] J. Cseh , A. Algora and P. O. Hess, in preparation.

[11] D. J. Rowe, P. Rochford and J. Repka, *J. Math. Phys.* **29**, 572 (1988).

[12] P. Rochford and D. J. Rowe, *Phys. Lett.* **B210**, 5 (1988).

[13] M. Jarrio, J. L. Wood and D. J. Rowe, *Nucl. Phys.* **A528**, 409 (1991).

[14] J. H. Hamilton et. al., *J. Phys.* **G20**, L85 (1994).

[15] A. Algora, J. Cseh and P. O. Hess, *J. Phys.* **G24**, 2111 (1998).

[16] A. Algora, J. Cseh and P. O. Hess, in preparation.

[17] Yu. F. Smirnov and Yu. M. Tchuvil'sky, *Phys. Lett.* **B134**, 25 (1984).

[18] G. G. Adamian, N. V. Antonenko and Yu. M. Tchuvil'sky, *Phys. Lett.* **B451**, 289 (1999).

[19] B. G. Wyborne, *Classical Groups for Physicists*, (John Wiley & Sons, New York, 1974).

[20] F. Iachello, *Phys. Rev.* **C23**, 2778 (1981);
F. Iachello and R.D. Levine, *J. Chem. Phys.* **77**, 3046 (1982).

[21] D. Janssen, R. V. Jolos and F. Dönau, *Nucl. Phys.* **A224**, 93 (1974).

[22] J. Cseh, *Phys. Lett.* **B281**, 173 (1992);
J. Cseh and G. Lévai, *Ann. Phys. (N.Y.)* **230**, 165 (1994).

[23] G. Lévai, J. Cseh and W. Scheid, *Phys. Rev.* **C46**, 548 (1992);
J. Cseh, G. Lévai and W. Scheid, *Phys. Rev.* **C48**, 1724 (1993);
Zs. Fülöp et. al., *Nucl. Phys.* **A604**, 286 (1996);
G. Lévai and J. Cseh, *Phys. Lett.* **B381**, 1 (1996);
J. Cseh, G. Lévai, P. O. Hess and W. Scheid, *Few-Body Systems* **29**, 61 (2000);
L. Hernandéz de la Pena, P.O. Hess, G. Lévai and A. Algora, *J. Phys.* **G27**, 2019 (2001).

[24] T. M. Schneidman, G. G. Adamian, N. V. Antonenko, R. V. Jolos and W. Scheid, *Proc. Int. Symp. Nucl. Struct. Phys., Göttingen, 2001*, eds: R. Casten et. al. (World Sci., Singapore, 2001) p.225.

[25] J. Cseh, R. K. Gupta and W. Scheid, *Phys. Lett.* **B299**, 205 (1993).

[26] J. P. Draayer, *Nucl. Phys.* **A520**, 259c (1990).

[27] G. Lévai, J. Cseh and P. Van Isacker, *Eur. Phys. J.*, in press.

[28] F. Iachello and P. Van Isacker, *The interacting boson-fermion model*, (Cambridge University Press, Cambridge, 1991).

[29] J. Cseh, *Phys. Rev.* **C50**, 2240 (1994).

[30] J. Cseh, *Proc. XXIV. Symp. Nucl. Phys. Taxco, Mexico, 2001*, in press; and to be published.

[31] A. Gal, *Ann. Phys. (N.Y.)* **49**, 341 (1968).

[32] H. Horiuchi, *Prog. Theor. Phys.* **58**, 204 (1977).

[33] V. Bargmann and M, Moshinsky, *Nucl. Phys.* **18**, 697 (1960).

[34] J. Cseh, G. Lévai, A. Ventura and L. Zuffi, *Phys. Rev.* **C58**, 2144 (1998).

[35] J. Cseh, *Proc. Int. Workshop on Symmetries and Spin, Praha, 2001*, in press.

[36] R. V. Jolos and P. von Brentano, *Phys. Rev.* **C60**, 064318 (2000).

Finite rank approximation for Skyrme interactions and quasiparticle RPA

A.P. Severyukhin[1], Ch. Stoyanov[2], V.V. Voronov[1] and N.V. Giai[3]

1 - Bogoliubov Laboratory of Theoretical Physics, JINR, 141980 Dubna,Russia
2 - Institute for Nuclear Research and Nuclear Energy, Boulevard Tzarigradsko Chausee 72, 1784 Sofia, Bulgaria
3 - Institut de Physique Nucleaire, F-91406 Orsay Cedex, France

Abstract

A finite rank separable approximation for the particle-hole RPA calculations with Skyrme interactions is extended to take into account the pairing. As an illustration of the method energies and transition probabilities for the quadrupole excitations in some nuclei are calculated. The values calculated within our approach are very close to ones that were calculated within QRPA with the total Skyrme interactions. They are in a reasonable agreement with experimental data.

1 Introduction

Many properties of the nuclear states can be described within the random phase approximation (RPA)[1, 2, 3, 4]. The most consistent models employ an effective interaction, which can describe, throughout the periodic table, the ground states in the framework of the Hartree-Fock (HF) approximation and the excited states in time-dependent HF, or the random phase approximation (RPA). The Gogny's interaction[5] and the Skyrme-type interactions[6] are very popular now. Such models are quite successful not only for predicting accurately nuclear ground state properties[7, 8] but also for calculating the main features of giant resonances in closed-shell nuclei[9, 10]. Taking into account of the pairing effects enables one to reproduce many properties of collective states in open-shell nuclei too[11, 12, 13, 14].

It is well known that due to the anharmonicity of vibrations there is a coupling between one-phonon and more complex states [2, 4]. The main difficulty is that the complexity of calculations beyond standard RPA increases rapidly with the size of the configuration space and one has to work within limited spaces. From another point of view more phenomenological models that assume some simple separable form for the residual nucleon-nucleon interaction while the mean field is modelized by an empirical potential well allow one to calculate nuclear excitations in very large configuration spaces since there is no need to diagonalize matrices whose dimensions grow with the size of a configuration space. The well-known quasiparticle-phonon model (QPM) of Soloviev et al.[4] belongs to such a model. Very detailed predictions can be made by QPM for nuclei away from closed shells[15].

A possibility to solve easily the RPA problem when the residual particle-hole (p-h) interaction is separable in considerably smaller configuration space than one for a non-separable interaction was the motivation for proposing in our previous work [16] a finite

rank approximation for the p-h interaction resulting from Skyrme-type forces. Thus, the self-consistent mean field can be calculated in the standard way with the original Skyrme interaction whereas the RPA solutions would be obtained with the finite rank approximation to the p-h matrix elements.

In the present work, we extend a finite rank approximation for p-h interactions of Skyrme type to take into account pairing paying a special attention for the quadrupole excitations in nuclei with very different mass numbers. As an application we present results of calculations for low-lying 2^+ states in some O, Ar, Sn and Pb isotopes.

2 Hamiltonian of the model and QRPA

We start from the effective Skyrme interaction[6] and use the notation of Ref.[17] containing explicit density dependence and all spin-exchange terms rather than the original form of Ref[6] where density dependence at the HF level was introduced by a three-body contact force and where some spin-exchange terms were dropped. The exact p-h residual interaction $\tilde{V}_{res}$ corresponding to the Skyrme force and including both direct and exchange terms can be obtained as the second derivative of the energy density functional with respect to the density[18]. Following our previous paper[16] we simplify $\tilde{V}_{res}$ by approximating it by its Landau-Migdal form in the momentum space:

$$V_{res}(\mathbf{k}_1,\mathbf{k}_2) = N_0^{-1}\sum_{l=0}^{1}\left[F_l + G_l\sigma_1\sigma_2 + (F_l^{'} + G_l^{'}\sigma_1\sigma_2)\tau_1\tau_2\right]P_l(\frac{\mathbf{k}_1\mathbf{k}_2}{k_F^2}), \tag{1}$$

where $\mathbf{k}_i$, σ_i and τ_i are the nucleon momentum, spin and isospin operators, and $N_0 = 2k_F m^*/\pi^2\hbar^2$ with k_F and m^* standing for the Fermi momentum and nucleon effective mass. For Skyrme interactions all Landau parameters with $l > 1$ are zero. Here, we keep only the $l = 0$ terms in V_{res} and in the coordinate representation one can write it in the following form:

$$V_{res}(\mathbf{r}_1,\mathbf{r}_2) = N_0^{-1}\left[F_0(r_1) + G_0(r_1)\sigma_1\sigma_2 + (F_0^{'}(r_1) + G_0^{'}(r_1)\sigma_1\sigma_2)\tau_1\tau_2\right]\delta(\mathbf{r}_1 - \mathbf{r}_2) \tag{2}$$

The expressions for $F_0, G_0, F_0^{'}, G_0^{'}$ in terms of the Skyrme force parameters can be found in Ref.[17]. Because of density dependence of the interaction the Landau parameters of Eq.(2) are functions of the coordinate $\mathbf{r}$. In what follows we use the second quantized representation and V_{res} can be written as:

$$\hat{V}_{res} = \frac{1}{2}\sum_{1234} V_{1234} : a_1^+ a_2^+ a_4 a_3 : \tag{3}$$

where a_1^+ (a_1) is the particle creation (annihilation) operator and 1 denotes the quantum numbers $(n_1 l_1 j_1 m_1)$.

$$V_{1234} = \int \phi_1^*(\mathbf{r}_1)\phi_2^*(\mathbf{r}_2)V_{res}(\mathbf{r}_1,\mathbf{r}_2)\phi_3(\mathbf{r}_1)\phi_4(\mathbf{r}_2)\mathbf{dr}_1\mathbf{dr}_2, \tag{4}$$

$$V_{1234} = \sum_{JM}\hat{J}^{-2}(-)^K\langle j_1 m_1 j_3 - m_3 \mid J - M\rangle\langle j_2 m_2 j_4 - m_4 \mid JM\rangle V_{1234}^J, \tag{5}$$

where $K = J + j_3 + j_4 - M - m_3 - m_4$ and

$$V_{1234}^J = \langle j_1||Y_J||j_3\rangle\langle j_2||Y_J||j_4\rangle I_M(j_1 j_2 j_3 j_4) - \sum_{L=J,J\pm1}\langle j_1||T_{JL}||j_3\rangle\langle j_2||T_{JL}||j_4\rangle I_S(j_1 j_2 j_3 j_4), \tag{6}$$

where $\langle j_1||Y_J||j_3\rangle$ is the reduced matrix element of the spherical harmonics $Y_{J\mu}$, $\hat{J} = \sqrt{2J+1}$, $T_{JL}^M(\hat{r},\sigma) = [Y_L \times \sigma]_J^M$ and $I_M(j_1 j_2 j_3 j_4)$, $I_S(j_1 j_2 j_3 j_4)$ are the radial integrals:

$$I_M(j_1 j_2 j_3 j_4) = N_0^{-1}\int_0^\infty (F_0(r) + F_0'(r)\tau_1\tau_2)\, u_{j_1}(r)u_{j_2}(r)u_{j_3}(r)u_{j_4}(r)\frac{dr}{r^2}, \tag{7}$$

$$I_S(j_1 j_2 j_3 j_4) = N_0^{-1}\int_0^\infty (G_0(r) + G_0'(r)\tau_1\tau_2)\, u_{j_1}(r)u_{j_2}(r)u_{j_3}(r)u_{j_4}(r)\frac{dr}{r^2}, \tag{8}$$

where radial wave functions $u(r)$ are related with the HF single-particle wave functions:

$$\phi_{i,m}(\mathbf{r_1}) = \frac{u_i(r_1)}{r_1}\mathcal{Y}_{l_i j_i}^m(\hat{r_1},\sigma_1)\,. \tag{9}$$

As it is shown in [16] the radial integrals can be calculated accurately by choosing a large enough cutoff radius R and using a n-point integration Gauss formula with abscissas and weights r_k, w_k. Thus the residual interaction can be presented as a sum of n separable terms.

So we employ the hamiltonian including an average nuclear HF field, pairing interactions, the isoscalar and isovector particle hole (p–h) residual forces in a finite rank separable form:

$$\begin{aligned} H = & \sum_\tau\left(\sum_{jm}^{\tau}(E_j - \lambda_\tau)a_{jm}^\dagger a_{jm} - \frac{1}{4}G_\tau^{(0)} : P_0^\dagger(\tau)P_0(\tau) : - \right. \\ & \frac{1}{2}\sum_{k=1}^{N}\sum_{q=\pm1}\sum_{\lambda\mu}\left[\left(\kappa_0^{(M,k)} + q\kappa_1^{(M,k)}\right) : M_{\lambda\mu}^{(k)+}(\tau)M_{\lambda\mu}^{(k)}(q\tau) : + \\ & \left.\sum_{L=\lambda,\lambda\pm1}\left(\kappa_0^{(S,k)} + q\kappa_1^{(S,k)}\right) : S_{\lambda L\mu}^{(k)+}(\tau)S_{\lambda L\mu}^{(k)}(q\tau) :\right]\Bigg) \end{aligned} \tag{10}$$

We sum over the proton(p) and neutron(n) indexes and the notation $\{\tau = (n,p)\}$ is used and a change $\tau \leftrightarrow -\tau$ means a change $p \leftrightarrow n$; k is a rank. The single-particle states are specified by the quantum numbers (jm); E_j are the single-particle energies; λ_τ is the chemical potential; $G_\tau^{(0)}$ is the strength in the p-p channel; $\kappa^{(Mk)}$ ($\kappa^{(Sk)}$) are the multipole (spin-multipole) strengths in the p–h channel and they can be expressed via the Landau parameters as:

$$\begin{pmatrix} \kappa_0^{(M,k)} \\ \kappa_1^{(M,k)} \\ \kappa_0^{(S,k)} \\ \kappa_1^{(S,k)} \end{pmatrix} = -N_0^{-1} \frac{Rw_k}{2r_k^2} \begin{pmatrix} F_0(r_k) \\ F_0'(r_k) \\ G_0(r_k) \\ G_0'(r_k) \end{pmatrix} \tag{11}$$

The monopole pair creation, the multipole and spin-multipole operators entering the normal products in (10) are defined as follows:

$$P_0^+(\tau) = \sum_{jm}{}^{\tau} (-1)^{j-m} a_{jm}^+ a_{j-m}^+,$$

$$M_{\lambda\mu}^{(k)+}(\tau) = \hat{\lambda}^{-1} \sum_{jj'mm'}{}^{\tau} (-1)^{j+m} \langle jmj'-m' \mid \lambda\mu\rangle f_{j'j}^{(\lambda k)}(\tau) a_{jm}^+ a_{j'm'},$$

$$S_{\lambda L\mu}^{(k)+}(\tau) = \hat{\lambda}^{-1} \sum_{jj'mm'}{}^{\tau} (-1)^{j+m} \langle jmj'-m' \mid \lambda\mu\rangle f_{j'j}^{(\lambda L k)}(\tau) a_{jm}^+ a_{j'm'},$$

where $f_{j'j}$ are the single particle radial matrix elements of the multipole and spin-multipole operators:

$$f_{j_1j_2}^{(\lambda k)} = u_{j_1}(r_k) u_{j_2}(r_k) i^{\lambda} \langle j_1 || Y_\lambda || j_2\rangle$$

$$f_{j_1j_2}^{(\lambda L k)} = u_{j_1}(r_k) u_{j_2}(r_k) i^{L} \langle j_1 || T_{\lambda L} || j_2\rangle$$

One can see that the hamiltonian (10) has the same form as the QPM hamiltonian with N separable terms, but in contrast to the QPM all parameters of this hamiltonian are expressed through parameters of the Skyrme forces.

In what follows we work in the quasiparticle representation, defined by the canonical Bogoliubov transformation:

$$a_{jm}^+ = u_j \alpha_{jm}^+ + (-1)^{j-m} v_j \alpha_{j-m}. \tag{12}$$

The hamiltonian (10) can be represented in terms of bifermion quasiparticle operators (and their conjugate ones) [4]:

$$B(jj';\lambda\mu) = \sum_{mm'} (-1)^{j'+m'} \langle jmj'm' \mid \lambda\mu\rangle \alpha_{jm}^+ \alpha_{j'-m'},$$

$$A^+(jj';\lambda\mu) = \sum_{mm'} \langle jmj'm' \mid \lambda\mu\rangle \alpha_{jm}^+ \alpha_{j'm'}^+.$$

We introduce the phonon creation operators

$$Q_{\lambda\mu i}^+ = \frac{1}{2} \sum_{jj'} \left(\psi_{jj'}^{\lambda i} A^+(jj';\lambda\mu) - (-1)^{\lambda-\mu} \varphi_{jj'}^{\lambda i} A(jj';\lambda-\mu) \right). \tag{13}$$

where the index λ denotes multipolarity and μ is its z-projection in the laboratory system. One assumes that the ground state is the QRPA phonon vacuum $\mid 0\rangle$, i.e. $Q_{\lambda\mu i} \mid 0\rangle = 0$. We define the excited states for this approximation by $Q_{\lambda\mu i}^+ \mid 0\rangle$. For the QRPA the following relation is valid:

$$\langle 0 \mid [Q_{\lambda\mu,i}, Q_{\lambda'\mu',i'}^+] \mid 0\rangle = \delta_{\lambda\lambda'}\delta_{\mu\mu'} \frac{1}{2} \sum_{jj'} \left(\psi_{jj'}^{\lambda i} \psi_{jj'}^{\lambda i'} - \varphi_{jj'}^{\lambda i} \varphi_{jj'}^{\lambda i'} \right)$$

The quasiparticle energies (ε_j), the chemical potentials (λ_τ), the energy gap and the coefficients u,v of the Bogoliubov transformations (12) are determined from the BCS equations with the single particle spectrum that is calculated within HF method with the effective Skyrme interactions [6]. Making use the linearized equation of motion approach [1]:

$$\langle 0 \mid \left[\delta Q_{\lambda\mu i}, \left[H, Q_{\lambda\mu i}^+\right]\right] \mid 0\rangle = \omega_{\lambda i} \langle 0 \mid \left[\delta Q_{\lambda\mu i}, Q_{\lambda\mu i}^+\right] \mid 0\rangle, \tag{14}$$

with the constrained condition:

$$\langle 0 \mid [Q_{\lambda\mu i}, Q_{\lambda\mu i'}^+] \mid 0\rangle = \delta_{ii'}, \tag{15}$$

one can derive the QRPA equations [3, 4].

$$\begin{pmatrix} \mathcal{A} & \mathcal{B} \\ -\mathcal{B} & -\mathcal{A} \end{pmatrix} \begin{pmatrix} \psi \\ \phi \end{pmatrix} = w \begin{pmatrix} \psi \\ \phi \end{pmatrix} \tag{16}$$

In QRPA problems there appear two types of interaction matrix elements, the $A^{(\lambda)}_{(j_1j_1')_\tau(j_2j_2')_{q\tau}}$ matrix related to forward-going graphs and the $B^{(\lambda)}_{(j_1j_1')_\tau(j_2j_2')_{q\tau}}$ matrix related to backward-going graphs. For our case we get the following expressions:

$$\begin{aligned} A^{(\lambda)}_{(j_1\geq j_1')_\tau(j_2\geq j_2')_{q\tau}} &= \varepsilon_{j_1j_1'}\delta_{j_2j_1}\delta_{j_2'j_1'}\delta_{q1} - \hat{\lambda}^{-2}\left(1+\delta_{j_2j_2'}\right)^{-1} \times \\ &\sum_{k=1}^{N} \Big[(\kappa_0^{(M,k)} + q\kappa_1^{(M,k)}) u_{j_1j_1'}^{(+)} f_{j_1j_1'}^{(\lambda k)}(\tau) u_{j_2j_2'}^{(+)} f_{j_2j_2'}^{(\lambda k)}(q\tau) + \\ &(\kappa_0^{(S,k)} + q\kappa_1^{(S,k)}) u_{j_1j_1'}^{(-)} f_{j_1j_1'}^{(\lambda\lambda k)}(\tau) u_{j_2j_2'}^{(-)} f_{j_2j_2'}^{(\lambda\lambda k)}(q\tau) \Big], \end{aligned} \tag{17}$$

$$\begin{aligned} B^{(\lambda)}_{(j_1\geq j_1')_\tau(j_2\geq j_2')_{q\tau}} &= -\hat{\lambda}^{-2}\left(1+\delta_{j_2j_2'}\right)^{-1} \times \\ &\sum_{k=1}^{N} \Big[(\kappa_0^{(M,k)} + q\kappa_1^{(M,k)}) u_{j_1j_1'}^{(+)} f_{j_1j_1'}^{(\lambda k)}(\tau) u_{j_2j_2'}^{(+)} f_{j_2j_2'}^{(\lambda k)}(q\tau) - \\ &(\kappa_0^{(S,k)} + q\kappa_1^{(S,k)}) u_{j_1j_1'}^{(-)} f_{j_1j_1'}^{(\lambda\lambda k)}(\tau) u_{j_2j_2'}^{(-)} f_{j_2j_2'}^{(\lambda\lambda k)}(q\tau) \Big], \end{aligned} \tag{18}$$

where $\varepsilon_{jj'} = \varepsilon_j + \varepsilon_{j'}$ and $u_{jj'}^{(\pm)} = u_j v_{j'} \pm v_j u_{j'}$.

One can find a prescription how to solve this system and to find the eigenenergies and phonon amplitudes in [16]. The matrix problems never exceed the dimensions $4N \times 4N$. The derived equations have the same form as the QRPA equations in the QPM [4, 19], but the single particle spectrum and parameters of the p-h residual interaction are calculated making use the Skyrme forces.

3 Details of calculations

In this work we use the standard parameterization SIII [20] for the Skyrme force. Spherical symmetry is assumed for the HF ground states. The pairing constants G_τ^0 are fixed to reproduce the odd-even mass difference of neighboring nuclei. As a result constant pairing gaps have values that are very close to $\Delta = 12.A^{-1/2}$ besides a case of semimagic nuclei. It is well known [11, 13] that the constant gap approximation leads to an overestimation of occupation probabilities for subshells that are far from the Fermi level and it is necessary to introduce a cut-off in the single-particle space. Above this cutoff subshells don't participate in the pairing effect. In our calculations we choose the BCS subspace to include all subshells lying below 5 MeV. In order to perform RPA calculations, the single-particle continuum is discretized [21] by diagonalizing the HF hamiltonian on a basis of twelve harmonic oscillator shells and cutting of the single-particle spectra at the energy 190 MeV. This is sufficient to exhaust practically all the energy-weighted sum rule (EWSR). As it was shown in our previous calculations [16] we have adopted the value N=24 for the finite rank approximation for the dipole and quadrupole excitations in Ar isotopes. An increasing of a mass number and a multipolarity of excitations demands of an increasing of a rank to keep an accuracy in calculations. Our investigations enable us to conclude that N=45 is enough for a multipolarity $\lambda \leq 3$ in nuclei with $A \leq 208$. Increasing N, for example, up to N=60 in ^{208}Pb changes results for energies and transition probabilities not more than by 1%, so all calculations in what follows have been done with N=45. Our calculations show that for the normal parity states one can neglect by the spin-multipole parts of interactions as a rule and this leads to the double reduction of the total matrix dimension. For example, for the quadrupole excitations in ^{206}Pb we need to diagonalize a matrix having a dimension 2N=90 instead of 1086 as it takes place for the exact diagonalization case. In our calculations for light nuclei a reduction of matrix dimensions due to the separable approximation is 3 or 4. So for heavy nuclei our approach gives a visible gain in comparison with an exact diagonalization. It is worth to point out that after solving the RPA problem with a separable interaction taking into account of the coupling with two-phonon configurations demands to diagonalize a matrix having a size that does not exceed 40 for the giant resonance calculations in heavy nuclei whereas one needs to diagonalize a matrix with a rank of an order of a few thousands at least for a nonseparable case.

4 Results of calculations

As a first example of calculations within our approach we demonstrate our results and experimental data [22] for the 2_1^+ state energies and transition probabilities $B(E2)$. They are shown in the table 1. One can see that there is a satisfactory agreement with experimental data. Results of our calculations for isotopes of O and Ar are close to ones within QRPA with the Skyrme forces [11, 23] and calculations fail to reproduce the B(E2)-value in ^{18}O. Making use of the SGII interaction[17] improves a description for the O isotopes and gives practically the same results for the Ar isotopes, but for Sn and Pb isotopes a description becomes much worse. Calculations with Ski4 forces don't change conclusion

Table 1: Energies and B(E2)-values for up-transitions to the first 2^+ states

Nucleus	Energy (MeV)		B(E2↑) (e^2fm^4)	
	Exp.	Theory	Exp.	Theory
^{18}O	1.98	4.75	45±2	14
^{20}O	1.67	4.17	28±2	20
^{36}Ar	1.97	1.91	300±30	310
^{38}Ar	2.17	2.51	130±10	110
^{40}Ar	1.46	2.17	330±40	290
^{112}Sn	1.26	1.49	2400±140	2600
^{114}Sn	1.30	1.51	2400±500	2100
^{206}Pb	0.80	0.96	1000±20	1700
^{208}Pb	4.09	5.35	3000±300	2000

mentioned above. A behaviour of the B(E2)-values in the Ar isotopes demonstrates clear effects of the pairing. The experimental and calculated B(E2)-value for ^{38}Ar is three times less than ones in ^{36,40}Ar. A closer of the neutron shell leads to the vanishing of the neutron pairing and a reduction of the proton gap. As a result there is a remarkable reduction of the E2 transition probability in ^{38}Ar. Some exceeding of calculated energies over experimental values indicates that there is a room for the two-phonon terms effects. As it was found in calculations that were performed within the QPM for ^{208}Pb [24] taking into account of the two-phonon configurations can shift down the 2_1^+ energy by more than 1 MeV. The B(E2)-value reduction is about 10% in this case. The study of an influence of the two-phonon configurations on properties of the low lying states within our approach is in progress now.

An additional information about a structure of the first 2^+ states can be extracted from an investigation of the ratio of the multipole transition matrix elements M_n/M_p that depends on the relative contribution of the proton and neutron configurations. In the framework of the collective model for the isoscalar excitations this ratio is equal to $M_n/M_p = N/Z$ and any deviation from this value can indicate on an isovector character of a state. The M_n/M_p ratio can be determined experimentally by using different external probes [25, 26, 27]. Recently [12, 23] the QRPA calculations with Skyrme forces for the M_n/M_p ratios for the 2_1^+ states in some O and Ar isotopes have been done. The microscopic calculations are in a good agreement with experimental data [23]. Our results support conclusions of papers [12, 23] about the isovector character of the 2_1^+ states in ^{18,20}O and ^{38}Ar. This conclusion is valid for any set of the Skyrme forces parameters discussed in this work.

5 Conclusion

A finite rank separable approximation for the particle-hole RPA calculations with Skyrme interactions that was proposed in our previous work is extended to take into account the pairing. The QRPA equations are derived for this case. These equations are used to study quadrupole excitations in nuclei with very different mass numbers. It is shown that the suggested approach enables one to reduce remarkably a rank of matrixes that must be diagonalized to perform structure calculations in very large spaces.

As an illustration of the method we have used the finite rank p-h interaction derived from the Skyrme force SIII to calculate the energies and transition probabilities for the 2_1^+ states in some O, Ar, Sn and Pb isotopes. The values calculated within our approach are very close to ones that were calculated in a framework of QRPA with the total Skyrme interactions. They are in a reasonable agreement with experimental data mostly. A developed approach can be generalized to take into account the coupling between the one- and two-phonon terms and such investigations are in progress now.

6 Acknowledgments

Authors thank Profs. D. Karadjov and W. Nawrocka for useful discussions. A.P.S. and V.V.V. thank the hospitality of IPN-Orsay where the main part of this work was done. This work is partly supported by IN2P3-JINR agreement and by the Bulgarian Science Foundation.

References

[1] D.J.Rowe, "Nuclear Collective Motion, Models and Theory" (Barnes and Noble, 1970).

[2] A. Bohr and B. Mottelson, "Nuclear Structure" **vol.2** (Benjamin, New York, 1975).

[3] P.Ring and P.Schuck, "The Nuclear Many Body Problem" (Springer, Berlin, 1980).

[4] V.G. Soloviev, "Theory of Atomic Nuclei: Quasiparticles and Phonons" (Institute of Physics, Bristol and Philadelphia, 1992).

[5] D. Gogny, in *Nuclear Self-consistent Fields*, eds. G. Ripka and M. Porneuf (North-Holland, Amsterdam, 1975).

[6] D. Vautherin and D.M. Brink, Phys. Rev. **C 5**, 626 (1972).

[7] H. Flocard and P. Quentin, Ann. Rev. Nucl. Part. Sci. **28**, 523 (1978).

[8] J. Dobaczewski, W. Nazarewicz, T.R. Werner, J.F. Berger, C.R. Chinn and J. Dechargé, Phys. Rev. **C 53**, 2809 (1996).

[9] G. Colò, P.F. Bortignon, N. Van Giai, A. Bracco and R.A. Broglia, Phys. Lett. **B276**, 279 (1992).

[10] G. Colò, N. Van Giai, P.F. Bortignon and R.A. Broglia, Phys. Rev. **C50**, 1496 (1994).

[11] E. Khan and Nguyen Van Giai, Phys. Lett. **B 472**, 253 (2000).

[12] E. Khan et al., Phys. Lett. **B 490**, 45 (2000).

[13] G. Colò and P.F. Bortignon, Nucl. Phys. **A696**, 427 (2001).

[14] G. Colò, N. Van Giai, P.F. Bortignon and M.R. Quaglia, Phys. Lett. **B485**, 362 (2000).

[15] S. Galès, Ch. Stoyanov and A.I. Vdovin, Phys. Rep. **166**, 127 (1988).

[16] Nguyen Van Giai, Ch. Stoyanov and V.V. Voronov, Phys. Rev. **C57**,1204 (1998).

[17] Nguyen Van Giai and H. Sagawa, Phys. Lett. **106 B**, 379 (1981).

[18] G.F. Bertsch and S.F. Tsai, Phys. Reports **18 C**, 126 (1975).

[19] V.G. Soloviev, Yad. Fiz. **50**, 40 (1989).

[20] M. Beiner, H. Flocard, Nguyen Van Giai and Ph. Quentin, Nucl. Phys. **A 238**, 29 (1975).

[21] J.P. Blaziot and D. Gogny, Nucl. Phys., **A284**, 429 (1977).

[22] S. Raman, C.W. Nestor Jr. and P. Tikkanen, At. Data and Nucl. Data Tables **78**, 1 (2001).

[23] E. Khan et al., Nucl. Phys. **A694**, 103 (2001).

[24] V.G. Soloviev, Ch. Stoyanov and V.V. Voronov, Nucl. Phys. **A399**, 141 (1983).

[25] A.M. Bernstein, V.R. Brown and V.A. Madsen, Comments Nucl. Part. Phys., **11**, 203 (1983).

[26] M.A. Kennedy, P.D. Cottle and K.W. Kemper, Phys. Rev., **C 46**, 1811, (1992).

[27] J.K. Jewell et al., Phys. Lett. **B 454**, 181 (1999).

EFFECT OF STRUCTURAL FORBIDDENNESS IN FUSION OF HEAVY NUCLEI

Yu.M.Tchuvil'sky[1,2,3], G.G.Adamian[2,3,4], N.V.Antonenko[2,3]
[1]*Institute of Nuclear Physics, Moscow State University, 119899 Moscow, Russia*
[2]*Joint Institute for Nuclear Research, 141980 Dubna, Russia*
[3]*Institut für Theoretische Physik der Justus-Liebig-Universität, D-35392 Giessen, Germany*
[4]*Institute of Nuclear Physics, Tashkent 702132, Uzbekistan*

With a microscopic approach based on the formalism of irreducible representations of the SU(3) group the influence of structural forbiddenness on the fusion of heavy nuclei and the dinuclear system phenomenon are investigated for different symmetric and asymmetric reactions used in the synthesis of heavy and superheavy nuclei. A large hindrance is obtained for the motion to smaller elongations of dinuclear systems. The comparison of the calculated energy thresholds for the complete fusion in different relevant collective variables shows that the dinuclear system prefers to evolve in the mass asymmetry coordinate by nucleon transfer to the compound nucleus.

With an algebraic description [1,2] we try to study the structural forbiddenness effect on the fusion of heavy nuclei and the factors decreasing forbiddenness, and the competition between two possible fusion channels. The first one (R-channel) is the transition of the dinuclear system (DNS) into the compound nucleus with increasing neck and decreasing relative distance R between the centers of interacting nuclei at fixed mass asymmetry $\eta = (A_2 - A_1)/A$ (A_1 and A_2 are the mass numbers of the DNS nuclei and $A = A_1 + A_2$). The second channel (η-channel) is the evolution of the DNS to the compound nucleus in mass asymmetry by nucleon transfer from a light nucleus to a heavy one [3–6] (DNS concept).

The concept of structural forbiddenness [1] is based on the difference created by action of the Pauli principle between the compound state and the heavy cluster state. If the wave functions of colliding ions are described with the oscillator quanta numbers N_{A_1} and N_{A_2}, the difference $n = N_A - N_{A_1} - N_{A_2}$ determines the minimal number of oscillator quanta for the wave function of relative motion characterizing by the number of nodes $(n - l)/2$ (l is the angular momentum of relative motion). This is referred to the Talmi-Moshinsky rule which holds good for light cluster channels. For heavy cluster channels the problem is essentially more complicated. For the fusion channel $A_1 + A_2 \to A$, with the wave function

$$\Psi_{A_1+A_2} = \hat{A}\{\Psi_{A_1}\Psi_{A_2}\phi(R)\}, \qquad (1)$$

where Ψ_{A_i} are the cluster wave functions which have the lowest numbers N_{A_i} allowed by Pauli principle, $\phi(R)$ is the function of their relative motion along collision axis z and $\hat{A}$ is operator of antisymmetrization, the minimal oscillator quanta $N_{A_1+A_2}$ is determined by application of the SU(3) group theory [1,2]. The fact is that $\Psi_{A_1+A_2}$ and Ψ_A belong to different SU(3) (or Sp(2,R) for deformed nuclei A_1 and A_2) representations. We have to construct the U(3) irreducible representation $[f_z f_y f_x]$ for $\Psi_{A_1+A_2}$ which possesses by minimal sum $f_x + f_y + f_z$ and does not vanish with antisymmetrization. The proper procedure for the construction of the vector of highest weight of this representation is the

use of the vector of highest weight for the wave function of the relative motion and the vectors of lowest weights for the wave functions of the fragments which possess by the maximal value of the sum $f_x^{(1)} + f_y^{(1)} + f_x^{(2)} + f_y^{(2)}$ (upper index denotes the fragment). The resulting $N_{A_1+A_2}$ value turns out to be essentially large than N_A if the mass of the lighter fragment is rather large. Therefore, in heavy ion physics we obtained the generalization of the Talmi-Moshinsky rule. The minimal difference $q = N_{A_1+A_2} - N_A$ is referred to the degree of structural forbiddenness for fusion channel $A_1 + A_2 \to A$. The wave function $\Psi_{A_1+A_2}$ of the DNS has nonvanishing overlap integral with wave function Ψ_A of the compound nucleus if $N_{A_1+A_2} \geq N_A + q$.

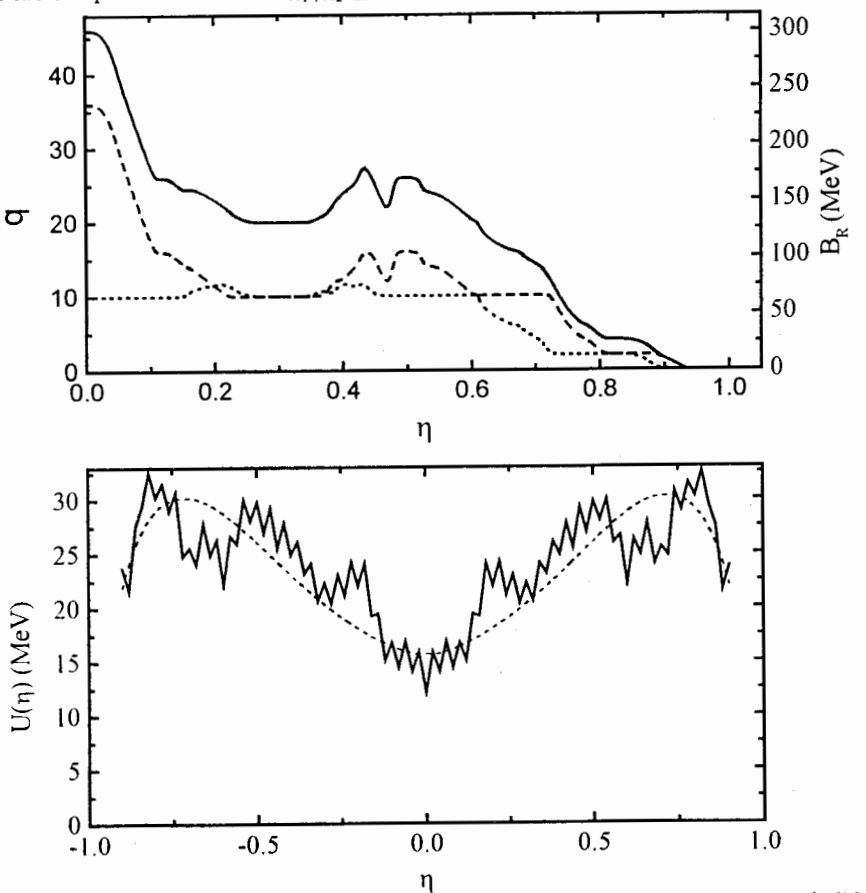

FIG. 1. The degree of structural forbiddenness q as a function of mass asymmetry η (solid line) in the DNS corresponding to ^{246}Fm compound nucleus (upper part). The contributions to q from protons and neutrons are presented by dotted and dashed lines, respectively. Potential energy of the DNS corresponding to ^{246}Fm compound nucleus as a function of mass asymmetry η at zero angular momentum (low part). Solid and dashed lines present the results obtained with realistic and liquid drop binding energies in (2), respectively. The spherical nuclei were taken in the DNS

The forbiddenness effect is model independent and the SU(3) approach is only the simple method to determine it. The numbers N_{A_i} may be larger than lowest ones allowed by the Pauli principle due to the same reasons as in the compound nucleus. As the result, the order of structural forbiddenness q slightly decreases. With the pole-to-pole orientation in the DNS consisting of the deformed nuclei the values of q are larger than ones for the DNS with the spherical nuclei. Since in the collisions near the Coulomb barrier this orientation effect is more important than other effects leading to the decrease of q, in our calculations with spherical nuclei we obtain the minimal value of q.

The quantity $B_R = \hbar\omega q$ ($\hbar\omega = 41\mathrm{MeV}A^{-1/3}$) is a qualitative estimation of the minimal energy thresholds for the fusion in relative distance R degree of freedom at fixed mass asymmetry η. If the excitation energy of system is much smaller than the value of B_R, the fusion process in the R-channel is strongly forbidden.

One can see in Fig. 1 that the dependence of q on η is not monotonic, the q-value is maximal for almost symmetric combinations and it decreases with increasing η. The neutron subsystem mainly contributes to the q-value for small mass asymmetry. Since the absolute values of q (or B_R) are large for not very asymmetric DNS, there is a strong hindrance for the evolution of these DNS to smaller R due to the large energy barrier between the initial DNS and compound shapes. The reason is likely that the shape change must proceed via intermediate shapes that have higher energy.

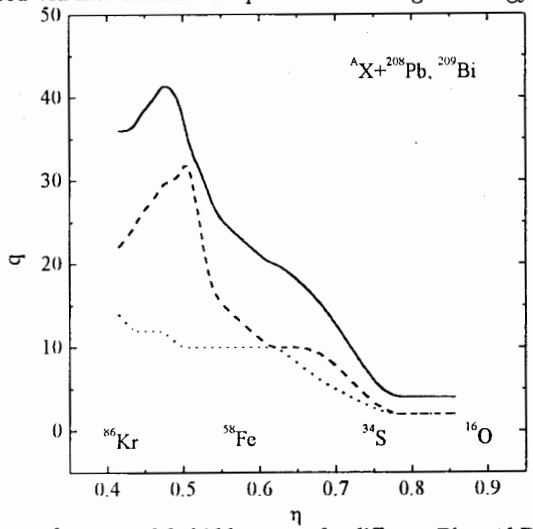

FIG. 2. The degree of structural forbiddenness q for different Pb- and Bi-based reactions as a function of mass asymmetry of the entrance DNS. The contributions to q from protons and neutrons are presented by dotted and dashed lines, respectively

The potential energy [4,5]

$$U(\eta) = B_1 + B_2 + V(R_m, \eta) - B_{12} \qquad (2)$$

of the DNS leading to the same ^{246}Fm compound nucleus as function of mass asymmetry η is presented in Fig. 1. In Eq. (2) B_1, B_2, and B_{12} are the realistic (for small excitation energy) or liquid drop (for large excitation energy) binding energies of the fragments and

the compound nucleus, respectively. The DNS are localized in the minimum of the pocket of the nucleus-nucleus potential $V(R,\eta)$ at $R = R_m \approx R_1 + R_2 + 0.5$ fm (R_1 and R_2 are the radii of the DNS nuclei). In the DNS concept [3–5] the complete fusion occurs through the η channel. It is in opposite to the macroscopic models in which the fusion is mainly considered as the motion in R-channel. The complete fusion in the η-channel is assumed to occur when the DNS overcomes the maximum of $U(\eta)$ (Businaro-Gallone point) at $\eta = \eta_{BG}$ [4] (Fig. 1). The value of $B_\eta = U(\eta_{BG}) - U(\eta_i)$ (η_i is η for the initial DNS) supplies the hindrance of complete fusion in the DNS concept. The energy required to overcome the fusion barrier B_η is contained in the DNS excitation energy. Starting with hypothesis that DNS configurations do not dissolve in the R-channel, the DNS fusion model gives impressive agreement with the experiment [4,5].

Table 1. Calculated with the DNS model [th.] [5] and experimental [exp.] [9] evaporation residue cross sections for several 1n Pb-based reactions. Calculated [th.] values of excitation energy E^*_{CN} of the compound nucleus are compared with the experimental [exp.] ones. The values of q, B_R and B_η are explained in the text.

Reactions	E^*_{CN} [th.] (MeV)	E^*_{CN} [exp.] (MeV)	B_η (MeV)	q	B_R (MeV)	σ_{1n} [th.]	σ_{1n} [exp.]
^{50}Ti+^{208}Pb $\rightarrow^{258}$ 104	16.1	16	4.7	20	129	14.3 nb	10 nb
^{54}Cr+^{208}Pb $\rightarrow^{262}$ 106	16.0	15.5	5.5	22	141	0.4 nb	0.5 nb
^{58}Fe+^{208}Pb $\rightarrow^{266}$ 108	15.5	14.8	7.2	24	153	48 pb	70 pb
^{64}Ni+^{208}Pb $\rightarrow^{272}$ 110	10.7	10.5	7.2	30	190	17 pb	15 pb
^{70}Zn+^{208}Pb $\rightarrow^{278}$ 112	9.8	10.0	8.8	40	251	1.8 pb	0.5 pb
^{70}Zn+^{209}Bi $\rightarrow^{279}$ 113	10.6		9.3	40	250	0.2 pb	

It is seen in Fig. 1 that the fusion barrier B_η for the initial DNS increases with decreasing η ($\eta < \eta_{BG}$). The decrease of the fusion cross section with η was experimentally confirmed [7]. The comparison of calculated energy thresholds for complete fusion in the R- and η- channels demonstrates the preference of the η-channel considered in the DNS concept. For $|\eta| > |\eta_{BG}|$, the very asymmetric systems can fuse in the η-channel as well as in the R-channel. As follows from our analysis, in the R-channel as well as in the η-channel the complete fusion in symmetric reactions ($\eta_i = 0$) yields smaller cross sections in comparison with asymmetric combinations. With the large q-values the nuclei of the DNS keep their individuality during the evolution to compound nucleus in η. The effect of structural forbiddenness is the one of reasons for the stability of the DNS against the dissolution into the R-channel. In addition, within the microscopical treatment [8] we obtained the large inertia and friction coefficients for the neck coordinate which supply the long lifetime for the DNS-type configuration and the applicability of our algebraic approach to calculate the energy threshold in the R-channel. There is strong correlation between large mass inertia and large degree of structural forbiddenness for the heavy DNS. Since the q-values are very large for heavy DNS and the fusion is quite fast process, the system has no time for destroying the "nuclear memory" about the structural forbiddenness [2,6]. This time, which is necessary to reorganize the densities of the system for the transition from frozen density to the adiabatic potential, is related to the characteristic time τ for the deformation (neck) degrees of freedom. The value of τ is

comparable with the fusion time and correspondingly the fusion process is mainly ruled by the frozen density potential.

For the reactions ^{123}Sn+^{123}Sn, ^{124}Sn+^{124}Sn, ^{132}Sn+^{132}Sn, ^{130}Xe+^{130}Xe, ^{136}Xe+^{136}Xe, ^{136}Xe+^{142}Ce, ^{136}Xe+^{170}Er and ^{128}Te+^{138}Ba we obtained q=46, 44, 40, 40, 40, 42, 44 and 40, respectively. Since the fusion probabilities in symmetric reactions with heavy nuclei are very small in the R and η-channels ($B_\eta > 20$ MeV), one can not expect large yields of evaporation residues in these reactions. In the reactions ^{209}Bi + ^{136}Xe and ^{208}Pb + ^{197}Au the dominance of the binary reaction channel at bombarding energy till 30 MeV/nucleon [11] is supported by large q–values 40 and 96, respectively.

For symmetric and Pb–, Bi–based reactions in Fig. 2 the obtained q-values are large enough for keeping the DNS configurations and their evolution in η or decay in R. The barrier in R-channel is much larger than one in η-channel but the trends of these barriers on the charge number Z_{CN} of compound nucleus are similar. The experimental [9] evaporation residues cross sections σ_{ER} are in agreement with the data calculated with the fusion in η [5] (see Table 1).

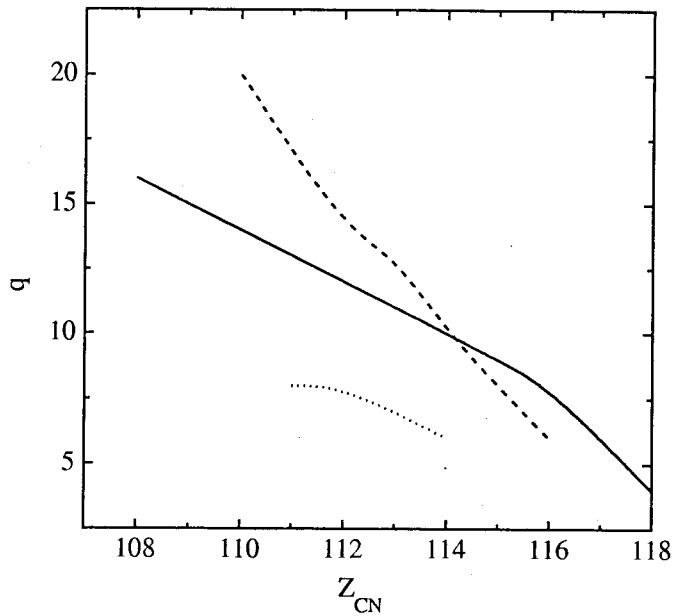

FIG. 3. Calculated values of q for actinide-based reactions ^{48}Ca+^{232}Th, ^{244}Pu, ^{243}Am, ^{248}Cm, ^{249}Cf (solid line), ^{40}Ar+^{232}Th, ^{244}Pu,^{243}Am,^{248}Cm, ^{249}Cf (dashed line) and ^{32}S+^{243}Am, ^{248}Cm,^{249}Cf (dotted line) as a function of atomic number Z_{CN} of the compound nucleus

The results of Fig. 3 show that q-value decreases with increasing atomic number of target-nucleus for actinide-based fusion reactions [10]. For the reaction ^{48}Ca+^{249}Cf→^{297}118, the q-value is the smallest one and B_R=25 MeV. The fusion barriers B_η in mass asymmetry are 7, 9, 11 and 15 MeV for the reactions ^{48}Ca+^{232}Th→^{280}110, ^{48}Ca+^{238}U→^{286}112, ^{48}Ca+^{244}Pu→^{292}114 and ^{48}Ca+^{249}Cf→^{297}114, respectively. For the reactions ^{238}U+^{50}Ti, ^{54}Cr, ^{58}Fe, ^{64}Ni, ^{70}Zn we obtained q=12, 10, 8, 8, 14, respectively.

For these reactions, the fusion barriers B_η are large (in comparison to the ones in reactions with ^{48}Ca) but much smaller than B_R. For very asymmetric actinide-based fusion reactions with $A_1 \leq 12$, B_R=B_η=0.

With the concept of structural forbiddenness we demonstrated large energy hindrance for the motion to smaller R in the initial DNS. Therefore, the internal fusion barrier in R seems to be much larger than the barrier in η. The actinide-based reactions with ^{48}Ca and lighter projectiles are seemed to be useful for producing superheavies beyond $Z = 114$.

This work was partly supported by RFBR, grant 00-02-16683.

[1] Yu.F.Smirnov and Yu.M.Tchuvil'sky, Phys.Lett.B 134 (1984) 25; O.F. Nemetz, V.G.Neudachin, A.T.Rudchik, Yu.F.Smirnov and Yu.M.Tchuvil'sky, Nucleon associations in the atomic nuclei and nuclear reactions of multinucleon transfers (Naukova Dumka, Kiev, 1988).

[2] G.G.Adamian, N.V.Antonenko, Yu.M.Tchuvil'sky, Phys.Lett.B 451 (1999) 289.

[3] V.V.Volkov, Izv. AN SSSR ser. fiz. 50 (1986) 1879.

[4] N.V.Antonenko, E.A.Cherepanov, A.K.Nasirov, V.B.Permjakov and V.V.Volkov, Phys. Lett. B 319 (1993) 425; Phys. Rev. C 51 (1995) 2635; G.G.Adamian, N.V.Antonenko and W.Scheid, Nucl. Phys. A 618 (1997) 176; G.G.Adamian, N.V.Antonenko, W.Scheid and V.V.Volkov, Nucl. Phys. A 627 (1997) 332; A 633 (1998) 154; A.Diaz-Torres, G.G.Adamian, N.V.Antonenko, W.Scheid, Phys. Rev. C 64 (2001) 024604.

[5] G.G.Adamian, N.V.Antonenko and W.Scheid, Nucl. Phys. A 678 (2000) 24.

[6] A.Diaz-Torres, G.G.Adamian, N.V.Antonenko, W.Scheid, Phys. Lett. B 481 (2000) 228; G.G.Adamian, N.V.Antonenko, A.Diaz-Torres, W.Scheid, Nucl. Phys. A 671 (2000) 245.

[7] H.Gäggeler et al., Z. Phys. A 316 (1984) 291, K.H.Schmidt, W.Morawek, Rep. Prog. Phys. 54 (1991) 949.

[8] G.G.Adamian, N.V.Antonenko, S.P.Ivanova, W.Scheid, Nucl. Phys. A 646 (1999) 29.

[9] S.Hofmann, G.Münzenberg, Rev. Mod. Phys. 72 (2000) 733; S.Hofmann et al., Preprint GSI-2002-01.

[10] A.V.Yeremin, V.K.Utyonkov and Yu.Ts.Oganessian *in* AIP Conf. Proc. 425 (1998) 16; Yu.Ts.Oganessian et al., Phys. Rev. Lett. 83 (1999) 3154; Nature 400 (1999) 242.

[11] W.U.Schröder, *in* Proc. Int. School- Seminar on Heavy Ion Physics (Dubna, 1993), edited by Yu.Ts.Oganessian and R.Kalpakchieva (JINR, Dubna, 1994) p.166.

Octupole deformation in the actinides and the Interacting Boson Model

N.V. Zamfir

WNSL, Yale University, New Haven, CT 06520, USA

The occurrence of nuclear octupole deformation in the framework of the Interacting Boson Model and the $SU_{spdf}(3)$ dynamical symmetry are discussed. The predictions of *spdf* calculations in the actinides that at medium spin there is an onset of octupole deformation are in agreement with phenomenological staggering index results.

I. INTRODUCTION

Octupole deformation in atomic nuclei have attracted over the years a widespread interest. The question of the existence of octupole deformation is still open and the evolution of octupole correlation is not yet very well understood. There is yet no definite answer which nuclei are octupole deformed, if any, or in which conditions strong octupole correlations occur. The difficulty arises from the fact that there are no specific established phenomenological criteria for the degree of octupole collectivity.

Experimentally, one of the most unique features of the presence of octupole modes is the appearance of alternating parity rotational bands in the form $0^+, 1^-, 2^+, 3^-, ..$ [1]. If the octupole degree of freedom is a vibration built on the ground state, as is typical in quadrupole deformed nuclei, the negative parity states appear at rather high excitation energies, well separated from the positive parity even members of the ground state band. If significant octupole deformation is present, the negative parity states lie much lower and can form an alternating parity sequence with the positive parity levels. Jolos and Brentano [2] related the observed parity splitting to the barrier height of the potential and the tunnelling effect, as a main source of the parity splitting, was calculated in the quasiclassical approximation [3]. It was shown by Jolos et al. [3] that there is a strong spin dependence of the parity splitting and a phenomenological unified staggering index can be introduced (see for ex. Ref. [2, 4]).

In this article, dedicated to Slava Jolos on the occasion of his 60th birthday, a rotational dynamical symmetry of the *spdf*-Interacting Boson Model related to the onset of octupole deformation will be discussed and the results for actinide nuclei will be presented.

II. ROTATIONAL DYNAMICAL SYMMETRY $SU_{\rm spdf}(3)$

Dynamical symmetries of the Interacting Boson Model (IBA) [5], as idealized limits of nuclear collectivity, play a major role in the study of positive parity states in nuclei. Although, the negative parity states were also successfully described in the framework of the IBA, none of the dynamical symmetries of the spdf model have been yet fully exploited. The dynamical symmetries of the associated group, U(16), were studied [6] and completely constructed and classified [7].

An interesting dynamical symmetry is the rotational limit defined by the group chain:

$$\begin{array}{ccccccccccccc} U_{spdf}(16) & \supset & U_{sd}(6) & \otimes & U_{pf}(10) & \supset & SU_{sd}(3) & \otimes & SU_{pf}(3) & \supset & SU_{spdf}(3) & \supset & O_{spdf}(3) \\ N_B & & N_+ & & N_- & & (\lambda_+\mu_+) & & (\lambda_-\mu_-) & & (\lambda\mu) & & J \end{array} \quad (1)$$

This subalgebra separately conserves the number of $s, d(N_+)$ and $p, f(N_-)$ bosons.

A simple dynamical symmetry Hamiltonian for this rotational limit is:

$$H = \epsilon_- \hat{N}_- - \kappa \hat{Q}_{spdf} \cdot \hat{Q}_{spdf} \quad (2)$$

where $\epsilon_- = \epsilon_p = \epsilon_f$ is the boson energy, $\hat{N}_- = \hat{n}_p + \hat{n}_f$ is the boson number operator, and $\hat{Q}_{spdf} = \hat{Q}_{sd} + \hat{Q}_{pf}$ is the quadrupole operator of $SU_{spdf}(3)$.

The spectrum is given by:

$$E = \epsilon_- N_- - \frac{\kappa}{2}[\lambda^2 + \mu^2 + \lambda\mu + 3(\lambda + \mu)] + \frac{3}{8}\kappa J(J+1) \quad (3)$$

Figure 1 shows a typical spectrum corresponding to this symmetry. The ground state and the first excited negative parity band are not dipole-octupole deformed, since $N_- = 0$ and 1, respectively. Rather, this deformation ($N_- = 2$ and 3, respectively) sets in at higher excitation energy (the right-most and left-most bands). If $\epsilon_-/\kappa(2N_B + 4) = 1$ these two bands will form a rotational band of alternating parity states $(0^+, 1^-, 2^+, 3^-, ...)$.

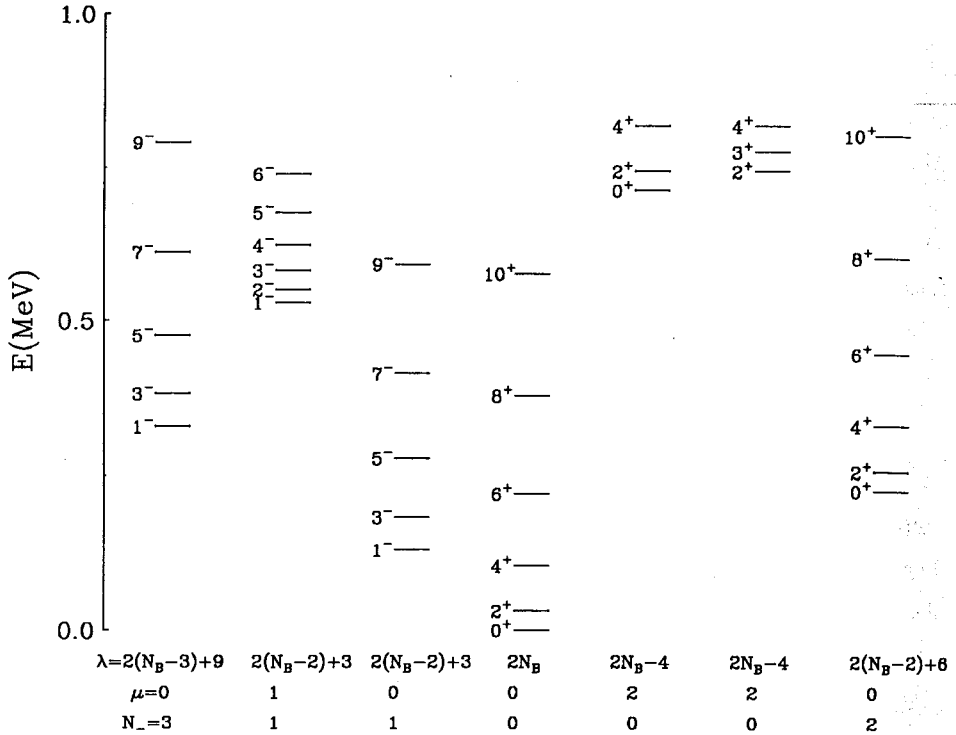

FIG. 1: Spectrum of the $SU_{spdf}(3)$ dynamical symmetry [Eq. (3)] for N_B(total number of bosons)=9, ϵ_-=0.4 MeV, κ=0.014 MeV. The number of negative parity bosons, N_-, and the rotational quantum numbers (λ, μ), are indicated for each band

III. IBA-SPDF CALCULATIONS FOR ACTINIDE NUCLEI

An extensive study of transitional and rotational actinides in the framework of the IBA-*spdf* model shows that, while the properties of the low-lying states can be understood without stable octupole deformation, higher spin states in some of these nuclei have properties which suggest that octupole deformation develops with increasing spin [8].

An Hamiltonian containing the essential degrees of freedom of the evolution from vibrational to rotational structure is:

$$H = \epsilon_d \hat{n}_d + \epsilon_p \hat{n}_p + \epsilon_f \hat{n}_f - \kappa \hat{Q}_{spdf} \cdot \hat{Q}_{spdf} \tag{4}$$

The numerical diagonalizations were done using the computer code OCTUPOLE [10]. The IBA calculations were performed for Rn, Ra, Th, U, and Pu nuclei and some of the results were previously reported in Refs. [8, 9]. The energy of the d boson was $\epsilon_d = 0.3$ Mev and the strength of the quadrupole-quadrupole interaction $\kappa = 0.014$ MeV. The presence of all terms in the Hamiltonian prevents the appearance of a pure dynamical symmetry. However, in some cases (^{224,226}Ra, ^{228}Th), as can be seen in Fig. 2, $\epsilon_p = \epsilon_f$, and, except for the non zero ϵ_d, it is precisely the Hamiltonian [Eq. (2)] for the above mentioned dynamical symmetry.

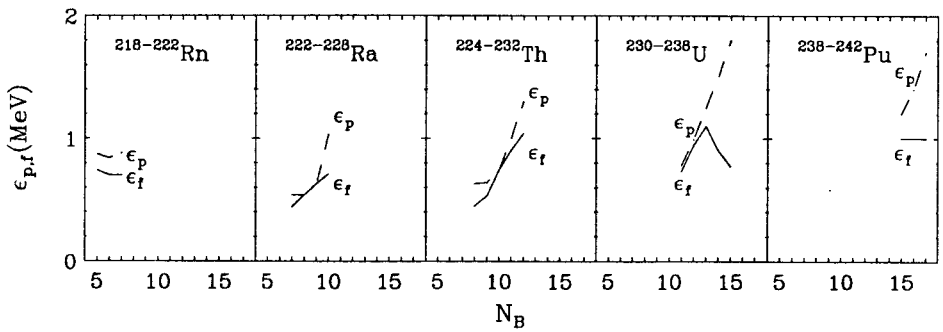

FIG. 2: The energy of the p and f bosons used in the IBA-*spdf* calculations

An important effect of the term $\epsilon_d \hat{n}_d$ is that the bands do not have now the same moment of inertia. The dipole-octupole deformed bands (the $K^\pi = 0^+$ band with N_-=2 and the $K^\pi = 0^-$ band with N_-=3) have a larger moment of inertia than the yrast positive and

negative parity bands. Consequently, at a medium spin the dipole-octupole states become yrast states. The content of pf bosons in yrast states for positive parity is 0 (at low spin) or 2 (at high spin) and, similarly, for negative parity states is 1 or 3 since the above Hamiltonian conserves separately the number of sd and pf bosons. An additional dipole-dipole interaction mixes the states with different pf components. If the interaction is very small the energies are only slightly affected. However, the pf content, due to the increasing with spin of the mutual interaction, is changed, especially at higher spin. The content of pf bosons in yrast states will increase with spin.

Figure 3 shows a comparison of the experimental spectra of ^{226}Ra and ^{228}Th with the IBA calculations. The positive parity band, labelled "a" contains almost no pf bosons at low spin and the band labelled "c" is primarily composed at low spin of $(pf)^2$ bosons. However, at higher spin ($J \sim 14\hbar$ for ^{226}Ra and $J \sim 20\hbar$ for ^{228}Th), the states in bands "a" and "c" mix strongly and the $(pf)^2$ character of the wave functions now appear in band "a". Similarly, the content of pf bosons in the negative parity yrast band $K^\pi = 0^-$ is increasing with spin from mainly $(pf)^1$ at low spin to $(pf)^3$ at high spin. Figure 4 shows that the amount of negative parity bosons in yrast states, i.e., the dipole-octupole deformation is increasing with spin with a sudden increase at spin $J \sim 14\hbar$ for ^{226}Ra and, although less evident, at $J \sim 20\hbar$ for ^{228}Th.

This behavior is mirrored by the data. Figure 5 shows the empirical spin-dependent signature splitting index S(J) [2, 4] for ^{226}Ra and ^{228}Th. The critical spin where $S(J) \sim 0$, i.e., where there is the onset of strong octupole correlations, is indeed $J \sim 14\hbar$ for ^{226}Ra and $J \sim 20\hbar$ for ^{228}Th.

IV. CONCLUSION

A systematic study of the transitional actinides in the framework of the Interacting Boson Model with s, p, d, and f bosons shows that some of these nuclei are very close to the rotational dynamical symmetry $SU_{\rm spdf}(3)$. Although, in the ground state these nuclei are not octupole deformed, the octupole correlations increase with spin and at medium spin there is an onset of octupole deformation, in agreement with phenomenological analysis.

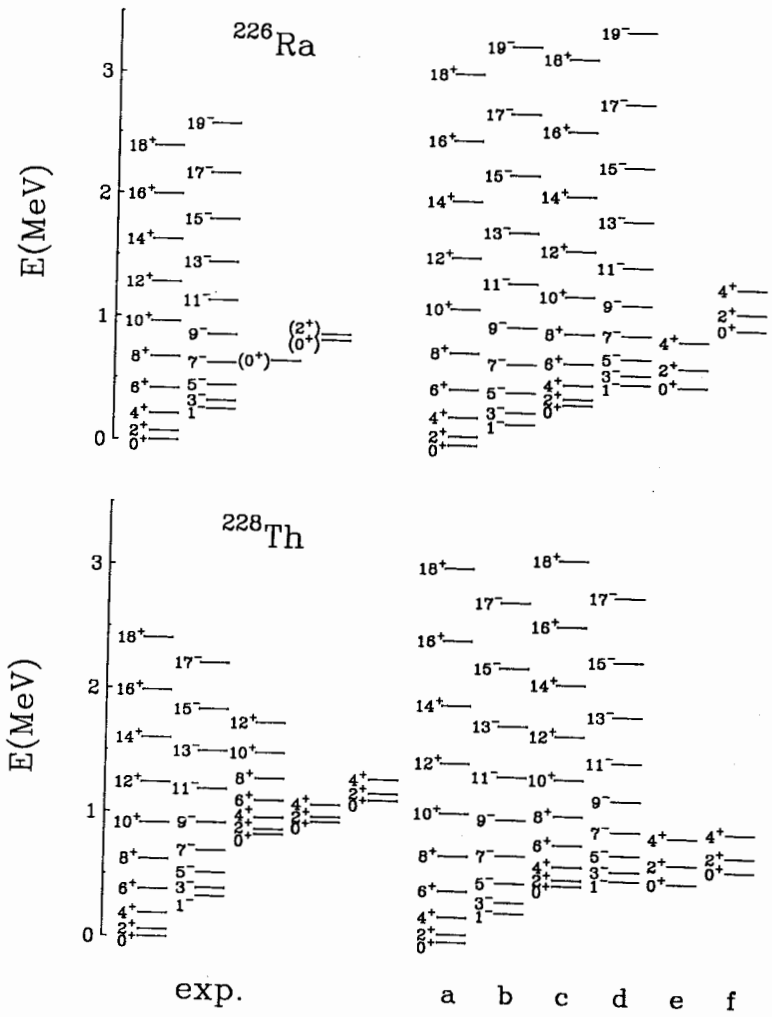

FIG. 3: Comparison of the experimental spectra of ^{226}Ra [11,12] and ^{228}Th [13-15] with IBA-*spdf* calculation with the Hamiltonian in Eq. (4) with the base containing up to 3 negative parity bosons) and a very small dipole-dipole interaction (0.0005 MeV). The other parameters are N_B=9, ϵ_d = 0.3 MeV, $\epsilon_p = \epsilon_f$ = 0.63 MeV, κ = 0.014 MeV for ^{226}Ra and N_B=10, ϵ_d = 0.3 MeV, $\epsilon_p = \epsilon_f$ = 0.74 MeV, κ = 0.014 MeV for ^{228}Th. At low spin, the pf composition in the bands is mainly n_{pf}=0(for band "a"), 1("b"), 2("c"), 3("d"), 0("e"), and 0("f")

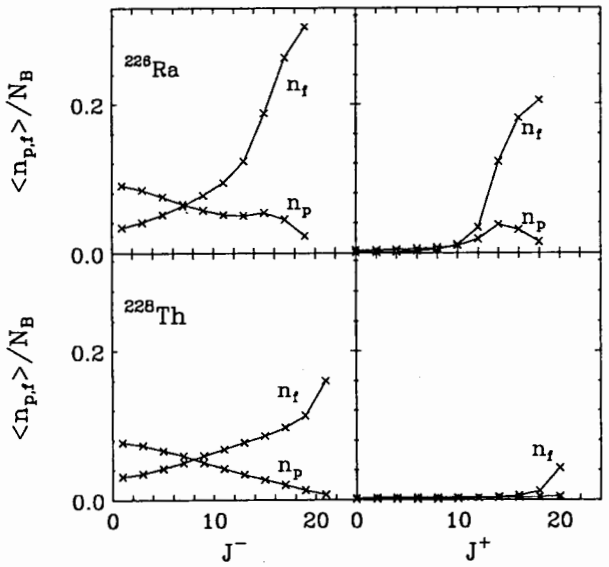

FIG. 4: Negative parity boson content in yrast states as a function of spin in ^{226}Ra and ^{228}Th for the calculation presented in Fig. 3

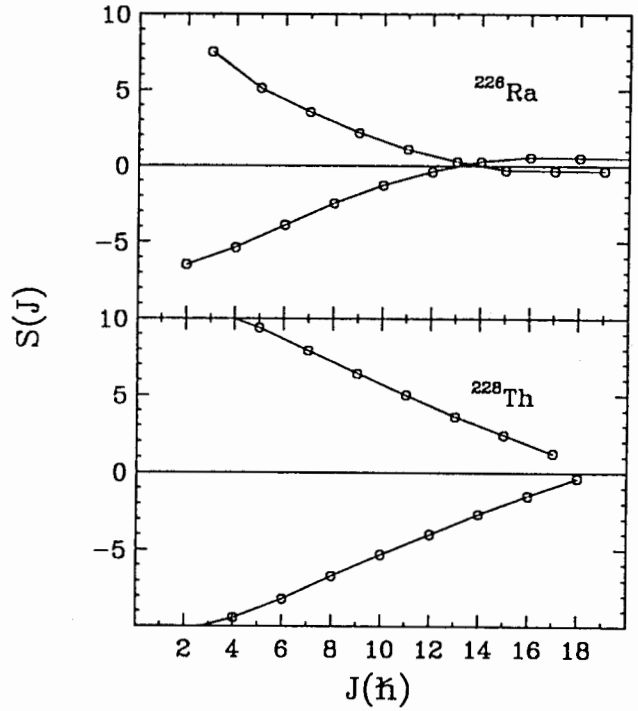

FIG. 5: Empirical signature splitting index $S(J) = [(E_J - E_{J-1}) - (E_{J-1} - E_{J-2})]/E_{2_1^+}$ for ^{226}Ra and ^{228}Th

ACKNOWLEDGMENTS

I am grateful to Dimitri Kusnezov for collaboration in the research presented here. Work supported by the USDOE Grands Nos. DE-FG02-91ER-40609 and DE-FG02-88ER-40417.

---

[1] A. Bohr and B. Mottelson, *Nuclear Structure*, Vol. 2, (Benjamin,Reading, MA, 1975).

[2] R.V. Jolos and P. von Brentano, Phys. Rev. C 49, R2301 (1994).

[3] R. Jolos, P. von Brentano, and F. Dönau, J. Phys. G 19, L1 (1993).

[4] N.V. Zamfir, P. von Brentano, and R.F. Casten, Phys. Rev. C49, R605 (1994).

[5] F. Iachello and A. Arima, *The Interacting Boson Model*, (Cambridge Univeristy Press, Cambridge, 1987).

[6] E.G. Nadjakov and I.N. Michailov, J. Phys. G 13, 1221 (1987).

[7] D. Kusnezov, J. Phys. A 22, 4271 (1989), 23, 5673 (1990).

[8] N.V. Zamfir and D. Kusnezov, Phys. Rev. C 63, 054306 (2001).

[9] N.V. Zamfir, in *Int. Symposium on Nuclear Structure Physics*, (World Scientific, Singapore, 2001), eds. R.F. Casten et al.

[10] D. Kusnezov, Computer code OCTUPOLE, unpublished.

[11] J.F.C. Cocks et al., Phys. Rev. Lett. 78, 2920 (1997).

[12] Y.A. Akovali, Nucl. Data Sheets, 77 433 (1996).

[13] T. Weber et al., Eur. Phys. J. A 3, 25 (1998).

[14] T. Weber, J. Gröger, C. Günther, J. de Boer, Eur. Phys. J. A 1, 39 (1998).

[15] Agda Artna-Cohen, Nucl. Data Sheets, 80, 723 (1997).

A soft mode in a finite Fermi-system: anharmonic effects near the instability point

Vladimir Zelevinsky[1,2] and Alexander Volya[2]
[1] *Department of Physics and Astronomy and*
[2] *National Superconducting Cyclotron Laboratory,*
Michigan State University, East Lansing, Michigan 48824-1321 USA

We consider a finite Fermi-system where the residual interactions create a soft mode of the excitation spectrum. Because of the large vibrational amplitude, the standard random phase approximation does not work in this situation. We develop a regular method for constructing the anharmonic potential and illustrate the application of the formalism by a simple model.

I. INTRODUCTION

The appearance of a soft collective mode of vibrational nature is quite common in nuclei and in other mesoscopic quantum systems, such as atomic clusters. The conventional theoretical way to handle this situation [1–4] goes along the standard line: mean field (MF) – residual interactions – random phase approximation (RPA). The MF determines the symmetry of the system around the ground state and corresponding elementary excitations, fermionic quasiparticles. The residual interactions include both coherent effects and collision-like processes responsible for the chaotization of motion and lead from a Fermi-gas to Fermi-liquid. The formation of coherent modes is described within the framework of the RPA where the quanta of those modes are treated as independent quasibosonic excitations [2,4]. In the low-lying states, kinematic corrections due to the fact that the quanta are built of fermions, as well as high order dynamic effects, can be accounted for perturbatively [2,5].

The RPA-type theories become insufficient when, in some region of the parameters, the vibrational frequency ω approaches zero. The vibrational amplitude then grows $\propto 1/\sqrt{\omega}$ revealing the instability of the MF. In a finite system, this is not necessarily a vestige of a phase transition or sharp restructuring of the system. Rather it might be a signature of the failure of the theoretical consideration based on the picture of harmonic vibrations. For instance, a low energy of the first excited quadrupole state does not mean that the nucleus becomes deformed. In the regime of large amplitude collective motion, we need to reject the harmonic approximation and find a way of calculating the anharmonic effects which cannot be here treated as small corrections.

The estimates [6], as well as more detailed unrestricted MF calculations, show that in the quadrupole case the effective potential is close to the γ-unstable [7] quartic one, $\sim \beta^4$, and the spherical symmetry of the MF still holds but only on average. The popular interacting boson model [8] with the phonon number fixed by a number of fermion pairs cannot describe the soft vibrational bands which stretch to very high spins. In this sense the phenomenological models [9–12] based on a specific form of the collective quadrupole

Hamiltonian are more successful. The onset of deformation occurs beyond the point of the RPA instability when some previously unoccupied configurations sharply lower their energy as a function of deformation and thereby select the equilibrium static value of γ, usually $\gamma = 0$. The macroscopic analog of this scenario would be the first order phase transition.

Below we consider a typical collective soft mode and show a way of constructing the effective nonperturbative anharmonic potential for large-amplitude collective motion starting with the full microscopic many-body Hamiltonian. We present only the skeleton of the formalism and apply it to the Lipkin model known as a testing ground of various theoretical approximations (the first version of this approach was published in [13]).

II. GENERALIZED DENSITY MATRIX

It is convenient to use the operator language with the generalized density matrix (GDM) as the main tool [14–17]. We consider a truncated single-particle space of orbitals $|1)$ of full dimension Ω. The GDM is the set of the operators

$$R_{12} = a_2^\dagger a_1 , \tag{1}$$

where a and $a^\dagger$ are fermionic operators in the second quantization (in a similar way, one can consider Bose-systems), the subscripts *1,2* form a matrix in single-particle space Ω, and each element R_{12} is an operator in the many-body Hilbert space. These operators generate a closed $SU(\Omega)$ Lie algebra given by the commutation relations

$$[R_{12},\, R_{34}] = \delta_{14} R_{32} - \delta_{23} R_{14} ; \tag{2}$$

the trace of the GDM in single-particle indices (tr) gives a number operator, $\mathrm{tr}(R) = N$. The GDM is Hermitian in the combined space of single-particle and many-body variables, $R_{12}^\dagger = R_{21}$.

The dynamics of the system are governed by a standard Hamiltonian which contains one-body and two-body terms,

$$H = \sum_{1,2} \epsilon_{12} a_1^\dagger a_2 + \frac{1}{4} \sum_{1,2,3,4} V_{12;34}\, a_1^\dagger a_2^\dagger a_3 a_4 , \tag{3}$$

where $\epsilon_{12} = \epsilon_{21}^*$, $V_{12;34} = V_{43;21}^*$, and we assume the antisymmetrized form of the two-body interaction. We define a self-consistent field W (similarly to R, an operator in the combined space) as a linear functional of the GDM,

$$W_{14}\{R\} \equiv \frac{1}{2} \sum_{2,3} V_{12;34} R_{32} = \frac{1}{2} \sum_{2,3} V_{12;34}\, a_2^\dagger a_3 . \tag{4}$$

The hamiltonian in eq. (3) can also be written in terms of the GDM.

The equations of motion for the creation and annihilation fermionic operators are

$$[a_1,\, H] = \sum_2 (\epsilon_{12} + W_{12})\, a_2 , \quad [a_1^\dagger,\, H] = -\sum_2 a_2^\dagger (\epsilon_{21} + W_{21}) , \tag{5}$$

whereas the total GDM (1) satisfies the nonlinear operator equation

$$[R,\, H] = [\epsilon + W\{R\},\, R] . \tag{6}$$

These equations are still exact. Here the commutators are understood to act in the combined space, for example,

$$[W, R]_{12} \equiv \sum_3 (W_{13} R_{32} - R_{13} W_{32}); \tag{7}$$

all elements are many-body operators.

III. MAPPING ONTO COLLECTIVE SPACE

Now we make two crucial assumptions: (i) there exists a "collective band" as a set of stationary states which are coupled by strong intraband transition amplitudes while the transitions to the states of a different nature are weak and can be ignored, or be taken into account perturbatively later; (ii) the nomenclature (quantum numbers) of the band states can be built with the aid of the operators of collective coordinates α and conjugate momenta π. These assumptions are fulfilled accurately [18] for low-lying quadrupole vibrations in medium and heavy spherical nuclei where it is known that the quadrupole transitions from the ground state are nearly saturated by the first excited 2^+ state, which in turn gives rise to transitions to the "two-phonon" triplet of states $0^+, 2^+$ and 4^+, and so on. This means that there is a good correspondence between the ideal quadrupole phonon space and realistic spectra in spite of the fact that the predictions of the naive model of harmonic quadrupole vibrations are badly violated. If so, the observed states can be generated by the quadrupole coordinate and momentum operators $\alpha_{2\mu}$ and $\pi_{2\mu}$ although the collective Hamiltonian $H(\alpha, \pi)$ might be very far from the harmonic one.

According to our assumptions, the collective subspace is spanned by the operators α and π with normal commutation relations

$$[\alpha,\, \pi] = i , \tag{8}$$

and their high order products. For simplicity we take here scalar quantities; the rotational tensor character can be introduced in a straightforward way. The general form of the effective Hermitian collective Hamiltonian acting within this subspace is

$$\mathcal{H} = \sum_{m,n} \frac{\Lambda^{(m\,n)}}{2mn} [\alpha^m,\, \pi^n]_+ . \tag{9}$$

Our goal is to derive the unknown c-number coefficients $\Lambda^{(mn)}$ from the microscopic Hamiltonian H, eq. (3). This can be done by the corresponding mapping of the exact operator equations of motion (6).

We are interested in the matrix elements of the equations of motion between collective states. Since the dynamics are saturated in the collective space, we leave as the intermediate states in those equations only the states within the band. Then operators R and W can be effectively represented by the functions of α and π similarly to (9),

$$\mathcal{R} = \sum_{m,n} \frac{r^{(m\,n)}}{2mn} [\alpha^m,\, \pi^n]_+ , \quad \mathcal{W} = \sum_{m,n} \frac{w^{(m\,n)}}{2mn} [\alpha^m,\, \pi^n]_+ . \tag{10}$$

The question of mapping is now formulated as a problem of finding a set of numbers $\Lambda^{(mn)}$ and quantities $r^{(mn)}$, $w^{(mn)}$ (matrices in single-particle space) which express the contributions of specific elementary excitations to a given collective operator. The corresponding parts of $r^{(mn)}$ and $w^{(mn)}$ are interrelated by the self-consistency conditions (4).

Physical arguments of time-reversal (T) invariance and the possibility of canonical transformations in the collective space, such as shifts and rescalings of collective variables, allow us to consider only $\Lambda^{(mn)}$ with even n and start the sum with the harmonic terms, $(mn) = (02)$ and (20), so that eq. (9) becomes ($\Lambda^{(02)} = 1/B$, $\Lambda^{(20)} = C$ give the mass and force parameters of the harmonic part)

$$\mathcal{H} = \frac{1}{2B}\pi^2 + \frac{C}{2}\alpha^2 + \frac{\Lambda^{(30)}}{3}\alpha^3 + \frac{\Lambda^{(12)}}{4}[\alpha,\pi^2]_+ + \frac{\Lambda^{(40)}}{4}\alpha^4 + \frac{\Lambda^{(04)}}{4}\pi^4 + \frac{\Lambda^{(22)}}{8}[\alpha^2,\pi^2]_+ + \dots . \tag{11}$$

Under our assumptions, the full operator equations of motion (6) should be satisfied inside the band. Therefore we require that in this space

$$[\mathcal{R},\, \mathcal{H} + \epsilon + \mathcal{W}\{\mathcal{R}\}] = 0 . \tag{12}$$

Commutators involving $\mathcal{H}$ and ϵ in the above expression are simple since $\mathcal{H}$ does not contain single-particle variables, whereas ϵ is a c-number matrix in the Hilbert space. The commutator of $\mathcal{W}$ with the GDM is more complex as both operators act in the combined space.

Below we show the lowest order equations. As seen from (12), it is convenient to introduce a self-consistent MF Hamiltonian as

$$h = \epsilon + \mathcal{W}\{\rho\} , \tag{13}$$

and a self-consistent RPA operator $\hat{L}$ defined [15,16] by its action on an arbitrary single-particle matrix r,

$$\hat{L}r = [h, r] + [\mathcal{W}\{r\},\, \rho] . \tag{14}$$

In eqs. (13) and (14) we used the ground state single-particle density matrix $\rho \equiv r^{(00)}$. The lowest static part, $(mn) = (00)$, produces a set of the MF equations

$$0 = [h,\, \rho] + i\delta^{(00)} , \tag{15}$$

where $\delta^{(00)}$ is a correction to the usual Hartree-Fock approximation from higher orders which changes the average MF single-particle occupancies (eigenvalues of ρ) due to the fluctuation effects coming from the soft mode [17]. The next set of equations corresponds to the parts linear in α and π operators (T-even and T-odd terms, respectively),

$$-i\Lambda^{(20)}r^{(01)} = \hat{L}r^{(10)} + i\delta^{(10)} , \tag{16}$$

$$i\Lambda^{(02)}r^{(10)} = \hat{L}r^{(01)} + i\delta^{(01)} . \tag{17}$$

These terms are analogous to the RPA although it is not assumed that the occupation numbers are 0 and 1. The following three equations in quadratic order are

$$-i\Lambda^{(20)}r^{(11)} - i\Lambda^{(30)}r^{(01)} = \frac{1}{2}\hat{L}r^{(20)} + [w^{(10)}, r^{(10)}] + i\delta^{(20)} , \tag{18}$$

$$-i\Lambda^{(20)}r^{(02)} + i\Lambda^{(02)}r^{(20)} + i\Lambda^{(12)}r^{(10)} = \hat{L}r^{(11)} + [w^{(10)}, r^{(01)}] + [w^{(01)}, r^{(10)}] + i\delta^{(11)} , \tag{19}$$

$$i\Lambda^{(02)}r^{(11)} - i\Lambda^{(12)}r^{(01)} = \frac{1}{2}\hat{L}r^{(02)} + [w^{(01)}, r^{(01)}] + i\delta^{(02)} . \tag{20}$$

We limit ourselves here to the fourth order of anharmonicities, i.e. cubic operators in equations of motion. The four corresponding equations are

$$\begin{aligned}
&-\frac{i}{2}\Lambda^{(20)}r^{(21)} - i\Lambda^{(30)}r^{(11)} - i\Lambda^{(40)}r^{(01)} = \frac{1}{3}\hat{L}r^{(30)} + \frac{1}{2}[w^{(20)}, r^{(10)}] + \frac{1}{2}[w^{(10)}, r^{(20)}] \\
&\qquad + i\delta^{(30)} , \\
&-i\Lambda^{(20)}r^{(12)} + i\Lambda^{(02)}r^{(30)} - i\Lambda^{(30)}r^{(02)} + i\Lambda^{(12)}r^{(20)} + \frac{i}{2}\Lambda^{(22)}r^{(10)} \\
&= \frac{1}{2}\hat{L}r^{(21)} + \frac{1}{2}[w^{(20)}, r^{(01)}] + [w^{(11)}, r^{(10)}] + \frac{1}{2}[w^{(01)}, r^{(20)}] + [w^{(10)}, r^{(11)}] + i\delta^{(21)} , \\
&-i\Lambda^{(20)}r^{(03)} + i\Lambda^{(02)}r^{(21)} + \frac{i}{2}\Lambda^{(12)}r^{(11)} - \frac{i}{2}\Lambda^{(22)}r^{(01)} \\
&= \frac{1}{2}\hat{L}r^{(12)} + \frac{1}{2}[w^{(02)}, r^{(10)}] + [w^{(11)}, r^{(01)}] + [w^{(01)}, r^{(11)}] + \frac{1}{2}[w^{(10)}, r^{(02)}] + i\delta^{(12)} , \\
&\frac{i}{2}\Lambda^{(02)}r^{(12)} - \frac{i}{2}\Lambda^{(12)}r^{(02)} + i\Lambda^{(04)}r^{(10)} = \frac{1}{3}\hat{L}r^{(03)} + \frac{1}{2}[w^{(02)}, r^{(01)}] + \frac{1}{2}[w^{(01)}, r^{(02)}] \\
&\qquad + i\delta^{(03)} .
\end{aligned} \tag{21}$$

The higher order corrections $\delta^{(i,j)}$ arise from the commutators $[\mathcal{R}, \mathcal{W}]$ and $[\mathcal{R}, \mathcal{H}]$,

$$\delta^{(00)} = \frac{1}{2}\left(\left[w^{(10)}, r^{(01)}\right]_+ - \left[w^{(01)}, r^{(10)}\right]_+ + \dots\right),$$

$$-\left(\frac{1}{2}\Lambda^{(20)}r^{(13)} - \frac{1}{2}\Lambda^{(02)}r^{(31)} + \frac{2}{3}\Lambda^{(30)}r^{(03)} - \frac{1}{4}\Lambda^{(12)}r^{(21)} + \dots\right) . \tag{22}$$

Each next term denoted by dots is four orders higher than the previous one. Furthermore, the lowest correction due to $[\mathcal{R}, \mathcal{W}]$ is always two orders higher, while the terms from $[\mathcal{R}, \mathcal{H}]$ are four orders higher, than the similar terms in the left hand side of (21). Their contributions become less important [6] because there the small statistical weight $\propto 1/\sqrt{\Omega}$ of the collective mode is not sufficiently compensated by the inverse powers of the low frequency ω. We can note parenthetically that this compensation can occur only in finite systems so that the whole approach is tailored for mesoscopic physics. Since the typical estimates for the realistic soft modes show the dominance of the quartic anharmonicity, we keep the main corrections to the RPA terms

$$\delta^{(10)} = \frac{1}{2}\left(\left[w^{(20)}, r^{(01)}\right]_+ - \left[w^{(01)}, r^{(20)}\right]_+ + \left[w^{(10)}, r^{(11)}\right]_+ - \left[w^{(11)}, r^{(10)}\right]_+\right) , \tag{23}$$

$$\delta^{(01)} = \frac{1}{2}\left(\left[w^{(11)}, r^{(01)}\right]_+ - \left[w^{(01)}, r^{(11)}\right]_+ + \left[w^{(10)}, r^{(02)}\right]_+ - \left[w^{(02)}, r^{(10)}\right]_+\right). \quad (24)$$

Let us stress here that the method suggested above differs from numerous attempts at boson expansion, see [5] and references therein. We do not map the wave functions from the microscopic space to a bosonic one. We also do not map directly the operators of observables. We map the *equations of motion* explicitly truncating the intermediate states. This method is regular, does not violate general principles, and, being in fact variational, allows for the further improvements by including other intermediate states.

IV. LIPKIN-MESHKOV-GLICK MODEL

Using the commonly accepted procedure of testing the validity of many-body approximation techniques, we apply the method to the two-level Lipkin-Meshkov-Glick (LMG) model [19]. The space contains two single-particle levels of energies $\pm\epsilon/2$ with a large degeneracy $\Omega/2$ of each of them. We label the Ω fermionic states by quantum numbers (σl), where $\sigma = \pm 1$ denotes one of the two single-particle levels and $l = 1, 2, \ldots, \Omega/2$ distinguishes the degenerate states on each orbital. The many-body Hamiltonian of the system is

$$H = \frac{\epsilon}{2}\sum_{\sigma,l}\sigma a^\dagger_{\sigma,l}a_{\sigma,l} + \frac{1}{2}V\sum_{\sigma,l,l'}a^\dagger_{\sigma,l}a^\dagger_{\sigma,l'}a_{-\sigma,l'}a_{-\sigma,l}\,. \quad (25)$$

The special feature of the problem is that the collective dynamics are expressed in terms of the quasimomentum operators $J_\pm, J_z$,

$$J_+ = J_-^\dagger = J_x + iJ_y = \sum_l a^\dagger_{+1,l}a_{-1,l}, \quad J_z = \frac{1}{2}\sum_{\sigma,l}\sigma a^\dagger_{\sigma,l}a_{\sigma,l}. \quad (26)$$

The Hamiltonian (25) can be expressed as

$$H = \epsilon J_z + \frac{1}{2}V(J_+^2 + J_-^2) = \epsilon J_z + V(J_x^2 - J_y^2). \quad (27)$$

The LGM model is ideally suited to our approximate mapping procedure. The SU(2) symmetry of the problem can be also combined with particle-hole symmetry, which allows us to limit the consideration to the cases with the particle number $N \le \Omega/2$, and discrete symmetries (we can take $V > 0$ without loss of generality). For the unperturbed system, $V = 0$, the ground state with all N particles on the lower level belongs to the largest representation $J = J_z = N/2$ with $\mathbf{J}^2 = [(N/2)+1](N/2)$, and then J_+ is an operator that creates a collective state. In this model the collective degrees of freedom are decoupled exactly, and we need to reproduce the equations of motion

$$[J_x, H] = -i\epsilon J_y - iV[J_y, J_z]_+, \quad [J_y, H] = i\epsilon J_x - iV[J_x, J_z]_+\,, \quad (28)$$

$$[J_z, H] = 2iV[J_x, J_y]_+\,, \quad (29)$$

in the mapped space of collective variables α , π , with a collective anharmonic Hamiltonian (11). The kinematic constraints, analogous to eq. (2, arise from the mapping of the

quasimomentum algebra onto a Heisenberg algebra of α and π. These constraints can be accounted for by the Holstein-Primakoff transformation

$$J_+ = J_-^\dagger = \mathcal{A}^\dagger\sqrt{2J - \mathcal{A}^\dagger\mathcal{A}} = \sqrt{2J + 1 - \mathcal{A}^\dagger\mathcal{A}}\,\mathcal{A}^\dagger, \quad J_z = -J + \mathcal{A}^\dagger\mathcal{A}\,, \quad (30)$$

where operators $\mathcal{A}$ and $\mathcal{A}^\dagger$ are bosonic annihilation and creation operators, $[\mathcal{A}, \mathcal{A}^\dagger] = 1$.

The RPA corresponds to keeping only quadratic terms in $\mathcal{A}$ and $\mathcal{A}^\dagger$ which leads to the RPA Hamiltonian

$$H_{\rm RPA} = -\epsilon\left(J + \frac{1}{2}\right) + \frac{\epsilon}{2}(\mathcal{A}^\dagger\mathcal{A} + \mathcal{A}\mathcal{A}^\dagger) + \frac{V}{4}\sqrt{16J^2 - 1}\left((\mathcal{A}^\dagger)^2 + \mathcal{A}^2\right). \quad (31)$$

The diagonalization of (31) results in the harmonic approximation with an RPA frequency [20]

$$\omega^2_{\rm RPA} = \epsilon^2 - V^2\left(4J^2 - \frac{1}{4}\right). \quad (32)$$

The instability point, $V^2 \approx \epsilon^2/(4J^2)$, exists in all J-subspaces emerging first for the largest J with a greater degree of collectivity.

The collective coordinate and momentum can be introduced with the aid of the canonical transformation

$$\mathcal{A} = \frac{1}{\sqrt{2}}(iu\alpha + v\pi), \quad \mathcal{A}^\dagger = \frac{1}{\sqrt{2}}(-iu\alpha + v\pi), \quad uv = -1. \quad (33)$$

The LMG model has only even order anharmonicities, and in our choice of expansion the correction to the n-th order will come from the $(n+2)$-th order in α and π. An expansion up to the sixth order retaining only quadratic and quartic terms is necessary for determining the effective quartic Hamiltonian. The appropriate choice of u and v as

$$u = \left(\epsilon + V\frac{16J^2 + 8J - 1}{2\sqrt{16J^2 - 1}}\right)^{1/2}, \quad v = -\frac{1}{u}, \quad (34)$$

sets a scale of the collective Hamiltonian at $B = 1$ and the parameters in eq. (11) as

$$\omega^2 = C = \epsilon^2 - V^2\frac{(16J^2 + 8J - 1)^2}{4(16J^2 - 1)} \approx \epsilon^2 - 4V^2J^2\,, \quad (35)$$

$$\Lambda^{(40)} = 2V\left(\frac{32J^3 - 2J - 1}{(16J^2 - 1)^{3/2}}\right)u^4 \approx V\,u^4, \quad \Lambda^{(04)} = -2V\left(\frac{32J^3 - 2J - 1}{(16J^2 - 1)^{3/2}}\right)v^4 \approx -V\,v^4. \quad (36)$$

At the instability point of $\omega \to 0$, assuming that $J \gg 1$, $\epsilon \gg V$, we obtain an approximate collective Hamiltonian ($V > 0$)

$$H = \frac{\pi^2}{2} + 4\epsilon^4\,V\,\alpha^4\,. \quad (37)$$

The negative π^4 term in the collective Hamiltonian is very small in the vicinity of the instability point in contrast to the quartic potential α^4 which has large matrix elements

because of the large amplitude of collective motion. This is a typical situation which emerges with a suitable choice of collective coordinates (T-even) and collective momenta (T-odd). The next order terms and, in general, coupling to non-collective space, will correct the behavior of the π^4 term but this is not important for low-lying states.

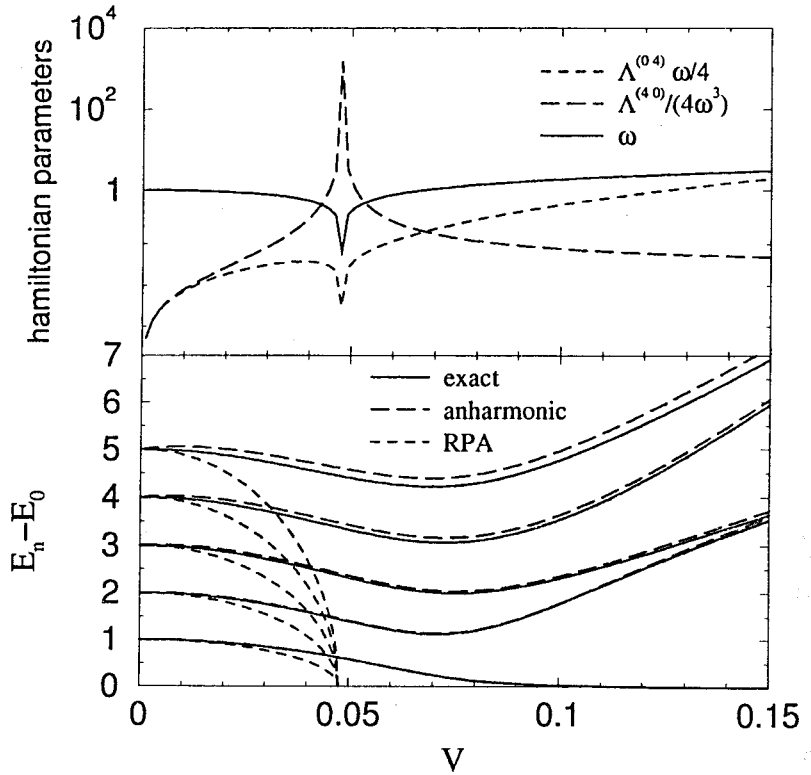

FIG. 1. Parameters of the collective Hamiltonian (harmonic frequency and quartic parameters) for the LGM model with $N = 20$ particles in the largest representation $J = 10$ as a function of the interaction strength V ($\epsilon = 1$), upper panel (note the logarithmic scale with the strong growth of $\Lambda^{(40)}$ at the point of the RPA instability); excitation energies of the first five states for the same case of the LMG, exact solution, solid lines; RPA solution, dotted lines; anharmonic oscillator solution with the π^4 term ignored, dashed lines, lower panel

In Fig. 1 we show the behavior of the harmonic term (ω) and quartic corrections $\Lambda^{(40)}$ and $\Lambda^{(04)}$ in the dimensionless normalization, upper panel, and present a comparison of the exact LMG model spectrum (solid lines), RPA solution (dotted lines), and an improved anharmonic oscillator solution with the ignored divergent π^4 part (at large V it should

be included along with the high order coordinate terms), lower panel. The anharmonic effects produce a dramatic improvement as compared to the RPA. At the point of the RPA instability, the contribution from the large quartic potential restores the stability. As the interaction strength V increases, the effective potential

$$U(\alpha) = \frac{1}{2}\omega^2\alpha^2 + \frac{1}{4}\Lambda^{(40)}\alpha^4 \tag{38}$$

evolves, Fig. 2, from the harmonic oscillator to a pure quartic oscillator at the instability point, and to the "Mexican hat" potential with two minima. In the last limit the lowest states of opposite parities located in the minima become degenerate as clearly seen in Fig. 2 ("chiral symmetry"). Contrary to the macroscopic second order phase transition, the higher states are located above the barrier and feel only the main quartic potential. A similar phenomenon should exist in soft nuclei beyond the RPA instability point when only the lowest states are influenced by the presence of the minima in the β coordinate; however, there the minima are connected along the γ coordinate which is absent in the LGM.

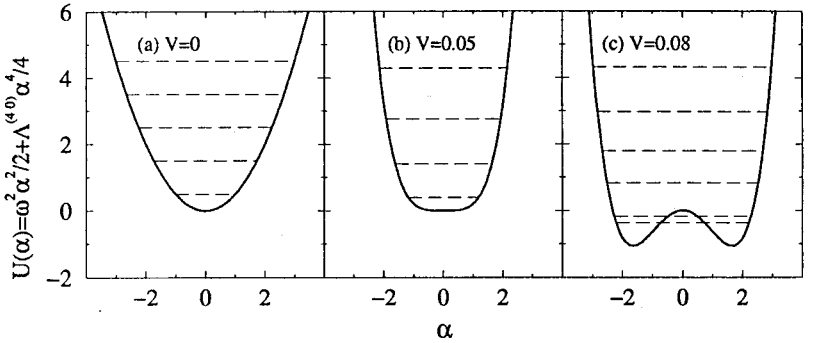

FIG. 2. The spectrum of the lowest levels in the model of Fig. 1, dashed lines, and the shape of the effective potential $U(\alpha)$ for (a) $V = 0$, the harmonic limit; (b) $V = 0.05$, pure quartic potential at the RPA instability point; (c) $V = 0.08$, beyond the instability point, the splitting of the levels of opposite parity (symmetry in J_z in the limit of $VJ^2 \gg \epsilon$) below the barrier decreases as V increases

V. CONCLUSION

We have suggested an alternative approach to the construction of a collective Hamiltonian for large amplitude collective motion in a finite Fermi system in the presence of a soft vibrational mode. In such a situation, the RPA is insufficient as near the RPA instability the anharmonic effects dominate. The advantages compared to conventional techniques, such as the generator coordinate method, are related to a fully quantum consideration which does not require the derivation of an approximate classical Hamiltonian

with the subsequent ill-defined procedure of requantization. It differs from the approaches utilizing various versions of the boson expansion in the variational character of the formalism. We can vary the collective space assuming the saturation of the exact operator equations of motion within a part of total Hilbert space. With our techniques we also avoid the slow convergence problem of the naive boson expansion.

Of course, the illustrative example of the Lipkin model is perfectly suited to our goal since the collective modes of this model are fully decoupled. However it emphasizes the predominance of the quartic anharmonicity near the RPA instability. Because of the convenient operator distinction between the coordinate and momentum parts, we concentrate the most important anharmonic effects in the quartic potential which has large matrix elements in the dangerous region of interest.

In realistic cases, the collective space is not decoupled completely. The effects of coupling to noncollective states lead to the spreading of the collective strength and the chaotization of motion in the region of high level density. To treat this situation as well, we can include the matrix elements of the GDM connecting the collective band with incoherent states. One promising approach would be to consider these states on average, making the random phase assumption on a new level of treatment. This would introduce an effective background for the collective mode to describe its spreading and damping.

The authors are thankful to D. Mulhall for assistance and criticism; they acknowledge support from the USA National Science Foundation.

---

[1] S.T. Belyaev, Mat. Fys. Medd. Dan. Vid. Selsk. **31**, No. 11 (1959).

[2] S.T. Belyaev and V.G. Zelevinsky, Nucl. Phys. **39** (1962) 582.

[3] P. Ring and P. Schuck, *The Nuclear Many-Body Problem* (Springer, Berlin - New York, 2000).

[4] V.G. Soloviev, *Theory of Atomic Nuclei; Quasiparticles and Phonons* (Institute of Physics, Bristol - Philadelphia, 1992).

[5] A. Klein and E.R. Marshalek, Rev. Mod. Phys. **63** (1991) 376.

[6] V.G. Zelevinsky, Int. J. Mod. Phys. **E2** (1993) 273.

[7] M. Jean and L. Wilets, Phys. Rev. **102** (1956) 788.

[8] F. Iachello and A. Arima, *The Interacting Boson Model* (University Press, Cambridge, 1987).

[9] O.K. Vorov and V.G. Zelevinsky, Sov. J. Nucl. Phys. **37** (1983) 830.

[10] O.K. Vorov and V.G. Zelevinsky, Nucl. Phys. **A439** (1985) 207.

[11] J. Armstrong and V. Zelevinsky, Preprint MSUCL-1098, April 1998; BAPS **44**, Part I, p. 397.

[12] F. Iachello, Phys. Rev. Lett. **85** (2000) 3580.

[13] V.G. Zelevinsky, in *Frontiers in Nuclear Physics* (Dubna, 1995) p. 243.

[14] S.T. Belyaev and V.G. Zelevinsky, Sov. J. Nucl. Phys. **16** (1973) 657.

[15] V.G. Zelevinsky, Nucl. Phys. **A337** (1980) 40.

[16] V.G. Zelevinsky, Prog. Theor. Phys. Suppl. **74-75** (1983) 251.

[17] . V.G. Zelevinsky, Nucl. Phys. **A555** (1993) 109.

[18] R.V. Jolos, P. von Brentano, N. Pietralla, and I. Schneiden, Nucl. Phys. **A618** (1997) 126.

[19] H. Lipkin, N. Meshkov, and A. Glick, Nucl. Phys. **62**, (1965) 188.

[20] N. Meshkov, A. Glick, and H. Lipkin, Nucl. Phys. **62** (1965) 199.

CONTENTS

Научное издание

Perspectives of Nuclear Structure and Nuclear Reactions

Collection of papers, dedicated to the 60th anniversary of the birthday of Rostislav Jolos

Перспективы в изучении структуры ядра и ядерных реакций

Сборник статей, посвященный 60-летию со дня рождения Р. В. Джолоса

E4-2002-66

Сборник отпечатан методом прямого репродуцирования с оригиналов, предоставленных оргкомитетом.

Ответственный за подготовку сборника к печати *Н. В. Антоненко.*

В сборнике использованы фотографии *Ю. А. Туманова*, а также снимки из семейного архива.

ЛР № 020579 от 23.06.97.
Подписано в печать 28.05.2002.
Формат 60 × 90/16. Бумага офсетная. Печать офсетная.
Усл. печ. л. 7,00. Уч.-изд. л. 12,48. Тираж 150 экз. Заказ № 53313.

Издательский отдел Объединенного института ядерных исследований
141980, г. Дубна, Московская обл., ул. Жолио-Кюри, 6.